

INFORMATION TO USERS

This manuscript has been reproduced from the microfilm master. UMI films the text directly from the original or copy submitted. Thus, some thesis and dissertation copies are in typewriter face, while others may be from any type of computer printer.

The quality of this reproduction is dependent upon the quality of the copy submitted. Broken or indistinct print, colored or poor quality illustrations and photographs, print bleedthrough, substandard margins, and improper alignment can adversely affect reproduction.

In the unlikely event that the author did not send UMI a complete manuscript and there are missing pages, these will be noted. Also, if unauthorized copyright material had to be removed, a note will indicate the deletion.

Oversize materials (e.g., maps, drawings, charts) are reproduced by sectioning the original, beginning at the upper left-hand corner and continuing from left to right in equal sections with small overlaps.

ProQuest Information and Learning
300 North Zeeb Road, Ann Arbor, MI 48106-1346 USA
800-521-0600

UMI[®]

NOTE TO USERS

**Page(s) missing in number only; text follows.
Microfilmed as received.**

154 & 158

This reproduction is the best copy available.

UMI

DISSERTATION

**CHROMOSOMAL INSTABILITIES IN HUMAN TUMOR AND IRRADIATED
NORMAL CELLS**

Submitted by

Lawrence C. Dugan

Department of Radiological Health Sciences

In partial fulfillment of the requirements

For the Degree of Doctor of Philosophy

Colorado State University

Fort Collins, Colorado

Summer 2002

UMI Number: 3063986

UMI[®]

UMI Microform 3063986

Copyright 2002 by ProQuest Information and Learning Company.
All rights reserved. This microform edition is protected against
unauthorized copying under Title 17, United States Code.

ProQuest Information and Learning Company
300 North Zeeb Road
P.O. Box 1346
Ann Arbor, MI 48106-1346

COLORADO STATE UNIVERSITY

MAY 30, 2002

WE HEREBY RECOMMEND THAT THE DISSERTATION
PREPARED UNDER OUR SUPERVISION BY LAWRENCE C.
DUGAN AND ENTITLED CHROMOSOMAL INSTABILITIES IN
HUMAN TUMOR AND IRRADIATED NORMAL CELLS BE
ACCEPTED AS FULFILLING IN PART THE REQUIREMENTS FOR
THE DEGREE OF DOCTOR OF PHILOSOPHY.

Committee on Graduate Work

James R. Bamberg
[Signature]
Michael G. Fox

[Signature]
J. Bedford
Adviser

[Signature]
Department Head

ABSTRACT OF DISSERTATION

CHROMOSOMAL INSTABILITIES IN HUMAN TUMOR AND IRRADIATED NORMAL CELLS

Radiation-induced genomic instability has been proposed as an initiating step in radiation-induced carcinogenesis. Numerous studies have established the occurrence of this phenomenon in various cells of both human and rodent origin. Genomic instability is considered to have been induced if new mutations or chromosomal aberrations occur in the progeny of cells surviving the radiation dose at a higher frequency than that for unirradiated cells. Such induced instability has been reported both *in vivo* and *in vitro* and for such genetic changes as delayed chromatid-type and chromosome-type aberrations, delayed mutations and delayed cell lethality. In many of these studies, however, the cells were not "normal" initially and in many cases involved tumor-derived cell lines. If radiation-induced genomic instability is indeed *the* initiating step involved in radiation-induced carcinogenesis, the phenomenon is clearly of much greater interest if it occurs especially in cells that are apparently normal at the outset. The induction of an "initiating" or early step in carcinogenesis would be less interesting in tumor cells that are already initiated by definition.

To this end, I studied a phenotypically normal human fibroblast cell line, (AG1521A) to determine whether they exhibit chromosomal instability in the progeny of surviving cells after exposure to low and high LET radiation. Radiation

exposures were administered while cells were in a non-cycling G_0 state and assays for instability were performed on both mixed populations of cells and clones of cells surviving the exposure. Several cytogenetic techniques were used to determine induced chromosomal instabilities. These included solid Giemsa staining and classical cytogenetic analysis, whole chromosome painting by fluorescence *in situ* hybridization (FISH) and multiplex fluorescence *in situ* hybridization (M-FISH).

I found no evidence for the induction of chromosomal instability in the phenotypically normal AG1521A human fibroblast cells after exposure to either high or low LET radiation following exposure of the cells in a G_0 state. Based on review of published literature and our own data, I conclude that radiation-induced chromosomal instability does not occur universally, at least in G_0 irradiated normal cells. I therefore suggest that induced instability may not be *the* initiating step in radiation carcinogenesis in all cases. This does not rule out the occurrence of the phenomenon, nor does it suggest a possible lack of importance for it in systems with some predisposing factor, such as alterations in normal DNA damage processing.

Nijmegen Breakage Syndrome results from a recessively inherited genetic disorder and among other things is characterized by hypersensitivity to ionizing radiation and chromosomal instability. NBS1 (nibrin or p95), the product of the NBS1 gene, complexes with Rad50 and Mre11 in response to DNA damage, especially double-strand breaks and is required for cell cycle control. The defect in DNA repair and the resulting hypersensitivity to ionizing radiation in cells from

NBS patients led us to hypothesize that exposure to ionizing radiation may lead to elevated levels of complex exchange aberrations at doses considerably lower than would produce a similar effect in repair competent cells. Elevated frequencies of spontaneous and radiation-induced chromatid-type and chromosome-type aberrations were detected in the NBS fibroblast cell line GM7166A compared to repair competent AG1521A fibroblasts. Furthermore, the proportion of radiation-induced aberrations that were complex was higher in the NBS fibroblasts than previously reported for normal human lymphoblasts as determined by mFISH. These results suggest that the major defect in this NBS cell line concerns the ability to correctly repair DNA damage and leads to elevated levels of both simple and complex exchange aberrations after exposure to ionizing radiation.

**Lawrence C. Dugan
Department of Radiological Health Sciences
Colorado State University
Fort Collins, Colorado 80523
Summer 2002**

ACKNOWLEDGEMENTS

No dissertation is written in a vacuum. Although the degree is conferred on one individual, so many contribute throughout the effort. To those who have provided encouragement, assistance and an ear to listen, I wish to give heartfelt thanks.

Joel Bedford has been beyond helpful. The number of times I complained to him that instability did not exist, regardless of what everyone else said, were always met with encouragement, understanding and insight. His ability to treat his students as equals and guide them through the tough times makes truly unique.

My committee members, Drs. Mike Fox, James Bamburg, Robert Ullrich and Charles Waldren provided much needed assistance on numerous occasions when the forest was hidden behind the trees.

Many thanks go to Sandy Wiggen and Julie Asmus whose secretarial and administrative assistance made so many problems simpler. Also, to the many members of our technical staff through the years, including Frank Herman, Kevin Colling, Shannon Flaugh, Amy Watson, Don Young, Colleen Harrington and Todd Harbitzreuther.

Special thanks to few individuals who were most helpful in the lab: Maria Muhlmann-Diaz and Allen Christian, who provided unending help with FISH techniques; Bob Dullea, who managed to teach a chemist what sterile techniques and cell culture were; Dianne Vannais, who provided so much help with

molecular biology and to Mike Cornforth and Brad Loucas at UTMB, who taught me mFISH so I could provide so many colorful images.

**To my wife Lori, who provided love, patience, understanding and the occasional
kick in the pants, I dedicate this work; I could not have done it without you.**

Table of Contents

Chapter 1

INTRODUCTION	1
Cancer in America	1
Chromosomal Aberrations and Cancer	1
Mutations, The Mutator Phenotype and Cancer	3
Genomic Instability and Cancer	7
Radiation Carcinogenesis	9
Initial Effects of Radiation	13
Delayed Effects of Radiation	16
Delayed Chromosome Aberrations	17
Delayed Mutations	32
Delayed Lethal Mutations/Delayed Reproductive Death	34
Instabilities for other Biological Endpoints	36
Lack of Radiation-induced Instability	37
Mechanism(s) of Radiation-induced Genomic Instability	41
Oxidative Stress	41
Genetic Variability	42
Telomeres	43
Is there an Emerging Pattern?	44
Objective of Dissertation	46

Chapter 2

Chromosomal Instability in Mixed Populations of Surviving Low Passage Normal Human Fibroblast-derived AG1521A Cells after G₀ Exposure to Low and High LET Radiation	49
---	-----------

ABSTRACT	49
INTRODUCTION	51
MATERIALS AND METHODS	57
Cell Culture	57
⁵⁶ Fe Irradiation at Brookhaven National Laboratory	57
¹³⁷ Cs Gamma-ray Irradiation	58
First Post-irradiation Mitosis Collection	58
Metaphase Spread Collection and Fixation	59
Plating Efficiency and Surviving Fraction.	59
Continuous Log-phase Incubation	60
Extended G ₀ Incubation	61
Classical Cytogenetic Analysis	61

Whole Chromosome Painting Probe Preparation	62
Fluorescence <i>in situ</i> Hybridization	63
Metaphase Analysis by FISH and Image Acquisition	64
Multiplex FISH	64
RESULTS	67
DISCUSSION	85

Chapter 3

Chromosomal Instability in Clones of HeLa Tumor Cells and Irradiated Normal Cells **98**

ABSTRACT	98
INTRODUCTION	100
MATERIALS AND METHODS	104
Numerical Instability in Clones of HeLa Cells	104
Chromosomal Instability In Clones of TK6 Cells	105
Isolation and Expansion of AG1521A Clones	105
Metaphase Spread Preparation	106
Chromosome Probe Preparation	107
Fluorescence <i>in situ</i> Hybridization	108
Image Acquisition	109
RESULTS	110
HeLa Cells: Assay for Numerical Chromosome Instability	110
Normal Ag1521A Human Fibroblasts: Assays for Radiation-induced Numerical and Structural Chromosomal Instability	114
DISCUSSION	121

Chapter 4

Chromosomal Aberrations in G₀-irradiated GM7166 Nijmegen Breakage Syndrome Fibroblasts **126**

ABSTRACT	126
INTRODUCTION	128
MATERIALS AND METHODS	134
Cell Culture	134
Irradiation	135
Premature Chromosome Condensation	135
Mitotic Cell Collection and Giemsa Staining	137
BrdU Incorporation and Detection	137
Multiplex FISH	138
RESULTS	139
Giemsa Staining: Classical Scoring of Aberrations	139
mFISH Analysis of Aberrations	139

Aberrations in PCC's	157
DISCUSSION	163
SUMMARY OF THE DISSERTATION	171
Bibliography	173

Figures and Tables

Chapter 1

Table 1-1	19
Figure 1-1	22

Chapter 2

Figure 2-1	55
Table 2-1	68
Figure 2-2	70
Figure 2-3	71
Figure 2-4	72
Figure 2-5	73
Figure 2-6	75
Figure 2-7	76
Figure 2-8	77
Figure 2-9	78
Figure 2-10	80
Table 2-2	81
Figure 2-11	83
Table 2-3	84
Figure 2-12	88
Figure 2-13	95

Chapter 3

Figure 3-1	111
Figure 3-2	113
Figure 3-3	115
Figure 3-4	117
Figure 3-5	119
Figure 3-6	120

Chapter 4

Table 4-1	140
Figure 4-1	141
Table 4-2	142
Table 4-3	143
Table 4-4	145
Figure 4-2	146

Figure 4-3	148
Figure 4-4	150
Figure 4-5	152
Figure 4-6	155
Figure 4-7	159
Figure 4-8	161
Table 4-5	165

INTRODUCTION

Cancer in America

In the United States, the lifetime risk for cancer is about 1 in 2 for males and 1 in 3 for females. Excluding $\sim 10^6$ cases of basal and squamous cell skin cancers/year, approximately 1.3×10^6 new cases of cancers will be diagnosed and an estimated 555,500 cancer deaths will occur in the United States in the year 2002 (1).

Ionizing radiation (IR) along with the use of tobacco and alcohol products, viral infections, exposure to UV radiation from the sun, chemical exposure, inherited genetic mutations, altered immune responses and altered hormone levels have all been implicated or directly linked to the onset of cancer.

Chromosome Aberrations and Cancer

Chromosome aberrations are abnormalities involving either the structure or number of chromosomes. These aberrations include deletions, duplications, inversions, translocations, aneuploidy, polyploidy or any other change from the normal pattern or karyotype. They are present in most if not all, human cancers. The association between chromosomal aberrations and cancer was suggested as long ago as 1902 by T. Boveri (2). However, a cause and effect relationship could not be established until more sophisticated methodologies were developed

for defining the aberrations more precisely. With the advent of chromosome banding in the early 1970's (3) (4), it became possible to unequivocally identify specific aberrations within particular tumors. One of the first chromosomal aberrations to clearly show a causative relationship to a human cancer was the Philadelphia chromosome (Ph) found in chronic myelogenous leukemia (CML). It was first identified by Nowell and Hungerford in 1960 (5) and later shown by Rowley in 1973 (6) to result from a translocation. The aberration involves a translocation between chromosomes 9 and 22, [t(9;22)(q34;p11)], that produces a chimeric oncoprotein due to the fusion of the BCR and ABL genes. Another such causative relationship is a translocation between chromosomes 8 and 14 [t(8;14)(q24;q32)] identified in 75% of the cases of Burkitt's lymphoma (7) (8). In this case the human *c-myc* gene is translocated into the immunoglobulin heavy chain locus leading to deregulation of this cell cycle proliferation proto-oncogene. In the other 25%, some 9% involve a [t(2;8)(p12;q24)] and 16% involve a [t(8;22)(q24;q11)] where *c-myc* is retained on chromosome 8 but genes that code for the light chains of the antibody on chromosome 2 or 22 are translocated to chromosome 8 (9). Currently, there are many such instances that have been identified, leaving little doubt of a cause and effect relationship between specific chromosomal aberrations and cancer.

Mutations, The Mutator Phenotype and Cancer

In addition to large mutations, smaller point mutations, loss of heterozygosity (LOH) and frame-shift mutations are also common in many cancers.

It has been accepted for some time that cancer is due to the accumulation of genetic changes in the DNA of a cell and the clonal expansion of the progeny of these altered cells. In the 1950's and 60's, Leslie Foulds developed the concept of tumor progression from an initiated cell to advanced, metastatic disease (10). In a 1976 *Science* paper, Nowell expanded upon this and proposed a model based on genomic instability and clonal selection. He hypothesized that "tumor progression results from acquired genetic variability within the original clone allowing sequential selection of more aggressive sublines (11)." It is still not clear, however, how cells manage to acquire the necessary number of genetic alterations based upon estimates that have been made on spontaneous mutation frequencies.

Normal spontaneous mutation rates have been estimated to be on the order of 10^{-8} mutations /locus /cell per generation (12). The human body contains on the order of 10^{14} cells, a small portion of which are stem cells. If only one or two dominant mutations were necessary to produce a cancer, then spontaneous mutation frequencies might account for the high frequency of cancer in the population (13). However, most cancers are found to contain many more than three alterations and therefore, cannot be explained on the basis of the accumulation of spontaneous mutations alone at the rates mentioned above.

For the sake of argument, if we assume 0.01% of the 10^{14} cells in a human are stem cells (10^{10} cells) and that stem cells are likely candidates for carcinogenesis and that mutations occur at a frequency of 10^{-6} /cell/generation, then in one generation there would be 10^4 mutants produced. If no new mutations were produced and no growth advantage was conferred on the cells due to the genetic changes, the mutants would remain at this frequency (10^{-6}) in the stem cell population.

However, if even a slight growth advantage was conferred on the cell by the mutation, over time the frequency of mutants in the stem cell population could dramatically increase. For example, if the generation time for normal stem cells, $N T_C$, in skin epithelial, is on the order of two weeks (14) (15), but if a mutation confers a growth advantage corresponding to a 2% faster growth rate, the mutant cell generation time, $M T_C$, would be 2 weeks \times 0.98 = 1.96 weeks vs. 2 weeks for the normal cells. We can now ask the question of how long would it take before the frequency of the mutants in the population increased from 10^{-6} to 10^{-4} (a 100-fold increase similar to that seen for radiation-induced delayed mutations by Little and coworkers (16)) if there were 10^6 mutant cells in the 10^{10} total stem cell population? This can be calculated as follows*:

For exponential growth in the normal population, the number of cells, N_t , present at time t , when the initial number, N_0 , is 10^{10} and the generation time, $N T_C$, is two weeks is:

* Footnote: An adult stem cell population does not grow exponentially, but maintains a constant size by allowing one cell to differentiate for every two new cells produced by cell division. So long as this differentiation is random, however, then the relative proportion of various sub-populations will be the same in the stem cell population as in an exponentially expanding population.

$$N_t = 10^{10} 2^{(t/2)}$$

Similarly, for exponential growth in the mutant population, the number of mutant cells, M_t , present at time t is:

$$M_t = 10^4 2^{(t/1.96)}$$

Therefore, to calculate the time, t (in weeks), when $M/N = 10^{-4}$, we solve for t in the expression:

$$M/N = 10^4 2^{(t/1.96)} / (10^{10} 2^{(t/2)}) = 10^{-4}, \text{ and show that}$$

$$t = 651 \text{ weeks or } 12.51 \text{ years}$$

Similarly, for a faster growth rate of 5% rather than 2%,

$$mT_c = 2 \text{ weeks} \times 0.95 = 1.9 \text{ weeks, and}$$

$$t = 252 \text{ weeks or } 4.86 \text{ years}$$

From such calculations, we see that the mutant fraction can become substantially elevated (100-fold or even much greater) in the total stem cell population within the lifetime of an individual (60-80 years) if the mutations confer even a slight growth advantage. Furthermore, the increase in mutant fraction might then allow for further mutations to occur in cells containing a previous mutation.

Now returning to the hypothesis that no growth advantage is conferred on the cells by the mutation we can ask the question: would it be possible for a second mutation to occur in a previously mutated stem cell within an adult lifespan of, say 40 years? If 10^4 mutant cells are produced per generation and 26 generations occur per year (1 generation/2 weeks), then the number of mutant cells produced in 40 years would be: $M_{40} = 10^4 \times 26 \text{ gener./yr} \times 40 \text{ yr} = 10^7$ mutants, a frequency of 10^{-3} in the stem cell population. The frequency of a

second mutant is also 10^{-3} . The probability of having both mutations would then be $(10^{-3})^2 = 10^{-6}$. Therefore, within the population of 10^7 mutants, 10 double mutants would be present, or an overall frequency of 10^{-9} . However, the probability of three or more mutations occurring in the same cell would become very small and unlikely in the 10^{10} cells in the stem cell population. Similar calculations by Loeb have led to the theory that although initiation of cancer resulting from one to two mutations is possible using typical spontaneous normal mutation rates, these rates cannot account for the multiple mutations seen in many human tumors and therefore do not account for the progression from an initiated state to a tumorigenic state (13) (17). Thus it has been proposed that an early event in tumor progression may be the mutation of a gene involved in maintaining genomic stability (11) and that this mutation leads to a mutator phenotype (13). This mutator phenotype then leads to an increase in the mutation rates of these cells (17). This accumulation of mutations, along with clonal expansion of cells containing multiple mutations, might then lead to tumor progression and account for the high frequency of cancer in the population.

In keeping with the "growth advantage" arguments discussed above, Bodmer and coworkers argue that an increase in mutation rate is not always necessary, but that the selection of mutants having some advantage over the initial population allows for clonal expansion of the mutant and the possibility for additional mutations to occur within cells of the clone. This could then lead to additional rounds of expansion of clones containing multiple mutations, all of which occurred at the same background frequency (12).

Genomic Instability and Cancer

Genomic instability is defined to be a state in which the acquisition of new alterations in the genome occurs at an elevated rate compared to that for spontaneous alterations. Evidence exists that most, if not all, cancers display the phenomenon of genomic instability. There appears to be two different levels at which the instability exists (18). At the nucleotide level, elevated levels of base changes involving a few nucleotides are sometimes found. At the chromosome level, rearrangements, losses and gains of whole or large portions of chromosomes are seen.

Instability involving base changes of only a few nucleotides includes substitutions, deletions and insertions and these occur in a low number of cancers. The most common occurrence of this type of instability is found in hereditary non-polyposis colorectal cancer (HNPCC). In HNPCC, microsatellite instability characterized by the presence of new alleles of di- and trinucleotide repeats is caused by mutations in mismatch repair genes, hMSH2, hMLH1 and hPMS2 (19).

Chromosomal instability is much more common in tumors. These instabilities can be seen as alterations in chromosome number (gains or losses), ploidy changes, chromosome translocations, deletions and gene amplifications.

Chromosome translocations are the products of the breakage and exchange of chromatin from two or more different chromosomes. Simple translocations involve only two chromosomes, while complex translocations

involve a greater number of chromosomes. Simple rearrangements might involve the repositioning of an oncogene leading to a decrease in the fidelity of cell cycle control as already mentioned above, for example in the case of Burkitt's lymphoma.

Complex translocations are often found in solid tumors and can involve numerous chromosomes. A recent comparison of four prostate cancer cell lines using multiplex-FISH identified the occurrence of multiple complex aberrations in all four cell lines (20).

Ploidy changes, including aneuploidy and polyploidy are common in solid tumors. Vogelstein and coworkers used fluorescence *in situ* hybridization of centromeric probes to show that changes in chromosome number occurred in chromosomally unstable colorectal cancer cell lines at 10-100x the rate seen in non-chromosomally unstable colorectal cancer cell lines (21).

Gene amplifications tend to occur in late-stage tumors and involve the amplification of a segment of DNA containing a single gene or a few genes. These amplifications are detected as small double-minute chromosomes or homogeneously staining regions within a chromosome (18). For example, Tlsty and coworkers estimated that the rate of spontaneous amplification of the gene encoding the CAD protein (whose enzymatic activities include carbamoyl-phosphate synthetase, aspartate transcarbamylase and dihydroorotase) was on the order of 10^{-4} events per cell per generation in highly tumorigenic rat liver epithelial cells compared to spontaneous rates of 10^{-6} events per cell per generation for nontumorigenic cells (22).

Radiation Carcinogenesis

As previously noted, radiation has been linked to the induction of cancer in humans and other mammals. It is estimated that ~2% of all cancer deaths are caused by radiation, most of which are melanomas due to solar UV exposure. Radon has been estimated to account for 5,000-20,000 cancer deaths per year (23). Medical treatment, such as radiotherapy and radiotherapy combined with chemotherapy, also contributes to cancer deaths (24).

In vitro Transformation

Transformation of cells *in vitro* appears to be a multi-step process that varies among species, with human cells being one of the least likely to transform, either spontaneously or via treatment by carcinogens(25). Furthermore, immortalization is required prior to transformation in culture. A comparison of spontaneous immortalization of fibroblasts by species is summarized as follows: mouse ($>10^{-5}$) >rat (10^{-6}), Chinese hamster (10^{-6}) >> Syrian hamster ($<10^{-6}$) >> human ($<<10^{-10}$) (26). In addition to immortality, transformed cells also possess the ability to grow colonies in soft agar (anchorage-independent growth), grow with minimal growth factor stimulus and can form tumors in nude mice (reviewed in (27)).

Quantitative radiation-induced "malignant transformation" of mammalian cells *in vitro* has been studied in several systems, including mouse 3T3, C3H10T_{1/2} cells and hamster embryo cells. Similar studies with human fibroblast

and epithelial cells have been notoriously unsuccessful, although more recent qualitative studies have met with some success. For such studies with C3H10T1/2 cells, cells are exposed to ionizing radiation (IR), subcultured and viable cells are expanded to confluence. Continued incubation eventually results in the growth of "transformed foci." Implanting sufficient numbers of these into nude mice can then be carried out to test for tumorigenicity. Early studies on C3H10T_{1/2} cells by Little and coworkers and others demonstrated a linearly increasing transformation frequency per viable cell up to about 4Gy X-rays followed by a plateau at around 2.3×10^{-3} transformants/ per viable cell for higher doses (28). Han and Elkind reported similar transformation frequencies, plateauing at $\sim 3 \times 10^{-3}$, in these cells after single X-ray doses, while single neutron doses led to a slightly higher plateau, 6×10^{-3} transformants/survivor (29). Miller and Hall also reported the transformation of these cells by acute and fractionated doses of radiation. Acute exposure produced more transformants per surviving cell at a total dose of ~ 150 rads compared to two split doses totaling 150 rads and given with a 5h interval. However, below this dose the inverse was true (30).

Elkind and coworkers demonstrated that DNA-PK_{cs} deficient SCID cells are more sensitive and show an enhanced IR-induced transformation frequency compared to C3H 10T1/2 mouse fibroblast cells (31).

Borek and coworkers, using transfection of DNA from cells transformed in vitro by X-irradiation, demonstrated that transformation resulted from genetic changes(32).

One major criticism of the C3H 10T1/2 and 3T3 cell systems first studied by Heidelberger (33) and (34) is that the cells are not 'normal' to begin with. They are, in fact, immortalized and tetraploid and contain perhaps several other unknown alterations. Immortalization, it appears is required as a separate step along the pathway to transformation in human cells (reviewed in (35))

Spontaneous *in vitro* transformation of normal human cells occurs at a frequency $\ll 10^{-10}$ (26). Early reports on the transformation of human diploid fibroblast cell lines, spontaneously or by chemical treatment or IR exposure, initially appeared successful, but almost all were later shown to be inaccurate and often due to contamination of cultures by other cell lines, reviewed in (25).

Prior immortalization of cell lines using viral vectors, including SV40, Epstein Barr, adenovirus and HPV, oncogenes (myc) or human telomerase reverse transcriptase (hTERT), greatly enhances the transformation frequency of human cells by IR. For example, Riches, *et al*, reported the radiation-induced transformation of a human thyroid epithelial cell line, HTori-3, that was previously immortalized by SV-40. They observed tumors in up to 80% of the nude mice transplanted with HTori-3 cells exposed to single or fractionated doses of ^{137}Cs γ -rays. Nude mice transplanted with HTori-3 cells exposed *in vitro* to single doses of 0.5, 1.0, 2.0, 3.0 and 4.0Gy yielded tumors in 40, 67, 53, 33 and 46% of the mice, respectively, compared to tumors developing in 9% of mice transplanted with unirradiated control cells. Mice transplanted with cells receiving three equal doses of 1 (75% of mice), 2 (80%) or 3Gy (83%) also yielded tumors. However, no excess tumors were seen in mice receiving cells given three fractions of 0.5

(20% of mice) or 4Gy (0%) compared to mice transplanted with unirradiated control cells (11%) (36). Similarly, SV-40 immortalized 267B1 human prostate epithelial cells were transformed by exposure to 30Gy X-irradiation in 2Gy fractions (37)

Human epithelial cells immortalized by transfection of hTERT were transformed after exposure to fractionated doses of γ -radiation. Control cells retained a diploid karyotype while cells exposed to 10x2Gy fractions became hypodiploid, exhibiting loss of Chr. 13 and amplification of 10p11.2. Cells exposed to 15x2Gy fractions were nearly tetraploid and contained derivative chromosomes. Anchorage-independent growth and serum-independent growth were detected in clones isolated from the cells exposed to higher doses. The authors were unable to isolate anchorage-independent growing clones after 1x2 up to 5x2Gy fractions (38).

In vivo Response to IR Exposure

Not long after the discovery of X-rays by Roentgen in 1895, their oncogenic potential was realized. The death of Thomas Edison's assistant, Mr. Daly, was due to cancer apparently induced by X-ray exposure from one of Edison's inventions ((39) (40) cited in (41)). The deaths by leukemia of Marie Curie, who discovered radium, and her daughter Irene, are believed to have been due to the radiation exposure they received during their work (cited in (42)).

Radiation is a double-edged sword. It can induce cancer and can be used to treat patients with cancer at the same time. Medical treatment of benign and

malignant diseases, using IR, has further demonstrated its oncogenic properties. Treatment of ankylosing spondylitis led to increased levels of leukemia, along with lung, esophageal and stomach cancer (reviewed in (43)). Treatment of tinea capitis (ringworm) by IR in childhood led to increased levels of skin cancer, along with thyroid and brain cancer in patients (reviewed in (43)). Children receiving radiation therapy for enlarged thymus were at elevated risk for thyroid, breast and skin cancer (reviewed in (43)). Numerous studies link the occurrence of second cancers to radiation therapy of primary cancer. These include leukemia, breast, colon, bone and thyroid, among others (reviewed in (43)).

The most important source of information on the *in vivo* effects of whole-body IR exposure has been the studies of the Japanese atomic bomb survivors. The major late effect of exposure has been an increase in certain cancers, especially leukemia and breast cancer(44).

Initial Effects of Radiation

Chromosomal Aberrations

Ionizing radiation exposure to cells *in vitro* and *in vivo* has been shown to produce dose-dependent increases in chromosome-type and chromatid-type aberration frequencies in the first post-irradiation mitosis. The cell cycle phase at which the exposure occurs has a great influence upon the types of aberrations seen in the next mitosis. Metaphase and G₁ or G₀ cells irradiated prior to DNA synthesis are found to contain predominantly chromosome-type aberrations,

including centric and acentric rings (intrachanges), terminal deletions, dicentric chromosomes and reciprocal translocations (inter-changes). A low frequency of chromatid aberrations, mainly gaps and breaks, can also be found in these cells. However, cells irradiated during S-phase or G2 contain elevated frequencies of chromatid-type aberrations, including chromatid exchange aberrations. It is important to note that chromatid-type aberrations can only be produced in the cell cycle immediately prior to mitotic analysis; otherwise, in subsequent cell divisions they will appear as derived chromosome-type aberrations.

Mutations

Spontaneous mutation frequencies in cultured mammalian cells have been measured for several gene loci. These include, for example, hypoxanthine-guanine phosphoribosyltransferase (*hprt*), adenine phosphoribosyltransferase (*aprt*) and thymidine kinase (*tk*). In general, spontaneous mutation rates for these genes in human cells are in the range of 10^{-6} - 10^{-8} mutations/locus/cell generation (reviewed in (12;13)). For example, background frequencies for *tk* and *hprt* mutations of $2-6 \times 10^{-6}$ were determined in human lymphoblastoid TK6 cells by Liber and coworkers (45). It should be noted that the majority of these spontaneously occurring mutations are point mutations, for instance, as shown for *hprt* mutants in lymphoblastoid human cells (46). Radiation-induced mutation frequencies at these loci have also been measured. For example, the average mutation frequency for the HPRT locus is approximately 2×10^{-7} per rad (47) and $1-5 \times 10^{-7}$ per rad for TK (45) (reviewed in (47)).

The kinds of mutations produced by ionizing radiation include detectable insertions and deletions, large genomic rearrangements (intergenic mutations) and point mutations (intragenic mutations).

Point mutations including base substitutions and frameshifts, as well as small deletions, were induced in the APRT locus of D422 *aprt* hemizygote CHO cells by exposure to 5Gy ^{137}Cs γ -rays. (48). In this system, of course, only null mutations (APRT⁻) can be isolated because selection, using 8-azaadenine, is toxic to cells containing the normal *aprt* gene.

Large genetic changes, especially deletions, at the HPRT locus have been induced by ionizing radiation exposure of V79 hamster cells (49) and in TK6 human B lymphoblastoid cells given multiple low doses (50).

The development and use of the A_L human-hamster hybrid cell line and the Thymidine kinase (TK⁺) system has allowed for more sensitive measurement of radiation-induced mutagenesis. The A_L system, developed by Waldren, *et al.* (51) uses a human-hamster hybrid cell containing a single copy of human chromosome 11 (h11). Several identifiable markers are present on the h11 chromosome and their presence or absence can be readily detected. Using this system, they have shown that mutant yield after exposure to X-radiation is not linear with very low doses and that the mutant yield per unit dose is ~200x higher than mutation assays for X-linked loci (52). Similarly, higher radiosensitivities for autosomally linked TK⁺ cells have been reported.

Comparisons of LET effects on mutation frequencies have been performed on a number of cell lines. Brown and Thacker isolated spontaneous, γ -ray, α -particle

and EMS-induced HPRT mutants from V79-4 hamster cells and determined that 70% of the IR-induced mutants resulted from large deletions while the spontaneous and EMS-derived mutants resulted from point mutations (53) (49). Alpha-particle irradiation of the TK⁺ TK6 and WTK1 human B lymphoblastoid cells was done by Amundson, *et al.* (54). The WTK1 cell line was less sensitive to IR exposure for survival but more susceptible to mutation at both the TK and HPRT loci compared to the TK6 cell line. Furthermore, the WTK1 line is much more mutable at the HPRT locus than at the TK locus after α -particle exposure. The authors attributed these results to the possible presence of an error-prone repair pathway that may not be present in the TK6 line and to the presence of a mutation in the p53 gene in the WTK1 line. This mutation might hinder the WTK1 cells ability to undergo p53-induced apoptosis, thereby leading to increased survival. In general, high LET radiation induces more mutants per mean lethal dose than low LET radiation (55).

Delayed Effects of Radiation in Cells

Radiation-induced Transmissible Genomic Instability in Mammalian Systems

A growing body of evidence indicates that a phenomenon of transmissible genomic instability can be induced in the progeny of cells surviving exposure to various ionizing radiations. Studies leading to this conclusion evolved out of the desire to examine the kinetics of radiation-induced *in vitro* transformation of mouse C3H 10T1/2 cells by Kennedy and Little (56). This transformation appeared to involve two distinct events, the first being a high frequency event

resulting directly from the exposure, the second a rare event occurring many generations after exposure and leading to the actual transformation (reviewed in (57)). This then led to the hypothesis that radiation induced a persistent transmissible genetic instability that enhanced the rate at which transformed cells arose in the progeny of the population (57). Several endpoints of radiation damage subject to this 'instability' phenotype have been studied to date. These include the appearance of delayed chromatid-type and chromosome-type aberrations, delayed gene mutations, delayed lethal mutations (also known as delayed reproductive death), delayed apoptosis, micronuclei formation, microsatellite instability and gene amplification. The high frequency in which these events have been reported to occur, up to 1 in 3 surviving cells for some of the induced chromosomal instabilities, at survival levels of 20-70%, seems to rule out the possibility that one or more "genome stability genes," such as a repair gene, would be mutated initially. The relationship between IR-induced genomic instability and IR-induced carcinogenesis has yet to be established, although, models have been proposed. Ullrich and Ponnaiya suggest that radiation-induced chromosomal instability in mammary epithelial cells might be a critical early event associated with the initiation of mammary cancer in BALB/C mice due to IR (58).

Delayed Chromosome Aberrations

Radiation-induced genomic instability has been reported as the delayed appearance of chromosomal aberrations in the progeny of cells surviving high

and low LET exposure. For purposes of discussion I have categorized these studies into two groups; the first involving cells that were initially "normal," or assumed to be normal and the second with cells that were in some respect abnormal at the onset. For ease of comparison, this second category also includes reports that analyzed apparently normal and abnormal cell systems under the same conditions. An overall comparison of cell systems detailed in the following sections is given in Table 1-1 and illustrated in Figure 1-1.

Studies Involving Apparently Normal Cells:

Research by Wright and Kadhim and their coworkers using apparently normal cells began in 1994. This group looked at individual clones from cells surviving irradiation and reported the induction of chromosomal instability in human bone marrow cells after exposure to 0.25 and 0.5Gy of α -particles. This was indicated by the appearance of non-clonal chromatid aberrations in G-banded metaphases from the clonal descendants of cells surviving exposure. Of four human subjects studied, only one unirradiated control colony from subject 1 contained an aberration in 1 of 49 metaphases analyzed from seven colonies. The phenomenon of induced chromosomal instability was detected in only two of the four subjects. Colonies from subject 1 had 0 aberrations in 37 cells from 6 colonies isolated after exposure to 0.5Gy. Analysis of clones from subject 2 colonies showed 3 of 8 colonies contained 10 metaphases with aberrations in 104 scored metaphases after 0.25Gy exposure. After 0.5Gy, 2 of 4 colonies contained aberrations of which 5 metaphases contained aberrations out of 20

Table 1-1

Comparison of systems used in reported radiation-induced instability research and described further within this text. Systems are compared based on normalcy of system, any known abnormalities, radiation used and whether or not instability was induced. For brevities sake, endpoints are not included.

Notes:

^a systems are defined as normal if they are non-immortal, did not derive from tumors, display wild-type radiosensitivity and contain no known DNA damage repair deficiencies, mutated tumor suppressor genes or activated oncogenes and display a stable karyotype

^b ? indicates systems where normalcy is not given or known although apparently healthy donors may have been used

^c apparently refers to systems where one or more characteristics of normalcy have been shown to exist with no abnormal characteristics present from 5 colonies isolated after exposure to 0.25Gy and 0 aberrations in 42 cells

Cell System	Normal ^a	Abnormality	Radiation used	Radiation-induced instability?	Reference no.
CBA/H murine bone marrow cells	No	Radiation-sensitive	X-rays, ²³⁹ Pu alpha-particles	Yes (alpha)	111
Human bone marrow cells	?		²³⁹ Pu alpha-particles	Yes (2 of 4 subjects)	59
CBA/H murine haemopoietic cells	No	Radiation-sensitive	²³⁹ Pu alpha-particles	Yes	67
DBA/2 murine haemopoietic cells	No	Radiation-sensitive	²³⁹ Pu alpha-particles	Yes	67
G57BL/6 murine haemopoietic cells	Appar. ^a		²³⁹ Pu alpha-particles	No	67
HF19 human lung fibroblasts	Appar.		X-rays, alpha, neutrons	Yes	60
HF12 human lung fibroblasts	Appar.		X-rays, alpha, neutrons	No	60
Human T-lymphocytes	?		³ He ²⁺ particles	Yes	61
GM10115	No	Human-hamster hybrid	X-rays	Yes	68
Human skin fibroblasts	?		Various heavy ions	Yes	62
Human T-lymphocytes	?		X-rays	Yes	64
V79 Chinese hamster lung cells	No	Immortal	X-rays	Yes	71
Human TK6 B-lymphoblastoid cells	No	Tumor-derived, immortal	X-rays, gamma rays	Yes	72
MCF10A human mammary epithelial cells	No	Immortal	X-rays, neutrons	Yes	73
BALB/c murine mammary epithelial cells	No	DNA damage repair deficient	Gamma-rays	Yes	74
C57BL/6 murine mammary epithelial cells	Appar.		Gamma-rays	No	74
Chinese hamster ovary (CHO) K-1 cells	No	P53 mutant, immortal	X-rays, alpha-particles	Yes	16
CHO K-1 cells	No	P53 mutant, immortal	UV	Yes	77
CHO K-1 cells	No	P53 mutant, immortal	X-rays	Yes	79
CHO K-1 cells	No	P53 mutant, immortal	Alpha-particles	Yes	16
EJ30 human epithelial cells	No	Tumor-derived, immortal	Gamma-rays	Yes	60
V79 Chinese hamster lung cells	No	Immortal	X-rays	Yes	63

Cell System	Normal*	Abnormality	Radiation used	Radiation-induced instability?	Reference no.
CHO K-1 cells	No	IP53 mutant, immortal	Gamma-rays	Yes	84
CHO cells	No	Immortal, transformed	X-rays	Yes	85
BALB/3T3 murine fibroblast cells	No	Radiation-sensitive	X-rays	Yes	85
V79 Chinese hamster lung cells	No	Immortal	X-rays, alpha-particles	Yes	88
Human embryo cells	?		X-rays	Yes	81
AG1522B human foreskin fibroblasts	Appar.		X-rays, ²³⁸ Pu alpha-particles	Yes	82
C3H 10T1/2 cells	No	Immortal, transformed	X-rays	Yes	89
CBA/Ca mice	No	Radiation-sensitive	Gamma rays (low dose rate)	No	95
HF19 human lung fibroblasts	Appa.		Auger electrons (125I)	No	93
CBA/H murine bone marrow cells	No	Radiation-sensitive	²²⁴ Ra alpha-particles	No	97
WTK1 human B-lymphoblastoid cells	No	Tumor-derived, immortal	Gamma-rays, ⁵⁶ Fe	No	109
AG1521A human foreskin fibroblasts	Appa.		Gamma-rays, ⁵⁶ Fe	no	Current study






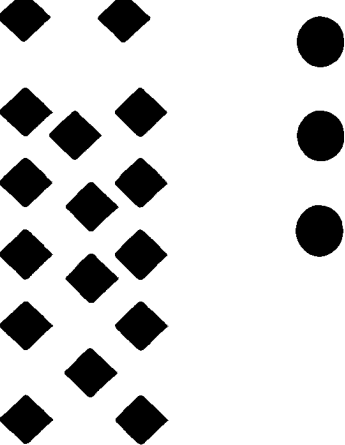

<u>Normal</u>		 
<u>Not established</u>		
<u>Abnormal</u>		
	<u>Induced Instability</u>	<u>No Induced Instability</u>

Figure 1-1

Comparison of the frequency of reports showing radiation-induced instability in rodent initially normal (◊), not established (◊) or initially abnormal (◆) and human initially normal (○), not established (⊕) or initially abnormal (●) cell systems as reviewed in Table 1-1.

scored. Subject 3 colonies had no metaphases containing aberrations in 54 total scored metaphases from 0.25Gy irradiated cells (2 colonies) or 0.5Gy-irradiated cells (3 colonies). Finally, subject 4 clones also contained metaphases with aberrations in colonies isolated after 0.25 and 0.5Gy exposures. After 0.25Gy exposure 2 of 5 clones contained a total of 6 metaphases with aberrations in 32 scored cells and after 0.5Gy 1 of 3 clones contained 4 metaphases with aberrations out of 37 scored cells. In subjects 2 and 4 60-75% of the aberrations were chromatid-type, with higher percentages seen in both cases in the cells from colonies isolated after 0.5Gy (59). It would appear that the aberration data given is for the colonies containing aberrations and not for all colonies scored. This report indicates that genetic variation most likely contributes to the induction of chromosomal instability by α -particle irradiation of human bone marrow cells.

This group expanded their efforts to the study of early passage apparently normal human diploid fibroblasts. Mixed surviving populations of HF19 normal human lung fibroblasts exposed to 1.5Gy X-rays, 0.5Gy neutrons or 0.4Gy α -particles showed persistent levels of 'unstable aberrations' (defined as including chromatid breaks, chromatid exchanges, chromosome fragments and minutes) from 3 to 35 population doublings post-irradiation. It was noted that a decrease in the percentage of aberrant cells was seen at 20 doublings after X-rays exposure followed by an increase at 35 generations. Control populations for the HF19 cell line contained from 2-6% aberrant cells, while irradiated populations contained from 20-40% aberrant cells. However, HF12 lung fibroblasts did not demonstrate radiation-induced instability after the same treatments as indicated by a decrease

in the percent aberrant cells from 3 to 35 generations in mixed surviving populations derived from irradiated cells (60).

This group then went on to demonstrate the induction of chromosomal instability in the progeny of human T-lymphocytes surviving exposure to only one α -particle from an α -particle microbeam. This was measured by an increase in chromatid-type aberrations 12-13 generations after exposure. Control samples from three experiments contained an average of 11.7 \pm 1.9% metaphases with aberrations, however, for irradiated cells, 22.0 \pm 2.4% of the metaphases contained aberrations, 86% of which were chromatid-type (61).

Studies on the induction of chromosomal instability in apparently normal human fibroblasts following irradiation with various heavy ions were carried out by Martins and coworkers (62). Non-cycling G0 human skin fibroblasts from a young donor were irradiated in the 19th passage after culture initiation with either neon (E = 10.74 MeV/ μ , LET = 386 keV/ μ m, fluence = 10⁶, 2x10⁶ or 4x10⁶ particles/cm²), argon (E = 10.52 MeV/ μ , LET = 1207 keV/ μ m, fluence = 10⁶, 2x10⁶ or 4x10⁶ particles/cm²) or lead (9.5MeV/ μ , LET = 13,600 keV/ μ m, fluence = 2x10⁶ particles/cm²) and metaphase cells from different post-irradiation passages were analyzed by R-banding. Twenty metaphases from non-irradiated cultures were analyzed and all were classified normal at the 20th passage after culture initiation. The investigators found elevated levels of non-random chromosome aberrations, mainly dicentrics, occurring around passage 20-25. These aberrations involved the telomeric regions of 13p, 13q, 1p, 16p and 16q. They also noticed that the radiation prolonged the lifespan of the cells, but did not

necessarily immortalize them (62). In a later report the researchers indicated that in chromosomally unstable populations, there were large variations in telomere-probe hybridization signals and no telomeric sequences detectable at the junctions of end-to-end associations, despite a lack of shortening of the mean telomere length measured by Southern blotting (63).

Holmberg and coworkers (64) demonstrated the appearance of radiation-induced chromosomal instability in the clonal progeny of human T-lymphocytes exposed to 3Gy of X-rays. Metaphase spreads from increasing numbers of days in culture were collected and analyzed by G-banding. Six non-irradiated clones were analyzed 2-4x from 19-69 days after isolation. The frequency of sporadic aberrations (defined as chromatid and chromosome breaks and rearrangements) ranged from 4-11% in the clones. Three irradiated clones were studied 4-7x between days 16 and 62. Sporadic aberrations occurred in many of the cells analyzed from these clones. In clone XI2, 25 cells out of 143 total cells analyzed contained sporadic aberrations. Similarly, in clone XI8 28 of 155 cells contained these types of aberrations and in clone XI9 43 of 130 cells did. They also observed the occurrence of clonal and subclonal (three or more cells in a specific cell clone having the same aberration) karyotypic abnormalities in the clonal progeny of X-irradiated cells (64).

Studies Involving Abnormal Cells:

In one early study, irradiated one-cell mouse embryos were analyzed during subsequent mitoses for chromosome aberrations. A consistent decrease

in aberration frequency was found from the first to second and third mitosis after X-irradiation, but not after neutron irradiation. In that case an increase was found from the second to the third mitosis (65).

Research on transmissible chromosomal instability by Wright and Kadhim and their laboratory coworkers at the MRC Radiobiology Unit in the UK began in 1992 using murine bone marrow cells. They analyzed individual clones from surviving irradiated cells and reported seeing increased levels of non-clonal chromatid-type aberrations in CBA/H murine bone marrow cells many generations after exposure to α -particle irradiations from 0.25 to 1Gy. However, they did not see the same effect after 3Gy X-irradiation. In the control colonies, only 7 of 59 colonies contained aberrations. In 432 scored metaphases, a total of 7 aberrations were seen and all were chromatid-type. Two of 86 colonies isolated after 3Gy X-rays contained a total of 4 different aberrations in 409 cells. In the α -particle irradiated samples, 12 colonies out of 27 total colonies scored contained a total of 79 aberrations in 228 scored metaphases. The majority of these aberrations were chromatid-type (53/79) (66).

Additional work by this group further demonstrated the effect of genetic variation on the induction of chromosomal instability by α -particle irradiation. Haemopoietic cells from radiation-sensitive CBA/H and DBA/2 mouse strains exposed to 0.5Gy of α -particle irradiation expressed chromosomal instability indicated by the appearance of increased frequencies of non-clonal aberrations, mostly chromatid-types, in cells from colonies isolated ~13 generations after exposure of bone marrow suspensions. In CBA/H mouse cells, 16 of 26 colonies

derived from exposed cells contained aberrant cells of which 9.7% of the metaphases analyzed (31/321) contained aberrations as compared to only 2 of 10 unirradiated control colonies containing a total of 2 aberrant metaphases in 143 scored, or 1.4%. In DBA/2 mouse cells, 14 of 23 colonies from irradiated cells contained aberrant cells of which 35 out of 335 scored metaphases, or 10.5%, contained aberrations compared to 4 of 18 colonies with aberrant cells and 4 of 213 metaphases or 1.9% from unirradiated control colonies. However, colonies from non-radiation sensitive C57BL/6 cells had much lower relative increases between irradiated and controls. In 5 of 26 colonies from irradiated cells, 11 of 312 metaphases, or 3.5%, contained aberrations compared to 1 of 16 colonies and 1 of 145 metaphases, 0.7%, from unirradiated control cells.. Furthermore, F1 progeny of these strains (C57BL/6 x CBA/H and C57BL/6 x DBA/2) indicated that resistance to the induction of chromosomal instability was a dominant trait. Finally, the authors indicated a correlation between superoxide generation and inducible chromosomal instability (67).

Research done by Morgan and his collaborators at UCSF has focused on the induction of chromosomal instability in a hamster-human hybrid cell line, GM10115, which contains a single copy of human chromosome 4 in a hamster background. Populations of cells derived from single cell clones surviving exposure to 5 or 10Gy of X-rays were analyzed using FISH with a human whole chromosome 4 FISH painting probe. In their studies they defined chromosomal instability as a cell that produced a colony containing two or more metaphases with rearrangements involving the h-4 chromosome in a total of 200 cells scored.

In five primary control colony isolates, no metaphases containing aberrations involving the h-4 were seen with 200 mitotic cells scored per clone. Three of six clonal isolates from irradiated cells from the first exposure to 10Gy showed delayed chromosomal instability by the above definition. Furthermore, the three clones showing delayed instability also yielded clonal populations with decreased plating efficiencies compared to the cell populations derived from other clones from irradiated cells. A second round of subcloning was then done. In this round, cells from each of the control and 10Gy-irradiated clones were exposed to an additional 0, 5 or 10Gy X-rays and recloned. Control clones derived from the original control clones continued to remain stable. In two subclones from the original C4 control, one aberration was seen in each clone. However, 4 out of 14 subclones derived from the exposure of initial control clones to 5Gy X-rays and 10 of 15 subclones derived from the exposure of initial control clones to 10Gy X-rays, showed delayed chromosomal instability. Subcloning of initially isolated clones from cells surviving exposure to 10Gy of X-rays indicated continued instability in two of the initial clones, designated X2 and X4, instability in one of three subclones from X1 (previously labeled stable) and a lack of instability in two subclones from X5 (previously labeled unstable). This X5 clone had only two aberrant metaphases in the initial 200 scored and therefore, it seems likely that isolating only three subclones could readily omit any aberrant cells from the initial clone. Finally, clonal isolates from cells surviving a second 10Gy exposure showed a reduced level of chromosomal instability compared to those from a single exposure(68).

Further work by this group using the GM10115 human-hamster hybrid cell demonstrated that the “kinds” of DNA double strand breaks are important in initiating the phenotype of induced chromosomal instability and not just DNA strand breaks in general. This was illustrated by the results that showed restriction enzyme cutting of DNA (a clean process) did not induce instability, while IR and a number of strand-breaking chemicals did. Here their criteria for the induction of instability was narrowed to three or more distinct metaphase subpopulations involving the rearrangement of the human chromosome 4 in 200 scored metaphase cells (69). They also demonstrated that in GM10115 human-hamster hybrid cells, an induction of chromosomal instability occurred at a rate of 3% per Gy of X-rays and a maximum frequency of ~30% was reached (70).

Jamali and Trott demonstrated a persistent increase in dicentric aberrations in V79 cells surviving exposures between 3 and 12Gy X-rays. Dicentric levels in unirradiated cells from 1-14 days after irradiation remained fairly constant around 0.025 dicentrics/cell, while levels in irradiated cells dropped from initially high, dose-dependent levels to persistent levels about 5x greater than in controls. Furthermore, a persistent increase in the level of apoptosis was detected in these same cultures (71).

Grosovsky and coworkers, studying non-normal, karyotypically stable (47, XY, +13, 14q+, 21p+), tumor-derived TK6 human B-lymphoblastoid cells, reported that up to 30% of the clones of cells surviving a dose of 2Gy X or γ -irradiation contained karyotypic heterogeneity. This was defined as a clone containing “two or more distinct metaphases, exhibiting non-identical

chromosomal abnormalities" in 10-20 G-banded metaphase spreads analyzed 50-60 generations after irradiation. No karyotypic heterogeneity was observed in unirradiated controls (72).

Ullrich's group at UTMB-Galveston investigated the induction of chromosomal instability in human MCF10A mammary epithelial cells after exposure to 0.43 MeV neutrons and ^{137}Cs γ -rays. MCF-10A cells are an immortalized cell line and arose spontaneously from fibrocystic breast tissue (cited in (73)). While they are not normal, they are also nontumorigenic and have a stable karyotype (48, XX, 3p-, 6p+, +8, 9p+, +16) (58). Near confluent cultures were trypsinized, pooled and either irradiated or held for controls. Cells were then plated onto collagen-coated dishes and incubated. Pooled populations of cells were analyzed every 5 generations after exposure for chromatid aberrations. Chromatid aberration frequencies per cell ranged from 0.02 to 0.06 in control populations for the neutron experiments and from 0.01 to 0.07 in control populations for the ^{137}Cs experiments. For 0.2Gy neutron-irradiated populations, initially elevated levels of chromatid aberrations (mainly gaps) persisted for the first 15 population doublings. After this, an increase was seen at 20-25 population doublings followed by some fluctuation in frequencies and an apparent increase in the later collections. A persistently elevated level (~1.5x background) was seen throughout the collection times. Increasing the dose to 0.4Gy appeared to have no additional effect. A slightly different effect was seen in the γ -irradiated populations. Initially low frequencies, similar to background, were detected in irradiated populations. These then increased with each

collection, peaking at 20 population doublings and then decreased to near background at 40 doublings (73). This group also demonstrated the genetic susceptibility of some mouse strains over others to radiation-induced chromosomal instability and to cancer induction. BALB/c mice are highly sensitive to radiation-induced mammary cancer and are susceptible to radiation-induced chromosomal instability after exposure to ^{137}Cs γ -rays measured by an increased frequency of chromatid-type aberrations 16 generations after exposure (74). Furthermore, cells from the BALB/c mouse have been shown to contain two polymorphisms in the gene encoding DNA-PK α , a protein required for non-homologous end-joining repair of DNA damage (75). C57BL/6 mice do not contain these polymorphisms and are not susceptible to either radiation-induced mammary cancer or chromosomal instability (75) (74).

Ullrich and Davis demonstrated that chromosomal instability could be induced *in vivo* after a whole-body irradiation dose of 3Gy ^{137}Cs γ -rays given to BALB/c mice. Mammary epithelial cells were removed from animals at various times after exposure and then cultured for 28 population doublings. Unirradiated control cells were isolated from animals of a similar age and maintained an aberration frequency near 0.1/cell throughout the culture. Cells isolated after 1, 4 and 16 weeks post-irradiation had persistently elevated aberration frequencies from 5 to 28 doublings and were on the order of 2.5-3.5x background. Cells isolated 24h after exposure showed elevated aberration frequencies at 5 doublings followed by a decrease to background by 10-15 doublings and then an increase to levels found in the other irradiated samples. Furthermore, they

demonstrated the occurrence of a dose effect for this system below 1Gy ^{137}Cs γ -rays and that fractionated dosage decreased the level of induced instability (76).

Research done on Chinese hamster ovary (CHO K-1) cells by Little and coworkers demonstrated that *Hprt* mutant clones from cells exposed to X- or α -particle irradiation and selected for slow-growth phenotype, were chromosomally unstable and contained non-clonal chromosome and chromatid-type aberrations (16).

Delayed mutations

Mutation of mammalian cells was assumed to occur within the first or second cell generation after exposure until the induction of delayed mutations in CHO cells was demonstrated by Stamato and colleagues after treatment with ethyl methyl sulfonate (EMS) (77) and later with UV-light (78).

Studies Involving Apparently Normal Cells:

No literature is cited in this section for cells that were apparently normal at the outset.

Studies Involving Abnormal Cells:

As mentioned above, work by Stamato and colleagues demonstrated that delayed mutations could be induced in the progeny of cells surviving exposure to a mutagenic agent. Treated or exposed cells that survived were grown into colonies and tested for X-linked glucose-6-phosphate dehydrogenase (G6PD)

activity by staining with nitroblue tetrazolium. Wild-type cells (functional G6PD⁺) stain dark blue, while mutants (G6PD⁻) have little or no staining. Some of the EMS-treated cells showed sectorized colonies that allowed for estimating the number of cell divisions in a colony from the origin of the mutation. If the original cell was a mutant, the entire colony stained white. If one of the daughter cells of the first division was a mutant and the other not, the colony was half white and half blue, and so on. Some clones could be seen where 1/16 of the cells were white and 15/16 of the cells were blue, clearly indicating the mutation occurred in a cell four generations after treatment. By further subculturing cells, they showed the mutational events occurred over a period of 10-14 generations after exposure (77).

In 1990, Little and coworkers reported that mutations at the hprt locus of CHO cells might be delayed 6-7 generations after exposure to X-rays. They also presented results showing the occurrence of delayed lethal mutations up to 30 generations after exposure. This was measured by reduced cloning efficiency amongst the progeny of surviving cells (79). Additional work on this phenomenon indicated that 8-9% of clones analyzed after exposure to X-rays or α -particles showed evidence of delayed mutations at this loci. Furthermore, the spectrum of delayed mutations was similar to that of spontaneous mutations, only at a higher frequency, 10^2 - 10^4 -fold above background. Whereas 75% of initial radiation-induced mutations involved partial or total gene deletions, less than 25% of the delayed mutations were of this type (16).

Loucas and Cornforth eliminated HPRT⁻ mutants produced directly in irradiated surviving EJ30 human tumor-derived epithelial cells after exposure to 4Gy ¹³⁷Cs γ-rays by incubation in HAT medium after irradiation, which kills HPRT⁻ mutants by blocking endogenous purine synthesis. They then selected for 6 thioguanine (6TG) resistant colonies (HPRT⁻ mutants) in medium containing 6TG (non-HAT). Their results indicate that a significant proportion of the HPRT⁻ mutants induced by IR were not caused by the direct effect of the exposure, but by a delayed effect (80).

Delayed lethal mutations/Delayed reproductive death

Delayed lethal mutations, also known as delayed reproductive death, has also been shown to be a late effect in cell cultures after exposure to ionizing radiation. It is characterized by the appearance of small-sized colonies and decreased plating efficiencies in cells surviving exposure and by the inheritance of these traits in their progeny compared to unirradiated control cells.

Studies Involving Apparently Normal Cells:

Suzuki and coworkers reported the occurrence of delayed reproductive death along with giant cell formation, chromosome bridges and micronuclei in the clonal progeny of normal human embryonic fibroblast-like cells surviving exposure to 6Gy X-rays. Primary clones (from initially irradiated cells and unirradiated control cells), secondary clones (from primary clones expanded for ~16-17 generations) and tertiary clones (from secondary clones expanded for a

total of 28-30 generations) had an average cloning efficiency of 16.4% while similar cloning of cells surviving irradiation had an average cloning efficiency of 7.2%, which persisted for over 40 generations after exposure (81).

Belyakov and coworkers reported micronuclei, apoptosis and delayed reproductive death in the progeny of AG1522B normal human fibroblasts surviving exposure to X-rays or α -particles. Delayed cloning efficiency was measured by subculturing cells from 0 to 30 days after exposure for colony formation. In X-irradiated samples, cloning efficiencies remained below controls for up to 14 days after exposure, but then approached background frequencies by 24-30 days after exposure. In α -particle experiments, cloning efficiencies remained below controls even after 30 days in culture prior to cloning (82).

Studies Involving Abnormal Cells:

In 1964 W. Sinclair published a report on small colony formation in cultured mammalian cells (V79 Chinese hamster lung cells) after exposure to X-irradiation. Small sized clones were compared to large size clones isolated at the same time, 13d after exposure. Small colonies showed slow growth, low plating efficiencies (delayed reproductive death) and increased radiosensitivity (83).

Seymour and coworkers reported that CHO K1 and primary sheep and human thyroid cells in colonies of cells surviving exposure to ^{60}Co γ -rays demonstrated reduced plating efficiencies upon recloning, in a dose-dependent manner. They characterized this phenomenon as a heritable lethal mutation occurring several generations after exposure (84). Gorgojo and Little also

reported the occurrence of a dose-dependent decrease in cloning efficiency of CHO K1 and BALB/3T3 cells after exposure to X-rays in populations arising from surviving cells many generations after exposure (85). This phenomenon was shown to be a dominant trait in hybrids of CHO clones. Clones of CHO cells surviving 12Gy X-irradiation were fused to two different 6TG/Oubain resistant CHO clonal cell lines. Reduced cloning efficiency was seen in these hybrids compared to hybrids involving wild-type CHO cells and the double mutants, indicating a dominant-acting trait. Furthermore, the reduced cloning efficiency of the hybrids paralleled the reduced cloning efficiency of the irradiated cell's clonal progeny (86).

Trott and coworkers also described the occurrence of delayed plating efficiencies in V79 cells after exposure to 300kVp X-rays or ^{238}Pu α -particles. Furthermore, they reported elevated levels of micronuclei that were associated with decreased plating efficiencies in the progeny of surviving cells (87) and in clones of cells surviving exposure (88).

Instabilities for Other Biological Endpoints

A number of other biological endpoints have been studied for the induction of instabilities by ionizing radiation. These include minisatellite sequences, giant cell formation and gene amplification. Some of these results are presented here.

Studies involving Abnormal Cells:

Paquette and Little compared the effects of *in vivo* tumor development vs. *in vitro* cell culture on minisatellite sequences of *in vitro* radiation-transformed mouse C3H/10T1/2 cells. They found that genomic instability of these sequences was enhanced *in vivo*, but not by *in vitro* culture, as measured by an increase in genomic rearrangements occurring *in vivo* in the same time frame and numbers of generations as *in vitro* cultures lacking in genomic (89). The relationship of this enhancement of induced instability *in vivo* in transplanted transformed cells and normal tumor development in animals however, has not been fully demonstrated.

Dubrova and coworkers demonstrated an elevated mutation rate at minisatellite loci in CBA/H mouse pre-meiotic spermatogonia after acute whole-body exposure to 0.5 and 1Gy of X-rays (90). The authors also demonstrated an increased minisatellite mutation frequency among children of parents living in the Mogilev area of Belarus, which was heavily polluted after the Chernobyl nuclear reactor accident, compared to control subjects the United Kingdom. The mutation rate was elevated in families where parental doses were higher, consistent with radiation induction of germ-line mutation (90).

Lack of radiation-induced instability

As summarized above, in most instances where radiation-induced genomic instability is consistently and repeatedly demonstrated, the cells tested are either tumor-derived, immortalized, or are already abnormal in some important aspect, such as regarding DNA repair capacity or growth control checkpoint genes. In cases where putatively "normal" cells have been used,

inconsistent results from one cell source to another were generally observed (59) (74) (67) (60).

Studies Involving Apparently Normal Cells:

In vivo measurement of radiation exposure has moved from classical solid staining and chromosome banding to the use of FISH painting due to its higher sensitivity of measuring chromosome aberrations, in particular stable translocations. The background frequency of translocation analysis, measured by FISH painting, is on the order of 10-fold higher than is seen in dicentric analysis. Therefore, increases at low dose levels are more readily detected. Studies using chromosome painting of lymphocyte chromosomes from victims of the Chernobyl accident indicated that the exposure did not lead to increasing frequencies of chromosome translocations in cells from exposed individuals. In 11 of 12 cases translocation frequencies remained constant for samples taken over a three-year period from Sept. 1991 to July 1994. In one case the occurrence of a clonal translocation observed with high frequency was detected and corrected for (91).

Analysis of lymphocytes from subjects exposed during a radiological accident in Tallinn, Estonia, showed mixed results as to induction of chromosomal instability. FISH analysis of *in vivo* samples, indicated no induction of chromosomal instability as measured by G-banded analysis of phytohemagglutinin-A (PHA) stimulated lymphocytes. However, long term *in vitro* culture of lymphocytes led to elevated levels of chromosomal aberrations in cultures from irradiated subjects. However, control subjects also had elevated

levels of chromosomal aberrations after long term *in vitro* culture, but with a lesser degree of complexity, i.e. fewer chromosomes involved in the aberrations compared to radiation exposed subjects (92).

HF19 human lung fibroblasts were exposed to [^{125}I]UdR and chromosomal analysis was performed on bulk cultures from 2 to 39d after treatment. ^{125}I is a low energy, short-range Auger electron emitter that deposits most of its energy within a few nanometers of its decay. The authors demonstrated a continued decrease in aberration frequency with increasing cell generations after exposure, indicating a lack of radiation-induced chromosomal instability (93).

Whitehouse and Tawn analyzed blood lymphocytes taken from radiation workers with internal deposits of plutonium. The samples were obtained between 10 and 20 years after the initial intake and analyzed by Giemsa or fluorescence plus Giemsa staining. The authors reported a decrease in the frequencies of chromatid-type aberrations over the period of the study, indicating a lack of transmissible chromosomal instability, despite increased levels of stable translocations due to continued *in vivo* irradiation of stem cells by internalized plutonium (94).

Studies Involving Abnormal Cells:

Abramsson-Zetterberg and coworkers studied the effects of low dose-rate ^{137}Cs γ -irradiation on micronuclei formation in CBA/Ca mice exposed *in utero*. They found no elevated frequencies of micronucleated erythrocytes, caused by

damage induced in erythroid stem cells, in samples from irradiated offspring taken 36d after birth compared to controls (95).

Martin and coworkers analyzed lymphocytes from a number of radiotherapy patients, who received fractionated doses from 35-80Gy, over a period of eight years after therapy. Samples were obtained and analyzed yearly, beginning with the first year after treatment. As expected, the authors detected a steady decrease in unstable chromosome aberrations; dicentrics and centric rings, although rates were not determined due to high variability in the data. However, no evidence of an increase in stable aberrations and no delayed appearance of dicentrics were seen. Furthermore, chromatid-type aberrations were initially low and remained at low levels throughout the analysis period. The authors interpret these results to indicate a lack of radiation-induced chromosomal instability in these 18 radiotherapy patients and present evidence from other similar studies yielding the same result (96).

Bouffler and coworkers reported the lack of radiation-induced chromosomal instability up to 100 days after exposure in CBA/H mouse bone marrow cells exposed to ^{224}Ra α -particles either *in vitro* or *in vivo*. The authors noted the sensitivity of the experimental system to manipulation as indicated by the presence of elevated yields of aberrations in short term cultures and by transplantation even in unirradiated cells (97).

Mechanism(s) of Radiation-induced Genomic Instability

Currently, no single mechanism has identified as the cause of radiation-induced genomic instability. It is quite possible that several mechanisms exist and are manifested in different endpoints used to describe the phenomenon. The following are some of the proposed mechanisms along with data supporting the theories.

Oxidative stress (superoxide radical)

Oxidative stress is a state where an imbalance exists between prooxidant production (hydrogen peroxide, superoxide, etc.) and antioxidant capacity (catalase, superoxide dismutase, NADPH, etc.). Persistent oxidative stress can lead to oxidative damage of DNA, RNA, proteins and lipids (98).

Sanford and coworkers demonstrated that when C3H mouse cells were incubated at atmospheric O₂ levels, (18%), they showed elevated levels of chromatid breaks and other chromosome abnormalities relative to cells grown at reduced O₂ levels of ~2%. The latter is more typical of oxygen tensions in many human tissues *in vivo*. (99).

It has been demonstrated that cells exposed to elevated levels of superoxide show elevated levels of chromatid-type aberrations (100) (101). Superoxide is converted to oxygen and hydrogen peroxide by superoxide dismutase. H₂O₂ can then be catalyzed by iron yielding more superoxide and hydroxyl radicals, which can further damage DNA.

Wright and coworkers analyzed the progeny of CBA/H mouse bone marrow cells (macrophages and granulocytes) exposed to different ionizing

radiations. They found persistently elevated levels of superoxide production in the cultures derived from irradiated cells compared to control cultures (102). They then carried out experiments to study a possible correlation between superoxide generation and inducible chromosomal instability in haemopoietic cells from radiation and radiation-induced chromosomal instability sensitive CBA/H and DBA/2 mice. Cell cultures from bone marrow samples from these mice were stimulated six days after culturing to produce a burst of superoxide and were analyzed 24 hours later for cytogenetic aberrations. These sensitive mouse strains showed aberrations in 16% of the metaphases studied, the majority of which were chromatid breaks. No such results occurred in resistant C57BL/6 cells analyzed in the same manner (67).

Genetic variability

Several studies clearly indicate a genetic variability in the induction of instability by ionizing radiation. Perhaps the strongest evidence is the work in Ullrich's lab involving mouse mammary epithelial cells. Cells from radiation-induced mammary cancer susceptible BALB/c mice were sensitive to IR-induced chromosomal instability, while non-sensitive C57BL/6 mouse cells were not (74). The evidence here is particularly interesting because, as already noted, they have demonstrated a DNA repair defect in BALB/c involving DNA PK_{cs} that is not present in C57BL or any other strain of mice they examined.

**The Possible Involvement of Telomeric and Telomeric-like Sequences in
Chromosomal Instabilities**

Telomeres are repetitive sequences at the ends of chromosomes. These (TTAGGG)_n repeat sequences, vary in length between species and in somatic cells have been shown to shorten with each round of DNA replication (103). Telomeric-like repeat sequences have been found within chromosomes as discrete bands in several species (104). The involvement of telomeric regions in the formation of dicentric aberrations in senescent human fibroblasts was demonstrated by Benn in both WI-38 and MRC-5 cells (105). Several reports linking telomeric sequences and radiation-induced instability have been published. Dicentrics and telomeric associations found in normal human fibroblast cells many generations after exposure to high LET radiation lacked the associated acentric fragments found in IR-induced dicentrics, indicating telomeric associations. Furthermore, these aberrations lacked a signal for telomeric sequences at the junctions, when analyzed by FISH. The authors proposed that this was due to telomeric shortening in the involved chromosomes (63).

Bailey and coworkers demonstrated that non-homologous end joining (NHEJ) DNA repair proteins are required for capping the ends of mammalian chromosomes to prevent their being identified as random DNA breaks which could lead to end-to-end chromosome fusions (106). Giaccia and coworkers demonstrated that interstitial telomeric sites in BL-10 and HA-1 CHO cells have a high propensity for radiation-induced exchanges (107). Day and coworkers

demonstrated that interstitial telomere-repeat-like sequences were involved in the sites of recombination between human and hamster chromosomes in GM10115 hybrid cells many generations after exposure to X-rays (108).

Schwartz and coworkers demonstrated that chromosomal instability in WTK1 human B lymphoblast cells was caused by telomere shortening and that exposure to IR only increased the number of cells within a clone that contained chromosome alterations, not the types of instability seen (109).

Is There an Emerging Pattern?

It has been demonstrated in numerous publications detailing experiments with a variety of cell and animal systems, that low and high LET radiation can induce a phenomenon of transmissible genomic instability (66), (68), (72), (76). However, it has also been shown that this phenomenon is not universal (59), (95), (97). Furthermore, the inability of researchers to clearly show any definitive mechanism associated with the onset of radiation-induced genomic instability and the conflicting data in experiments using the same cell lines or animal models, led us to propose a broad scoped research project.

Several of the experiments described above used apparently normal cell lines as the basis for analysis. However, most of the work described was done in cell lines that were derived from tumors, or contained alterations in normal DNA repair pathways or tumor suppressor genes. Although it is important and often necessary to study abnormal systems, one might clearly want to determine the responses in phenotypically normal systems, especially if we are trying to prove

the phenomenon is universal. Therefore, we chose to study a phenotypically normal human fibroblast cell line, AG1521 that exhibits normal response to ionizing radiation and has wild-type TP53 (110) and was available in a low passage number.

Chromatid aberrations have been used to describe transmissible chromosomal instability in several reports and yet have little known biological significance. Therefore, we wanted to determine whether an elevated level of chromatid-type aberrations led directly to an increase in the frequency of stable chromosome-type aberrations, which are more relevant since they are found in numerous cancers and genetic diseases.

Finally, although data exists for the induction of chromosomal instability in both pooled populations and clonal descendents of cells surviving exposure to IR, few, if any, compare both systems. Since one or more highly unstable clones could lead to elevated levels of chromatid aberrations in pooled populations of cells, we decided to compare the outcomes of surviving cells in both systems.

Objective of Dissertation

The objective of this dissertation was to determine whether chromosomal instabilities could be induced in normal human fibroblasts exposed to ionizing radiation while in a non-cycling G0 phase. In most cell renewal tissues the majority of cells exist in a G0 state, they are not in a 100% cycling state. These cultured G0 cells were exposed to equitoxic doses ^{137}Cs γ -rays at CSU or to 1 GeV/nucleon ^{56}Fe particles at Brookhaven National Laboratory's Alternating Gradient Synchrotron. The doses of ^{56}Fe nuclei were chosen to give an average of 1 particle traversal per cell nucleus.

Chapter two details the efforts undertaken to detect radiation-induced chromosomal instability in pooled populations of cells kept in continuous log-phase culture after exposure to γ -radiation or ^{56}Fe particle irradiation. Cell populations were analyzed at regular intervals for the presence of chromatid-type aberrations by Giemsa staining of mitotic cells. Chromosomal instability was deemed to have been induced if a statistically significant increase in chromatid-type aberrations was seen at any analysis point. To meet the criteria of induced instability, this increase needed to be higher than that from background levels in parallel samples of unirradiated cells and higher than that from earlier sample times. Since it is known that chromatid-type aberrations can become derived chromosome-type aberrations, we then compared early post-irradiation generation cells against late post-irradiation generation cells for the presence of new stable translocations that might have arisen from earlier chromatid symmetrical interchanges. This was done using a multi-probe, two-color FISH

analysis involving chromosomes 1-5. Some of these populations were also analyzed for all scorable aberrations using multiplex FISH, which uses a combinatorial labeling scheme involving five different fluorochromes and computer imaging software to pseudocolor the 22 pairs of homologues and the X and Y-chromosomes into distinguishable colors. Chromosomal instability was deemed to have been induced if a significant increase in aberrations was found in later generations compared to earlier samples and the increases were significantly above any that occurred in the unirradiated cultures. The possible occurrence of clonal expansion, if detected, needs to be corrected for here in order that all the aberrations scored are newly arising aberrations not found in the first generation irradiated cells.

Chapter three deals with the efforts to detect instability in numerous individual clones, each derived from a single isolated cell surviving the same exposures as for the studies detailed in Chapter two. This study was carried out using a single color. multi-probe combination for FISH whole chromosome painting of chromosomes 1, 2, 4 and X and analysis of mitotic cells 20-25 generations post-irradiation. Clones were classified as unstable if in 30-50 cells scored 3 or more different karyotypic subpopulations were observed involving either structural or numerical aberrations or a combination of both types.

The final chapter (four) describes the cytogenetic analysis of a Nijmegen breakage syndrome (NBS) fibroblast cell line, GM7166, exposed to ^{137}Cs γ -rays and compared to the normal human fibroblast line used above, AG1521. NBS patients are highly sensitive to IR and are predisposed to lymphoma and

leukemia. First post-irradiation mitotic cells were scored for chromatid-type and chromosome-type aberrations using solid Giemsa staining. These cells were also analyzed for complex exchange aberration frequencies using mFISH analysis. This study was initiated with one purpose being to compare induced instabilities in a repair deficient human cell. While the comprehensive instability study was not possible in this time frame, the initial characterization was felt to be worth including.

CHAPTER 2

Chromosomal Instability in Mixed Populations of Surviving Low Passage Normal Human Fibroblast-derived AG1521A Cells After G0 Exposure to Low and High LET Radiation

ABSTRACT

Exposure of cells to ionizing radiation has been shown to induce several forms of transmissible genomic instability, including cytologically visible chromosomal instability. Furthermore, exposure to ionizing radiation has been shown to lead to *in vitro* cell transformation and cancer in animals and humans. Since a connection between chromosome abnormalities and cancer has been established, it has been suggested that radiation-induced chromosomal instability may be an initial or at least a very early step in this process of radiation-induced carcinogenesis.

Support for this notion requires that the phenomenon be established with cell populations that are "normal" at the outset. With this aim in mind, I exposed phenotypically normal, AG1521A, human fibroblast cultures to high LET, 1 GeV/nucleon ^{56}Fe nuclei or low LET ^{137}Cs γ -rays while in a temporarily non-cycling G0 state. We used this exposure condition to better simulate cell renewal tissues *in vivo*. Mixed populations of cells surviving exposure were analyzed after various cell population generations using a number of cytogenetic endpoints,

including chromatid-type aberrations frequencies, stable aberration frequencies and complex aberration frequencies using Giemsa staining, whole chromosome painting by fluorescence *in situ* hybridization (WCP-FISH) and multiplex-FISH (mFISH).

I was unable to detect an induction of chromosomal instability due to the IR exposure in the progeny of surviving cells by any of the analyses used. Furthermore, the development of chromosomal instability that was seen in very late generations was common in both control and irradiated samples and was indicative of cells at or near senescence.

INTRODUCTION

Cancer is a multistep process whereby a single cell and its progeny, within a population of surrounding cells, acquire multiple genetic alterations leading to loss of proper control of cell proliferation and tissue function. If left unchecked, cancers can progress and lead to the death of the organism. Ionizing radiation (IR) has been used for many years to kill cells for cancer treatment, but exposure has also been shown to transform mammalian cells in culture and to lead to cancer in humans. The mechanisms by which IR initiates and promotes this process are still not fully understood. Radiation-induced transmissible genomic instability has been proposed as an early mechanism in the initiation of this process (58).

IR has been reported to induce transmissible chromosomal instability in the progeny of surviving cells as detected by elevated levels of chromatid-type and/or chromosome-type aberrations compared to controls many generations after exposure. This has been shown in mixed (non-clonal) populations of human fibroblasts (62) (60) and in murine (74) and human (73) mammary epithelial cells. Studies of clonal descendents of exposed murine (111) and human bone marrow cells (59), human lymphoblastoid cells (72) and human-hamster hybrid cells (68) have also reported the occurrence of this phenomenon.

The perception that developed after several such reports was that this phenomenon could possibly be used in a general way to explain the initial steps in radiation-induced carcinogenesis. If indeed radiation-induced genomic instability is *the* initiating step involved in radiation-induced carcinogenesis, then

it should occur especially in those cells that are apparently normal at the outset. Cells containing abnormalities in tumor suppressor responses or DNA damage repair processes, such as found in many of the cells used in the above mentioned experiments, would already contain a precondition that may be necessary for induction of instability upon exposure to IR. If so, IR would not be an initiating step, but more of a switch that accelerates or turns on this pre-existing condition. This switch might also be flipped by a number of other exogenous or endogenous insults, such as chemical or biological exposure or oxidative stress inherent in the cell.

To determine if this phenomenon is indeed universal and not dependent on a pre-existing condition and could therefore be *the* initial step in radiation-induced carcinogenesis, we set out to study it in an apparently normal human fibroblast cell line. Studies were done in both mixed, non-clonal populations of cells and clonal descendents of cells surviving exposure. I will focus in this chapter on the results from studying mixed populations and the next chapter will discuss the analysis of clonal isolates.

The basic idea for the mixed cell population studies was to irradiate numerous confluent flasks of cells that were then left to complete the processing of the induced DNA damage. Control and irradiated samples were then collected and subcultured to examine aberrations in the first post-irradiation mitosis. Parallel samples were also set up for continuous log-phase incubation and to determine plating efficiency and surviving fraction. In some cases cultures were maintained for extended periods of G₀ incubation. To measure instability it is

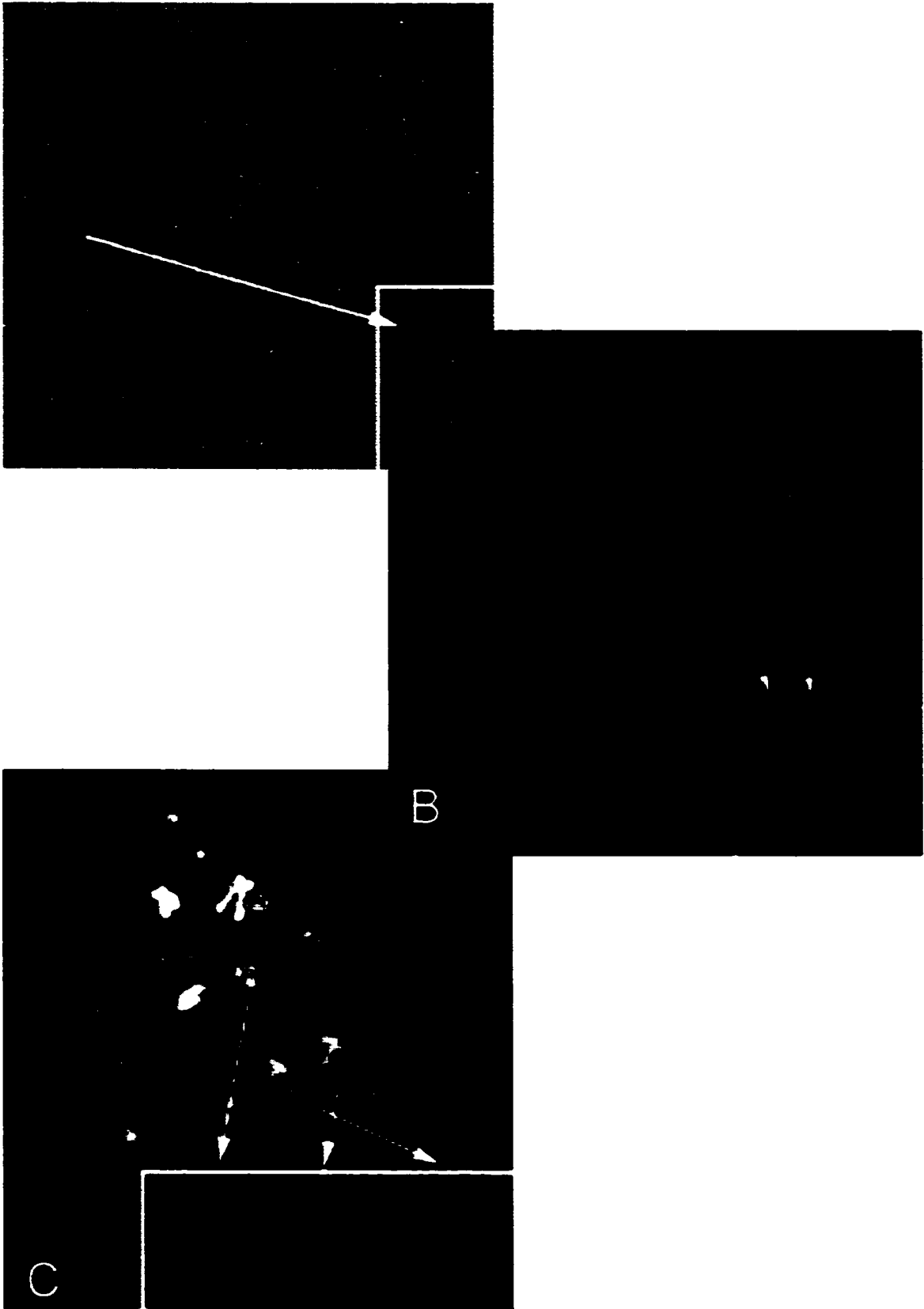
necessary to determine whether there is an increase in the appearance of new aberrations many generations after exposure. So, for log-phase cultures, flasks were allowed to reach ~75% confluence, within 7-10 days and cells were then harvested and replated at a lower density (1/10th dilution) for continued log-phase incubation. Furthermore, at each subculturing, cells were plated for collection of the next mitosis. These mitotic collections were later analyzed by staining with Giemsa and in certain cases with hybridization of whole chromosome painting probes. In these experiments chromosomal instability was considered to have been induced if new chromosomal aberrations occur in the progeny of cells surviving the radiation exposure at a level higher than the level of stable aberrations at the first mitosis. Further, to attribute such elevated aberration rates to irradiation, the absolute increase would have to exceed that for unirradiated controls.

Solid staining with Giemsa allows for the rapid detection of all chromatid-type aberrations and of most chromosome-type aberrations. However, stable translocations and complex aberrations involving multiple chromosomes are rarely, if ever, detected with this method. The use of whole chromosome probe fluorescence *in situ* hybridization (WCP-FISH) and mFISH does allow for the detection of these types of aberrations, although the costs can become prohibitive depending on the number of samples required for analysis. A visual comparison of the analysis criteria is illustrated in Figure 2-1. Panel A shows a chromatid break aberration detected in a Giemsa stained cell. Panel B shows an apparently simple reciprocal translocation detected by WCP-FISH involving

chromosome 2 (red) and a DAPI counterstained chromosome (blue). In Panel C a complex aberration is shown as detected by mFISH. In this case the aberration involved a translocation between chromosome 13 (pink) and 6 (bronze) that has an insertion of DNA from chromosome 4 (blue) in one part of the translocation. The truncated chromosome 4 is also shown.

Figure 2-1

Analysis methods used in this portion of the study are shown in this figure. Solid Giemsa staining is illustrated in panel A showing a chromatid break. Panel B illustrates the use of the FISH technique using whole chromosome painting probes for chromosomes 1 and 5 (blue-green) and chromosomes 2, 3 and 4 (red). Dapi counterstained chromosomes are shown in dark blue. A reciprocal translocation involving chromosome 2 (red) and an unlabeled chromosome is shown in the box. Panel C illustrates the use of mFISH for aberration detection. Each chromosome is labeled with up to three different fluorochromes of a possible five fluorochromes used for labeling. Image analysis software captures images for each of the five fluorochromes along with the DAPI counterstain and then pseudocolors the chromosomes. Identification of individual chromosomes and aberrant chromosomes is done by examining their labeling patterns and comparing against the known color scheme. A complex chromosome aberration is shown here involving an insertion of chromosome 4 (blue) into a translocation between chromosome 6 (bronze) and 13 (pink).



MATERIALS AND METHODS

Cell Culture

Low passage number (P4-P5) AG 1521A normal, diploid, human fibroblasts were obtained from American Type Culture Collection (ATCC). A passage is defined as a 1:10 dilution of a confluent T25 flask and consists of 3-4 population doublings for this cell line. Cells were cultured in α -MEM medium (Gibco BRL, Grand Island, NY) supplemented with 15% fetal bovine serum (FBS) (Summit Labs, Ft. Collins, CO) and incubated at 37°C in a humidified atmosphere of 5% CO₂ in air. Confluent T25 flasks were split 1:10 into new T25 flasks. This was repeated until the required number of flasks was available. Upon reaching confluence, fresh medium was placed in all flasks to stimulate any cycling cells through mitosis.

⁵⁶Fe Irradiation at Brookhaven National Laboratory

Four days prior to irradiation the confluent flasks were completely filled with medium, capped and sealed with melted paraffin wax. The flasks were then hand-carried or shipped overnight by commercial carrier to Brookhaven National laboratory (BNL) for irradiation. Cells were irradiated to a dose of 1.25 Gy in the plateau region of the Bragg curve of a beam of 1GeV/nucleon ⁵⁶Fe particles that produced on average one track per cell nucleus. Controls were not irradiated. After irradiation the cells were hand-carried back to CSU. A complete description

of the 1 GeV/nucleon ^{56}Fe beam at BNL's Alternating Gradient Synchrotron is given in (112).

^{137}Cs γ -ray Irradiation

The dose of γ -rays used was adjusted to yield approximately the same level of effect as the ^{56}Fe exposure for cell survival and first post-irradiation mitosis aberration scoring. Three days after the final medium change, cells were irradiated at CSU using a 6000Ci JL Shepherd Mark-1 ^{137}Cs irradiator (J.L. Shepherd, CA). A dose of 5 Gy was given at a dose rate of 3.9 Gy/min. The dose rate was obtained from the slope of a calibration curve created from data obtained by thermoluminescence dosimetry (TLD) readings over a range of exposure times from 0.01 to 0.1 min.

1st Post-irradiation Mitosis Collection

Upon returning to CSU, high LET irradiated cells and controls were incubated overnight. Low LET irradiated cells and controls were also incubated overnight, allowing for DNA repair to take place. All flasks of cells given the same dose were pooled and counted. 3×10^5 control cells and 8×10^5 cells exposed to 1.25 Gy of 1 GeV/nucleon ^{56}Fe particles were placed into 3xT25 flasks each along with 10^{-5} M 5-bromo-2'-deoxyuridine (BrdU) (Sigma, St. Louis, MO). Colcemid (Gibco BRL, Grand Island, NY) was added to a control and a sample flask 30, 36 and 42 hrs after subculture, at a concentration of $0.1 \mu\text{g/ml}$, to block cycling cells entering mitosis in metaphase. Samples were collected and fixed 6 hrs after colcemid

addition. Giemsa staining for BrdU incorporation following the procedure of Benn and Perle (113) allowed for the elimination of 2nd division cells from scoring results as indicated by the presence of harlequin stained chromosomes.

Metaphase Spread Collection and Fixation

Six hrs after colcemid addition, the cells were trypsinized, spun down and incubated for 15 min at 37°C in 12 ml 0.075 M KCl hypotonic solution. The hypotonic solution allows the cells to swell and helps remove cytoplasmic material that can interfere with resolution after staining and hybridization procedures. The time, temperature and volume of hypotonic KCl solution are critical for best mFISH analysis. Two ml of freshly prepared 3:1 methanol: acetic acid (fix) was then added, followed by an additional 15 min incubation at room temperature. The cells were spun down again. Next, 4ml of fix was added dropwise and incubated for 15 min at room temperature followed by centrifugation. This step was then repeated. Finally, the cells were resuspended in 1-2 ml fix and dropped onto cold, wet, ethanol-washed microscope slides. Slides were then allowed to air-dry and then stored desiccated at 37°C for up to one week or at room temperature for longer periods.

Plating Efficiency and Surviving Fraction

Pooled cells were also subcultured for determination of plating efficiency (PE) and surviving fraction (SF) by colony formation. For this, 200 unirradiated control cells were inoculated into 3x100 mm dishes. For cultures given 1.25 Gy ⁵⁸Fe or 5

Gy γ -irradiation, 2000 cells were inoculated, also into 3x100mm dishes. The dishes were then incubated at 37°C in a humidified atmosphere of 5% CO₂ in air for 10-14 days without disturbance, except for the addition of 10 ml medium after 7 days, to allow for colony formation. Methanol: acetic acid fix was then added for one min, removed and followed by a second fix. The colonies were then stained with a 1% crystal violet solution for 5-10 min. After rinsing, the flasks were allowed to dry and colonies were then counted. Only colonies containing greater than 50-60 cells were counted.

Continuous Log-phase Incubation

For measurement of aberration frequencies after various cell generations had elapsed in log-phase culture, mixed samples were inoculated for continuous log-phase growth. At the start of the experiment 5×10^4 unirradiated control cells and 3×10^5 irradiated cells were each plated into T75 flasks. The medium was changed after one day. Cultures were incubated for one week and then harvested for mitotic collection and for subculture. 5×10^4 unirradiated control cells and an equal number of cells from the irradiated population were replated to continue the log-phase growth. In some experiments, at the time of subculture cells were again plated for PE. In all cases 3×10^5 cells were inoculated for mitotic collection and fixation of the next mitosis (see above for method). This procedure was repeated for up to 45 generations or until it appeared that the cultures were senescing and no longer reproductively viable. Any cells remaining from each collection were then frozen down into liquid N₂ using 10% DMSO as a

cryoprotectant. From subculture initiation to the harvest 5-7 days later, approximately 5 generations elapsed. Allowing for a plating efficiency of approximately 50%, this corresponds to a 32-fold increase in 5 days with a one day generation time.

Extended G0 Incubation

An additional subculture was done for some experiments where a separate flask was plated, grown to confluence and held in confluence, with weekly medium changes, until the end of the experiment. Cells were then subcultured and allowed to progress to the next mitosis for mitotic harvest or frozen. The purpose here was to determine whether the development of instability might be governed by "time in culture" rather than "number of generations." For this portion of the experiment, then, it was possible to have two subsets of samples; both of which had experienced the same time in culture, but one had experienced in one case 15 or in another case 25 more population doublings than the other.

Classical Cytogenetic Analysis

Slides were coded by a second party to prevent the analyst from knowing which sample was being scored. They were then stained in a Coplin jar containing 10% Giemsa stain in pH 6.8 buffer solution for 4-5 min. Slides were then thoroughly washed in H₂O and air-dried. Coverslips were then mounted and allowed to dry overnight. Metaphase spreads containing 45-46 chromosomes were then scored

for all samples. A minimum of 100 spreads were scored for each sample unless this was not possible for reasons of low mitotic index.

Whole Chromosome Painting Probe Preparation

DOP-amplifiable whole chromosome probe libraries for human chromosomes #1-5 were kindly provided by Dr. Allen Christian of Lawrence Livermore National Laboratory. The libraries were combined as follows and amplified or direct-labeled; C1+C5, 1:6; C2+C3+C4, 1:2:6. The amplification was done in a 30 μ l volume containing 12U Thermo-Sequenase polymerase (USB, Cleveland, OH), 3 μ l ThermoSequenase reaction buffer, 4 μ M each dTTP, dCTP, dATP and dGTP (Roche Molecular, Indianapolis, IN), 4 μ M Telenius primer (5'-CCGATCGAGNNNNNNATGTGG-3') (MMR, Fort Collins, CO) and 100 ng DNA. The reaction was run in a MJR Thermocycler (MJ Research, Boston, MA) using a heating, annealing and extension profile of 95°C for 5 min followed by 24 cycles of 94°C for 1min, 56°C for 1min, 72°C for 3 min. This was followed by 5 min at 72°C and a hold at 4°C until samples were removed. Products were purified for labeling using Qiagen's Qiaquick PCR Purification Kit (Qiagen, Santa Clarita, CA) following the manufacturer's instructions. The labeling was done in a 50 μ l volume containing 20 U ThermoSequenase polymerase (USB, Cleveland, OH), 5 μ l ThermoSequenase reaction buffer, 200 μ M each dTTP, dCTP, dATP and dGTP (Roche Molecular, Indianapolis, IN), 4 μ M Telenius primer (MMR, Fort Collins, CO) and 10 ng DNA. In addition, 200 μ M FITC-dUTP (Roche Molecular,

Indianapolis, IN) (chromosomes 1+5) or tetramethylrhodamine-dUTP (Roche Molecular, Indianapolis, IN) (chromosomes 2+3+4) was added.

Fluorescence *in situ* Hybridization

The hapten- or direct-labeled PCR products were combined and mixed with a 20-fold excess of human Cot-1 DNA (Roche Molecular, Indianapolis, IN) and precipitated overnight at -4°C by adding 1/20th volume 3 M sodium acetate and 2x volume 100% ethanol. The probe mix was spun down, rinsed 2x in 70% ethanol, dried and resuspended in a hybridization mixture. The hybridization mixture consisted of 50% formamide, 2x SSC and 20% dextran sulfate. Coded, aged (desiccated 1-3 days at 37°C) slides were dried in an ethanol series consisting of 2 min rinses in 70, 85 and 100% ethanol. The slides were air-dried and then denatured in 70% formamide, 30% 2x SSC at 72°C for 2min. The slides were then run through the ethanol series again and air-dried. While the slides were being prepared, 30 µl of the hybridization mixture was being denatured in a thermocycler by heating to 84°C for 10 min followed by a 45-60 min hold at 37°C to allow reannealing of repetitive sequences between the unlabelled Cot-1 DNA and the labeled repetitive DNA in the probe. The hybridization cocktail was then placed on the prepared slides and a 22x50 mm coverslip was then placed over the hybridization mix and sealed with rubber cement to prevent evaporation. The slides were placed in a sealed box and incubated for 18-36 hrs. After incubation the coverslips were gently removed and the slides were washed. This involved 2 rinses for 5 min each in 50% formamide, 2x SSC at 45°C followed by 2 rinses in

2x SSC for 5 min at 45°C followed by 2 rinses in 1xPN buffer for 3 min each at RT. 30 µl of antifade solution containing 42 ng/ml DAPI was then placed on the slide and covered with a coverslip.

Metaphase Analysis by FISH and Image Acquisition

Probe-hybridized metaphase spreads of mixed populations of cells were then viewed and scored on an Olympus Provis AX-70 fluorescence microscope (Olympus, Melville, NY). A minimum of 100 metaphases was scored per sample. Metaphase spreads were photographed on an Olympus Provis AX-70 fluorescence microscope (Olympus, Melville, NY) using a Photometrics SenSys cooled CCD camera (Photometrics, Tuscon, AZ). Images were acquired and processed using Applied Imaging's PowerGene MacProbe software (Applied Imaging, Santa Clara, CA).

Multiplex FISH (mFISH)

Vysis' SpectraVysion Assay mFISH probe set (Vysis, Downers Grove, IL) was used following the manufacturer's instructions, with slight modifications. Fixed cell suspensions were dropped in the middle 1/3 of the slide, allowing for maximum metaphase density in a 22x22 mm area. One to three day old slides that had been kept at room temperature were dried in acetone for 10 min followed by air-drying. Slides were then soaked in 1x PN buffer for 3 min at RT followed by 5 min in RT 2x SSC. Slides were then incubated for 60 min in 100 µg/ml, DNase free (boiled 10 min) RNase A (Roche Molecular, Indianapolis, IN)

in 2x SSC at 37°C. This was followed by rinsing 2x in 2x SSC at RT for 5 min rinse. Slides were then incubated for 5 min in 0.1µg/ml Proteinase K (Roche Molecular, Indianapolis, IN) in 20 mM Tris-HCl, pH 7.4, 2 mM CaCl₂ at 37°C. Slides were then rinsed 2x in phosphate buffered saline (PBS) at RT for 5 min/rinse. Next, the slides were fixed in 3.7% formaldehyde in PBS for 2 min at RT followed by 2 additional PBS rinses. Slides were then run through an ethanol series consisting of 3 min rinses in 70%, 85% and 100% ethanol. They were air-dried and then denatured in 70% formamide, 30% SSC for 2 min followed by a second ethanol series and air-drying. When the slides were nearly ready, 10 µl/slide of SpectraVysion assay probe cocktail was denatured at 72°C for 5 min. The metaphase spreads were checked at this point for faded chromosomes and minimal cytoplasmic residue. Due to the high cost of the probe, multiple slides/sample were prepared up to this point. Only the best slide was then used. The denatured probe cocktail was then dropped onto the prepared slide, covered with a 22x22 mm coverslip and sealed with rubber cement. The slides were placed in a sealed box and incubated for 1-2 days at 37°C. Following incubation, the coverslips were gently removed and the slides were immediately immersed in 0.4x SSC/0.3% Igepal CA-630 (Sigma, St. Louis, MO.) at 72°C. Slides were agitated for 1-3 seconds and removed after 2 min. The slides were then rinsed in RT 2x SSC/0.1% Igepal CA-630 for 5 sec to 1 min. The slides were then rinsed for 3 min in 1x PN buffer at RT. Finally, 10 µl of DAPI III counterstain (Vysis, Downers Grove, IL) was dropped onto slide and covered with a 25x25 mm coverslip. Metaphase spreads were photographed on an Olympus Provis

fluorescence microscope (Olympus, Melville, NY) using a Photometrics SenSys cooled CCD camera (Photometrics, Tuscon, AZ). Images were acquired and processed using Applied Imaging's PowerGene mFISH software (Applied Imaging, Santa Clara, CA).

RESULTS

Survival fractions for G_0 irradiations of AG1521A cells by ^{137}Cs γ -rays or $1\text{GeV}/\mu\text{m}$ ^{56}Fe nuclei were $\sim 10\%$ as determined by colony forming ability 10-14 days after plating. First post-irradiation mitotic cells were collected and analyzed by solid Giemsa staining. Results are summarized in Table 2-1. In 221 cells exposed to 5Gy ^{137}Cs γ -rays, 125 dicentrics were scored (0.57 dic/cell). In 171 cells exposed to 1.25Gy ^{56}Fe particles, 91 dicentrics were scored (0.53/cell). One dicentric was detected in a total of 342 control cells.

Results of aberration scoring of continuous log-phase incubated cells surviving exposure to 5Gy ^{137}Cs γ -rays are shown in Figures 2-2 through 2-5. Chromatid-type aberration frequencies obtained by solid Giemsa staining are shown for γ -experiment #1 in Figure 2-2 and γ -experiment #2 in Figure 2-3. Pooled results are shown in Figure 2-4. It was clear from these experiments that no delayed increase in the levels of chromatid-type aberrations in irradiated samples occurred for any of the sampling times ranging from 7 to 35 post-irradiation cell generations.

Apparently simple exchange frequencies obtained by whole chromosome painting -FISH (WCP-FISH) with chromosome 1-5 probes on γ -experiment #1 samples are shown in Figure 2-5. Continuous log-phase cultures and cultures held for extended G_0 incubations after 8 generations were all analyzed by the WCP- FISH method. The frequency of exchanges, expressed as bi-color exchange pairs, involving chromosomes 1-5 was higher in the first generation, as expected, since both lethal unstable exchanges (asymmetrical) and non-lethal

Table 2-1

Aberration scoring by solid Giemsa staining of 1st post-irradiation mitotic cells, minimum 100 cells per sample.

	No. Cells	No. Aberrations	Chromatid-type aberrations/cell	Chromosome-type aberrations/cell	Dicentrics/cell
0 Gy Control	342	11	0.03	0.003	0.003
5 Gy ¹³⁷Cs γ-rays	100	117	0.04	1.13	0.57
1.25 Gy ⁶⁰Fe particles	171	193	0.04	1.09	0.53

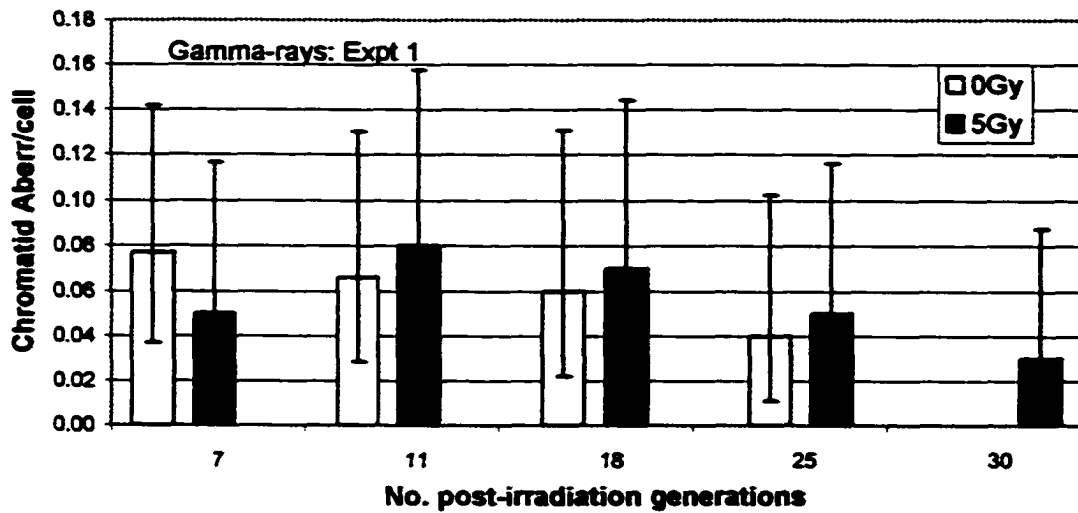


Figure 2-2

Chromatid aberration frequencies in mixed populations of cells surviving 5Gy ^{137}Cs γ -irradiation (γ -experiment 1) and held in continuous log-phase culture. Error bars are 95% confidence intervals using Poisson statistics.

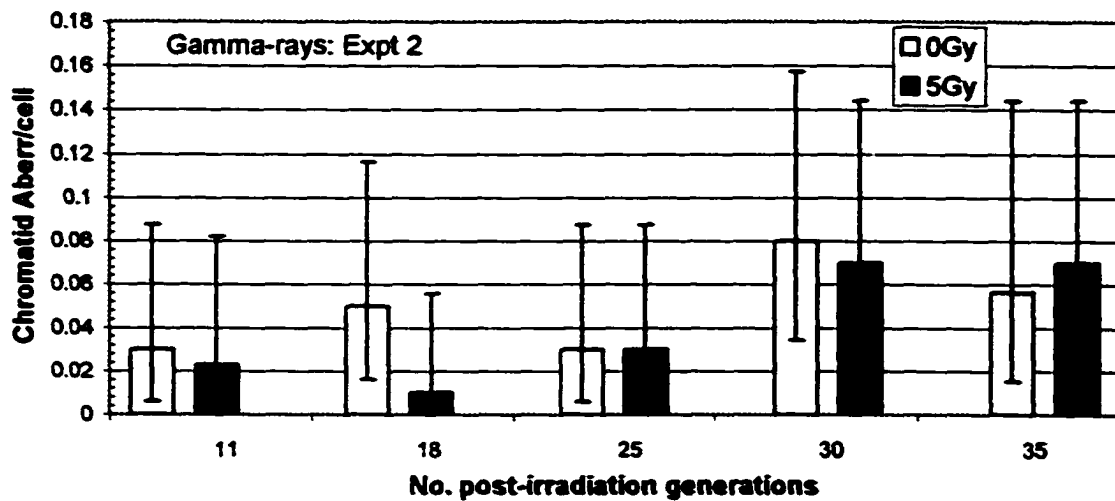


Figure 2-3

Chromatid aberration frequencies in mixed populations of cells surviving 5Gy ^{137}Cs γ -irradiation (γ -experiment 2) and held in continuous log-phase culture. Error bars are 95% confidence intervals using Poisson statistics.

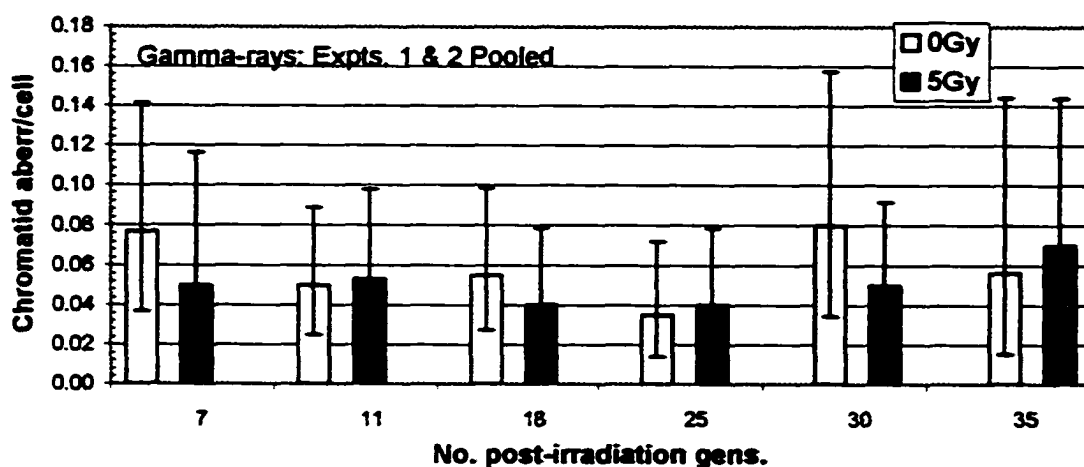


Figure 2-4

Chromatid aberration frequencies in mixed populations of cells surviving 5Gy ¹³⁷Cs γ -irradiation (pooled data from γ -experiments 1 & 2) and held in continuous log-phase culture. Error bars are 95% confidence intervals using Poisson statistics.

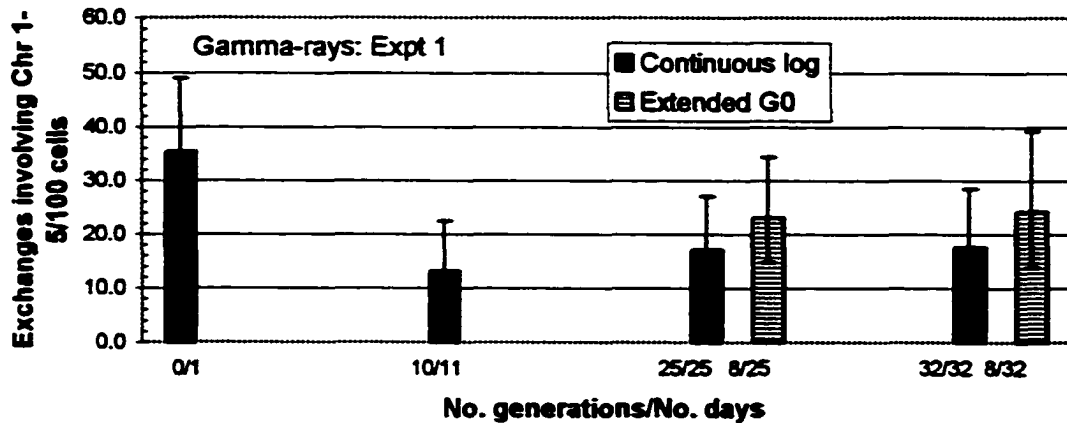


Figure 2-5

Comparison of apparently simple exchange (SE) aberration frequencies measured by 2-color whole chromosome painting FISH (WCP-FISH) using chromosomes 1-5 in mixed populations of cells surviving exposure to 5Gy ^{137}Cs γ -rays. Chromosomes 1&5 were labeled green and chromosomes 2-4 were labeled red to identify aberrations amongst the labeled chromosomes. Cultures were either kept in continuous log-phase growth, or held in G0 for extended periods after several post-irradiation cycles. Error bars are 95% confidence intervals using poisson statistics.

Note: only 1 exchange aberration was seen in a total of 547 control cells scored from all sample points.

stable exchanges (symmetrical) were present. In later generation samples the value dropped to about half this value. This would also be expected if there was no instability induced because the initial frequency of symmetrical and asymmetrical aberrations is about equal (114) In each of the later samples the frequency did not change with the number of generations during continuous log-phase culture or as a function of time in culture with minimal number of generations.

Results of aberration scoring of continuous log-phase incubated cells surviving exposure to 1.25 Gy ^{56}Fe particles are shown in Figures 2-6 through 2-10. Chromatid-type aberration frequencies obtained by solid Giemsa staining of mitotic collections from Fe-experiment #1 (BNL-3) are shown in Figure 2-6 and for Fe-experiment #2 (BNL-4). Pooled results are shown in Figure 2-8. An elevated frequency of chromatid-type aberrations in the sample population in Fe-experiment #1 can be seen at generations 16 and 21 compared to the frequency at generation 10. However, these results were not duplicated in Fe-experiment #2. Therefore, the results from these experiments indicate that there was no significant increase in the appearance of delayed chromatid-type aberrations in irradiated samples for any of the sampling times ranging from 10 to 35 post-irradiation generations.

Apparently simple exchange frequencies obtained by WCP-FISH with chromosome 1-5 probes on Fe-experiment #1 samples are shown in Figure 2-9. Continuous log-phase cultures and cultures held for extended G0 incubations after 15 generations were all analyzed by the WCP- FISH method. The frequency

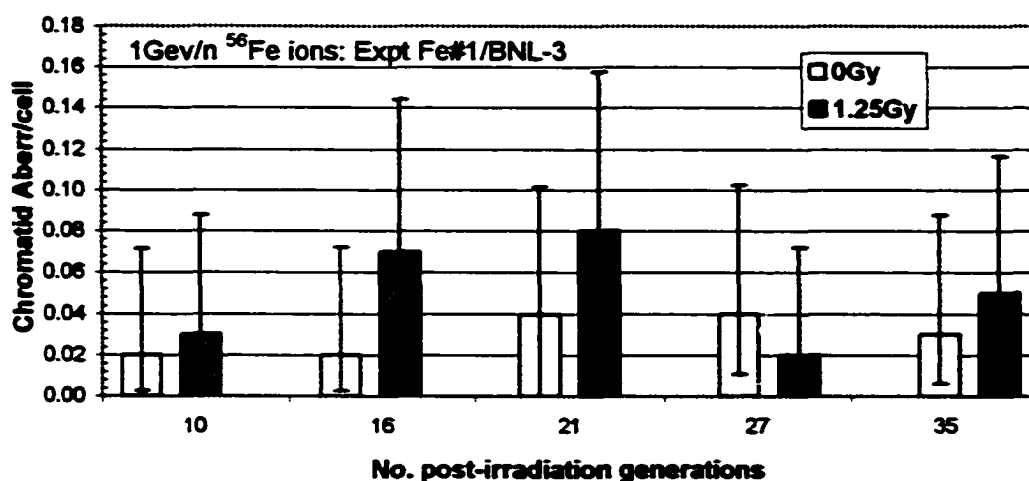


Figure 2-6

Chromatid aberration frequencies in mixed populations of cells surviving 1.25Gy ^{56}Fe particle irradiation (Fe-experiment #1: BNL-3) and held in continuous log-phase culture. Error bars are 95% confidence intervals using Poisson statistics.

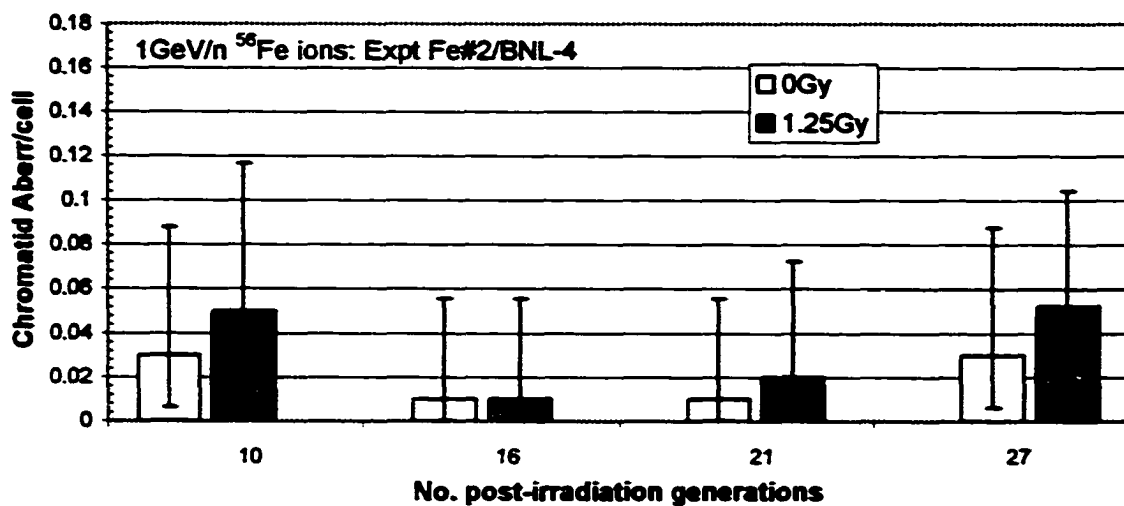


Figure 2-7

Chromatid aberration frequencies in mixed populations of cells surviving 1.25Gy ⁵⁶Fe particle irradiation (Fe-experiment #2: BNL-4) and held in continuous log-phase culture. Error bars are 95% confidence intervals using Poisson statistics.

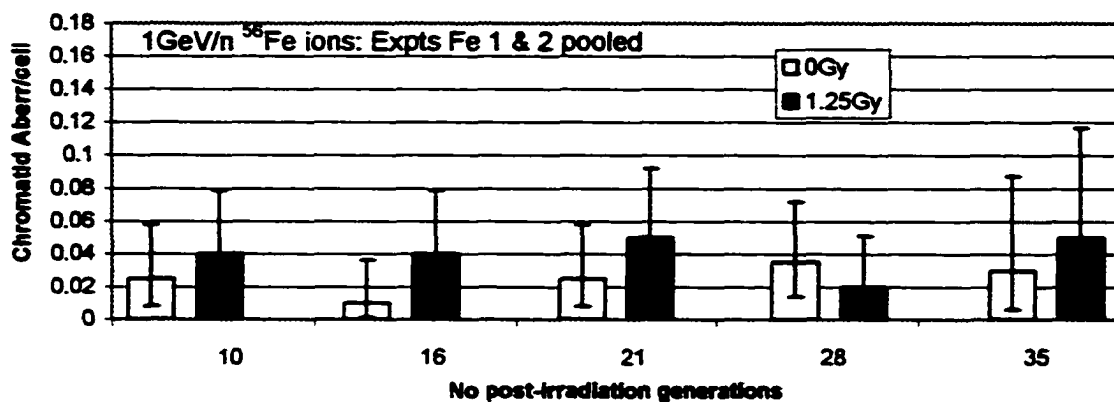


Figure 2-8

Chromatid aberration frequencies in mixed populations of cells surviving 1.25Gy ⁵⁶Fe particle irradiation (data are pooled from Fe-experiments #1 & #2) and held in continuous log-phase culture. Error bars are 95% confidence intervals using Poisson statistics.

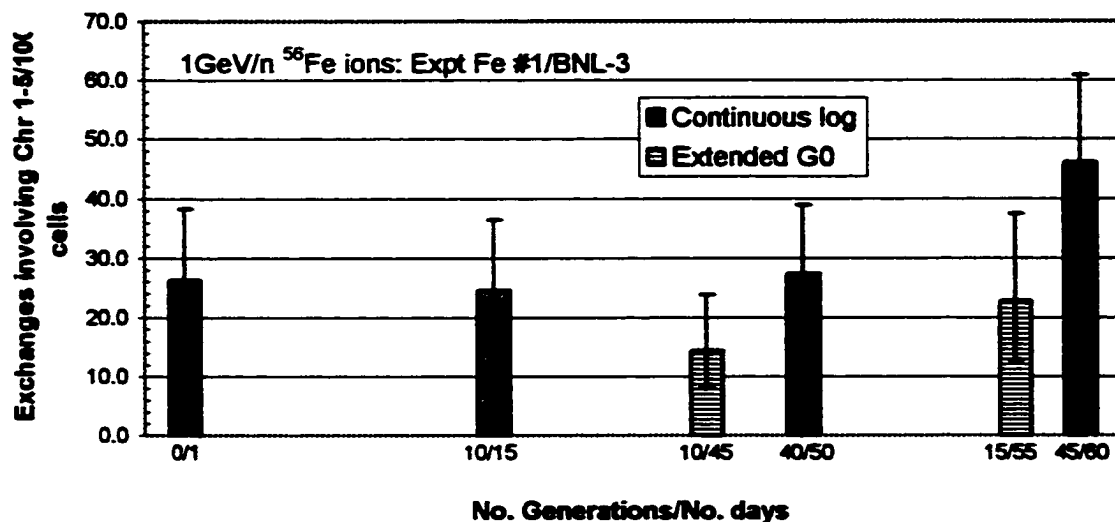


Figure 2-9

Comparison of apparently simple exchange aberration frequencies measured by 2-color whole chromosome painting FISH (WCP-FISH) using chromosomes 1-5 in pooled populations of cells surviving exposure to 1.25Gy ⁵⁶Fe nuclei (Fe-experiment 1; BNL-3). Chromosomes 1& 5 were labeled green and chromosomes 2-4 were labeled red to identify aberrations amongst the labeled chromosomes. Cultures were either kept in continuous log-phase growth, or held in G0 for extended periods after several post-irradiation cycles. Error bars are 95% confidence intervals using poisson statistics.

Note: 0 exchange aberrations were seen in a total of 533 control cells scored from the different sample points.

of exchanges, expressed as bi-color exchange pairs, involving chromosomes 1-5 was similar at the first post-irradiation mitosis and at the 10th and 40th post-irradiation generation mitosis. However, a significant increase was detected at the 45th post-irradiation mitosis ($p = 0.001$, student's t-test).

Total aberration frequencies obtained by multiplex-FISH (mFISH) analysis of Fe-experiment #1 samples are shown in Figure 2-10 and tabulated in Table 2-2. A low background level of aberrations was detected in control samples at generations 10 and 30. However, at generation 45 this frequency increased over 12-fold from these points. This change in total aberration frequency per cell was due to increases in the number of chromatid-type aberrations and dicentrics detected and to an increase in the number of cells with ploidy changes.

In the sample populations, a similar total aberration per cell frequency was detected at both 10 and 30 generations and was due to the presence of symmetrical aberrations. This frequency was in line with expected values based on the asymmetrical aberration frequency determined by solid Giemsa stained scoring of first post-irradiation mitotic cells. At the 40th generation a slight increase was detected. The frequency was also within experimental error for the expected value. However, at the 45th generation we detected a significant increase in total aberration frequency per cell. As with the control population at this generation, the increase was due to the observance of chromatid-type aberrations along with dicentrics and cells with ploidy changes. However, unlike in the control population, an elevated level of symmetrical exchanges was also detected in the sample population at the 45th generation. Overall, the total

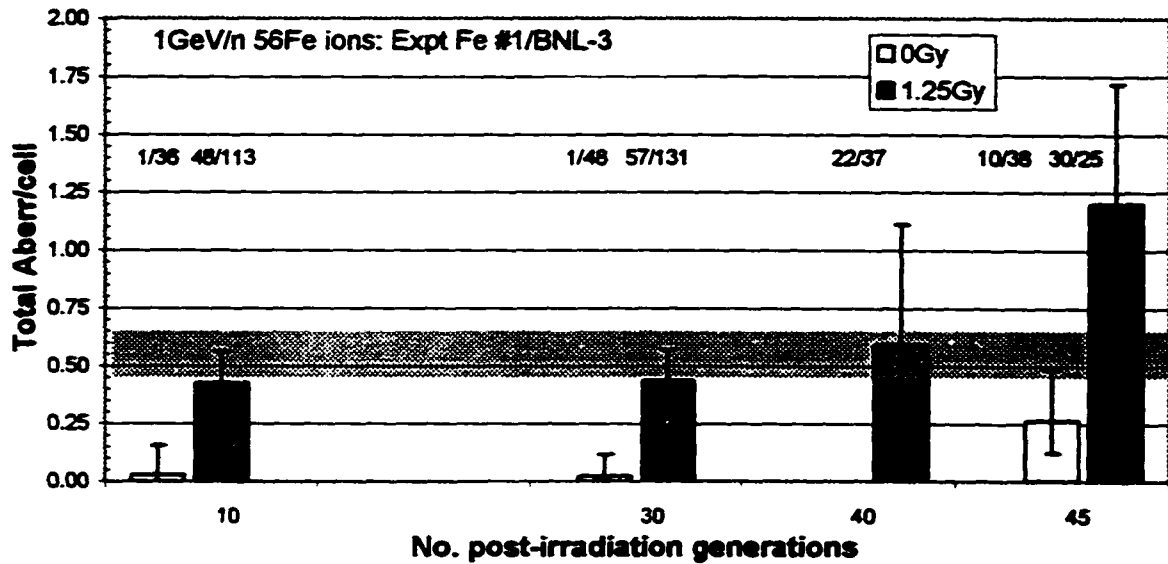


Figure 2-10

Total aberrations scored by mFISH in mixed populations of cells surviving 1.25Gy ⁵⁶Fe particle irradiation (Fe-experiment #1) and held in continuous log-phase culture. Error bars are 95% confidence intervals using Poisson statistics. Gray box indicates expected stable (symmetrical) aberration frequency based on dicentric (asymmetrical) frequency in 1st post-irradiation mitotic cells scored by Giemsa (0.53/cell). Note: no control cells were scored at 40 generations.

Table 2-2

Aberration frequencies for Fe-experiment #1 mitotic collections analyzed using mFISH. Chromatid-type aberrations seen were all gaps and breaks except for one sister chromatid union in control generation 45 cells. Chromosome-type aberrations included acentric rings, interstitial deletions, terminal deletions, dicentrics (Dic), asymmetrical exchanges, symmetrical exchanges (SE) and complex aberrations. Ploidy aberrations included aneuploidy, tetraploidy and endoreduplication. NS = not scored.

Dose, Gy	No. Gen.	No. Cells Scored	Chrom atid- type /cell	Chromo some- type /cell	Ploi dy /cell	SE /cell	Dic /cell	Complex ab /Exchange ab
0	10	36	0.0	0.03	0.0	0.03	0.0	0.0
	30	48	0.0	0.02	0.0	0.0	0.0	0.0
	40	0	NS	NS	NS	NS	NS	NS
	45	38	0.11	0.11	0.05	0.0	0.11	0.0
1.25	10	113	0.01	0.42	0.0	0.30	0.0	0.14
	30	131	0.01	0.41	0.0	0.23	0.0	0.11
	40	37	0.03	0.57	0.0	0.38	0.0	0.09
	45	25	0.20	0.92	0.08	0.72	0.08	0.10

aberration frequency per cell increased 2.75-fold from the 30th to the 45th post-irradiation generation as compared to a 12.6-fold increase in the control population in the same sample period.

A reciprocal translocation involving chromosomes 4 and 5 was identified by FISH analysis and an mFISH image of it is shown in Figure 2-11. The frequency of this aberration per sample point and the occurrence of other aberrations in cells containing this aberration are given in Table 2-3.



Figure 2-11

Reciprocal translocation involving chromosomes 4 (light green) and 5(red). C5p telomere translocated to C4 q-arm, C4q-arm translocated to C5p telomere region.

No. post-irrad. generations	Frq Chr 4q-C5ptel exchange	Frq Chr 4q-5ptel exchange + other ab.
10	0.006	0.0
30	0.065	0.0
40	0.40	.025
45	0.55	0.10

Table 2-3

Change in frequency of cells containing chromosome 4q – chromosome 5ptel symmetrical exchange with generation number found in mixed population study of cells surviving exposure to 1.25Gy ⁵⁶Fe nuclei (Fe-Experiment #1). Also, frequency of cells containing this exchange and other aberrations. An attempt was made to clone these cells containing this exchange at generation 30, but was unsuccessful. This aberration apparently provided a growth advantage to the cells, but did not immortalize them.

DISCUSSION

The objective of this research was to determine if radiation-induced chromosomal instability is a phenomenon that applies to normal cells in general as well as the immortalized, transformed or tumor cells in which this has been studied. A further aim was to determine whether the induction might be basically different for different LET radiations, at equitoxic doses, in AG1521A normal, human fibroblasts. For these experiments cells were irradiated in G₀ with either 5Gy ¹³⁷Cs γ-rays or 1.25Gy ⁵⁶Fe nuclei. These doses yielded equitoxic cell killing (~10% survival) as determined by colony forming ability. Also, analysis of aberration frequencies in 1st post-irradiation mitotic cells yielded nearly identical chromatid-type (0.4/cell) and chromosome-type (1.13 vs. 1.09/cell, respectively) aberration frequencies. Dicentric frequencies were also the similar (0.57 vs. 0.53/cell). Therefore, these doses yielded similar cell killing and induced aberration frequencies at the first post-irradiation mitosis and were therefore appropriate for comparison on the basis of an "equitoxic" initial dose.

Mixed populations of cells held in continuous log-phase culture were analyzed after regular mitotic collections for chromatid-type aberration frequencies. Two independent experiments were analyzed for each irradiation type. In only one of the four experiments (BNL-3) using 1GeV/μ ⁵⁶Fe ions, was there ever any indication of a slightly elevated chromatid-type aberration frequency at any of the sample points. For this experiment the estimated mean chromatid-type aberration frequency rose from 0.03/cell at 10 generations to 0.07/cell at 16 generations and 0.08/cell at 21 generations. Although the

estimated mean chromatid-type aberration frequency for the control population was 0.02/cell at 10 and 16 generations, the estimate doubled to 0.04/cell at 21 generations.

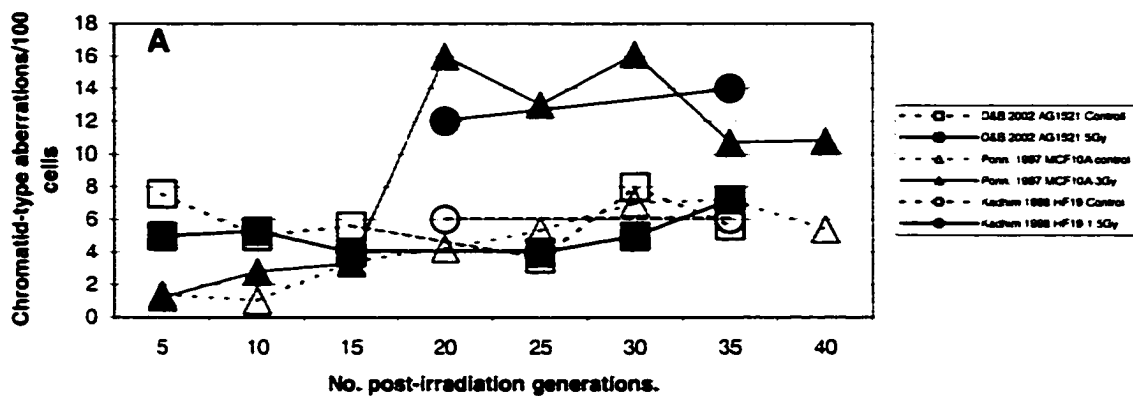
To compare these results with those from other laboratories, the data were replotted along with data from MCF10A human mammary epithelial cells (115), HF19 normal human lung fibroblasts (116) and CV123 human lymphoblastoid cells (117). As shown in Figure 2-12 chromatid-type aberration frequencies for both our unirradiated control and irradiated sample populations after exposure to either low LET or high LET radiation fall within reported background levels in human HF19 lung fibroblasts (60), human CV123 lymphoblastoid cells (117) and human MCF10A mammary epithelial cells (73). These results underscore the inconsistency and emphasize the lack of radiation-induced chromosomal instability in AG1521A fibroblasts using chromatid-type aberrations in mixed populations of cells analyzed many generations after radiation exposure as an endpoint.

Chromatid aberrations are produced in the cell generation immediately prior to mitosis and some, especially symmetrical interchanges, may become derived chromosome-type aberrations if they remain in a daughter cell and are carried to subsequent generations. To this end we hypothesized that if chromatid aberrations had any biological significance for carcinogenesis, it would be in their ability to produce elevated levels of stable, derived chromosome-type aberrations

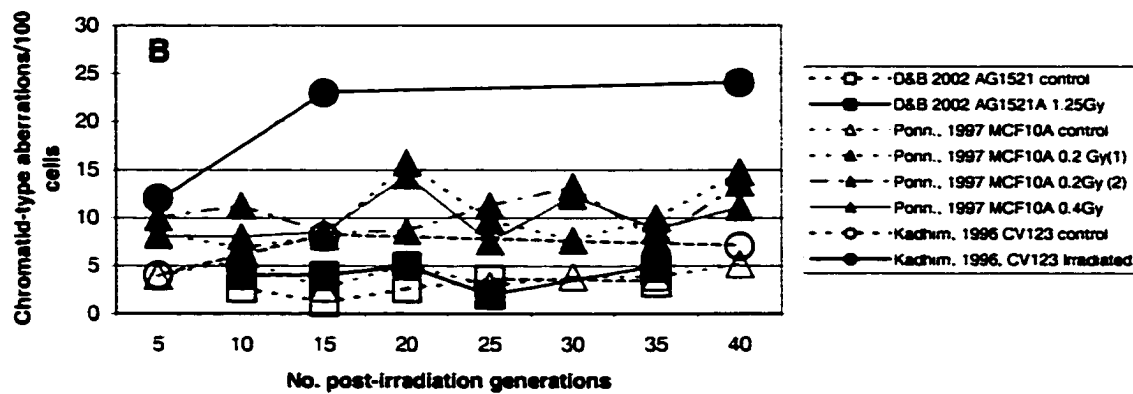
Figure 2-12

Comparison of reported chromatid-type aberration frequencies in mixed populations of various cell types after low and high LET radiation exposures. Panel A compares low LET radiation results from our work with AG1521A fibroblast cells (control: □, irradiated: ■), Ponnaiya, et al, 1997 MCF10A epithelial cells (control: Δ, irradiated: ▲), Kadhim, et al, 1998 HF19 fibroblast cells (control: ○, irradiated: ●). Panel B compares high LET results from our work with AG1521A fibroblast cells (control: □, irradiated: ■), Ponnaiya, et al, 1997 MCF10A epithelial cells (control: Δ, irradiated: ▲) and Kadhim, et al, 1996 CV123 lymphoblast cells (control: ◇ irradiated: ◆)

Low LET (X or gamma-rays)



High LET (Neutrons, alpha-particles or ^{56}Fe)



that would be carried to later cell generations. Therefore, to analyze this phenomenon, we compared early vs. late generation cell populations for the presence of stable chromosome-type interchanges using whole chromosome probe FISH. This would, of course, measure only interchange aberrations derived from chromatid interchanges or new chromosome types arising in later generations and it is perhaps noteworthy that most chromatid-type aberrations seen in our own, as well as other studies were chromatid gaps and breaks with very few exchanges.

WCP-FISH analysis of the first experiment of mixed populations of descendants of cells surviving 5Gy ^{137}Cs γ -ray exposure showed an initial frequency of interchanges at the first mitosis of about 0.65/cell. This included both asymmetrical (0.29/cell) and symmetrical aberrations (0.36/cell). Only data for symmetrical interchanges is shown in Figure 2-5. By the 10th generation the lethal aberrations were essentially eliminated and a frequency of symmetrical interchanges of 0.15/cell was detected (Figure 2-5). This aberration frequency then leveled off and remained fairly constant through the 32nd post-irradiation generation. Furthermore, cell populations that were incubated in log phase for 8 generations and then allowed to enter and persist in a G0 state, did not show any increase in change in exchange frequency after 25 or 32 total days in culture. Taken together, these results indicate that no induced instability occurred in these cell populations up to 32 generations after exposure, as measured by simple exchange frequencies using WCP-FISH.

Similar WCP-FISH analysis of the first Fe experiment (BNL-3) of mixed populations of descendents of cells surviving 1.25Gy ^{56}Fe nuclei exposure showed no change in apparently simple exchange aberration frequency from the 1st post-irradiation mitosis to the 35th (Figure 2-9). Again, the data shown for the first mitosis shows only the symmetrical interchanges. An elevated level does appear at the 40th generation, however these cells are nearing the end of their replicative lifespan and this change in aberration frequency may be due to the approach and onset of senescence. A slight increase was also seen in cells incubated for 15 generations of continuous log-phase growth followed by G0 incubation for a total of 55 days in culture compared to 10 generations and 45 total days in culture. After a total of 60 days in culture there were 22 exchanges/100 cells compared to 15 exchanges/100 cells after 45 days.

Calculations using the formula of Lucas et al (118) were performed to determine if symmetrical interchange aberration frequencies in the 1st post-irradiation mitosis, scored by C1-5 WCP-FISH, were within expectations for the whole genome. Dicentric frequencies were 0.57/cell for the 1st mitosis after ^{137}Cs -irradiation and 0.53/cell after ^{56}Fe irradiation. Assuming one symmetrical interchange is created for each detected dicentric (asymmetrical interchange) (114), the total genomic frequency of symmetrical interchanges (F_G) should also be 0.57/cell and 0.53/cell, respectively. Chromosomes 1+5 (painted green) account for 15% of the haploid genome ($f_{p(1+5)}$), while chromosomes 2, 3 & 4 (painted red) account for 22% ($f_{p(2+3+4)}$). Using Lucas' formula, we can determine

the expected frequency of interchanges involving painted chromosomes for each color group, F_p :

$$F_p = 2.05(fp)(1-fp)F_G$$

For cells exposed to 5Gy ^{137}Cs :

$$F_{P(1+5)} = 2.05(.15)(.85).57 = 0.15/\text{cell}$$

$$F_{P(2+3+4)} = 2.05(.22).78).57 = 0.20/\text{cell}$$

$$F_{P(1+5)+(2+3+4)} = F_{P(1+5)} + F_{P(2+3+4)} = 0.35/\text{cell}$$

For cells exposed to 1.25Gy ^{56}Fe nuclei:

$$F_{P(1+5)} = 2.05(.15)(.85).53 = 0.14/\text{cell}$$

$$F_{P(2+3+4)} = 2.05(.22).78).53 = 0.19/\text{cell}$$

$$F_{P(1+5)+(2+3+4)} = F_{P(1+5)} + F_{P(2+3+4)} = 0.33/\text{cell}$$

Our results for symmetrical exchange aberrations involving chromosomes 1-5 in the 1st post-irradiation mitosis are within experimental error of these calculations. For 1st mitosis cells after 5Gy ^{137}Cs γ -irradiation, 0.35 ab/cell were seen involving chr,1-5 and for 1st mitosis cells after 1.25Gy ^{56}Fe nuclei irradiation, 0.26ab/cell for were seen. Some error may be due to mis-scoring of dicentric and symmetrical exchange aberrations due to the lack of a centromeric probe in combination with the whole chromosome probes (114), but the agreement is well within expected sampling error.

Analysis of the data for mis-scoring indicates an error of <10%. Sixty-five painted simple exchange aberrations (dicentrics + symmetricals) were detected in 102 analyzed 1st M cells exposed to 5Gy ^{137}Cs . Of these, 29 were dicentrics and 36 were SEs. Assuming a 1:1 ratio, we should have scored 32-33 of each.

Therefore, 3–4 aberrations, or 5%, may have been mis-scored. Of 104 1st M cells analyzed from the population irradiated with 1.25Gy ⁵⁶Fe, 62 painted simple exchange aberrations were scored, 35 dicentrics and 27 SEs. Again assuming a 1:1 ratio, we should have seen 31 of each, indicating that ~4 aberrations, or 6%, were mis-scored.

A comparison of total aberrations per cell was also performed on the Experiment 1 descendants of cells surviving exposure to 1.25Gy ⁵⁶Fe nuclei using multiplex-FISH (mFISH) (Figure 2-10). It can be seen from the data in Table 2-2 that as the populations neared senescence (~generation 45) an increase in the types and frequencies of aberrations occurred. In both control and sample populations, elevated levels of chromatid-type aberrations (mostly gaps and breaks) along with ploidy changes, dicentrics (without acentric fragments) and other chromosome-type aberrations were detected. These aberrations are expected to be present at senescence based on previous reports dating back several decades (119) (105). It is noteworthy to point out that in the sample population we also detected an elevated level of symmetrical exchanges (SE) from early collection points to the sample taken at 45 generations after exposure. SE frequencies ranged from 0.23/cell to 0.38/cell at earlier points, but jumped to 0.72/cell at 45 generations. To the best of the author's knowledge, this has not been previously reported. It would appear from these results that high LET (1GeV/nucleon ⁵⁶Fe nuclei) exposure to non-cycling cells enhanced the chromosomal instability detected at senescence as indicated by a greater increase in aberration frequency than seen in the control population.

Complex aberrations involving multiple chromosomes are commonly found in solid tumors (reviewed in (18)), therefore we looked specifically for any change in their frequency in the Fe-experiment 1 samples analyzed by mFISH. Complex aberration frequencies remained fairly constant throughout the experiment on a per cell basis. At 10 generations the frequency was 0.06/cell, at 30 generations it was 0.04/cell, at 40 generations it was 0.05/cell and at 45 generations it was 0.12/cell. However, complex aberration frequencies on a per aberration frequency remained fairly constant at 0.14, 0.11, 0.09 and 0.10 for 10, 30, 40 and 45 generations, respectively.

An interesting outcome of the FISH and mFISH analysis was the detection within the population of cells surviving exposure to 1.25Gy ⁵⁶Fe nuclei of a stable clone containing an IR-induced translocation. This cell line also appeared to acquire a growth advantage over the other cells in the population in the later generations. The aberration, shown in Figure 2-11, was an exchange between the sub-telomeric region of one copy of chromosome 5 and the q-arm of a chromosome 4. It was detected at a very low frequency in the 10th generation (1 copy in 171 cells, 0.006/cell) and increased somewhat by the 30th generation (3 copies in 46 cells, 0.065/cell). However, at the 40th generation, the frequency of cells containing this aberration was greatly elevated (100 copies in 252 cells, 0.4/cell) and continued to take over the population at the 45th generation (106 copies in 194 cells, 0.55/cell). Furthermore, the frequency of cells containing this chromosome 4-5 exchange but with other additional, but various different aberrations, also increased from the 40th to the 45th generation. The types of new

aberrations seen were similar to those detected in both the control and sample populations seen in the 45th post-irradiation generation and included chromatid-type aberrations, dicentrics and ploidy changes.

Calculations are presented below to answer the question of whether this clone actually possessed a growth advantage such that an original irradiated cell with this aberration could have been responsible. I assume an average doubling time for log-phase populations of AG1521A cells, $N T_C$, of 1 day, as typically seen in our lab. What would the doubling time, $M T_C$, in the aberrant clone have to be to account for a change in frequency from 3 in 46 cells at 30 generations to 40 in 100 cells at 40 generations?

The number of normal (N) cells at time $t =$

$$N N_t = N N_0 2^{t/T_C} = (93.5)2^{(10/1)}$$

The number of aberrant, or mutant (M) cells at time $t =$

$$M N_t = M N_0 2^{t/T_C} = (6.5)2^{(10/M T_C)}$$

Since we know the fraction of aberrant cells at 40 generations, $M N_t / (N N_t + M N_t) = 40/100$, we can solve for the mutant doubling time, given that $t = 10$ days:

$$40/100 = ((6.5)2^{(10/M T_C)})/((93.5(2)^{10}) + ((6.5)2^{(10/M T_C)}))$$

$$M T_C = 0.75 \text{ days}$$

This corresponds to a doubling time of 18 hours, which is faster by 2-6 hrs than most known cultured normal and tumor cell lines of human origin, although not totally unlikely. This is further illustrated in Figure 2-13, panel A, where multiple doubling times were compared to a normal doubling time of 1 day. It can be seen

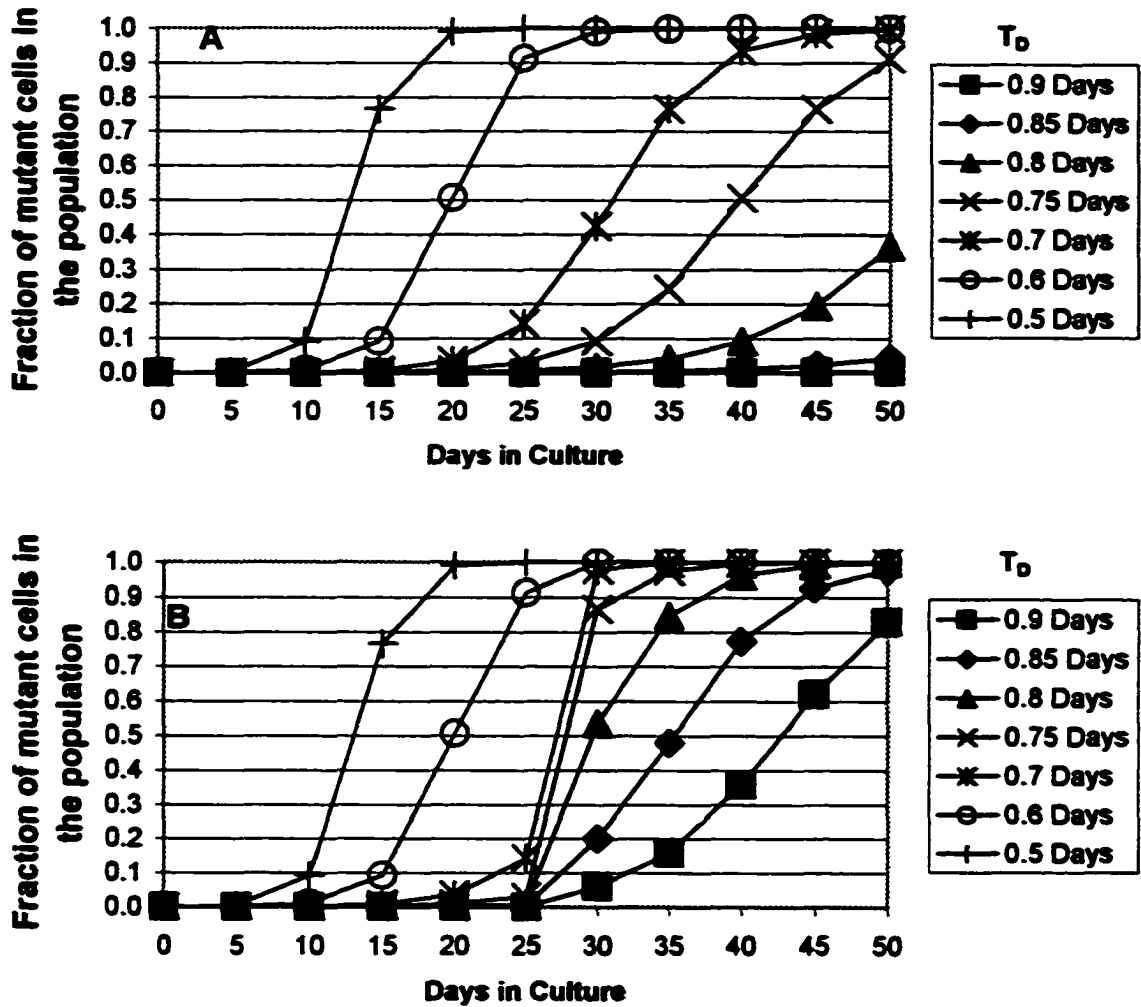


Figure 2-13

Comparison of mutant fractions in normal populations containing one initial mutant cell with a shortened doubling time through a prolonged culture. Panel A illustrates the effect of a decreased doubling time, T_D , for the mutant in a population of "wild type" cells with a constant doubling time of 1 day. Panel B illustrates the same effect, but in this case at 30 generations the doubling time for the normal population was increased to 1.25 days, assuming they were entering senescence. Results are based on an initial culture containing 10^4 viable cells.

that a decrease to around 0.75 days (18 hrs) would be required for a mutant fraction, F_M , to be near 40-50% at 40 population doublings for the normal cells.

However, if we assume that an 18 hr doubling time is beyond the ability of a human cell line, we still have another possible explanation for our results. If a 10% reduction in doubling time occurred in the mutant due to the IR exposure and persisted throughout the log-phase culture, and if at ~30 generations, as the normal population neared senescence, a 25% increase (from 24-30h) in the normal cell population doubling time occurred, then by 40 days in culture the mutant fraction would jump from ~6% to ~40%, as we saw for the clone of cells containing this particular C4-5 translocation.

Attempts to isolate clones containing this aberration and determine doubling times were unsuccessful. No cells grew to independent and expandable cell lines after plating 600 generation 30 cells (theoretically 39 contained the aberration of interest) for single-cell clones, nor did any foci develop after long-term incubation (>4 weeks) of a confluent monolayer of very late generation cells (>40 post-irradiation generations).

These results indicate that this clone, although possessing an apparent growth advantage over the rest of the population in the late generations, did not obtain immortality or become transformed, nor was it any more unstable than the population of cells from where it derived. It must be noted that the aberration frequencies given in Figures 2-9 and 2-10 were corrected for the presence of this clone in the population.

Endpoints including chromatid aberration frequency, stable translocation frequency, complex aberration frequency and total aberration frequency all failed to show a significant increase with increasing generations compared to controls until the population reached senescence. The same types of aberrations were detected by mFISH at generation 45 in both control and irradiated populations from Fe-experiment 1, except for an increase in symmetrical exchanges in the descendant population from the irradiated cells, as would be expected as cells reached the end of their replicative lifespan. Since the increase in aberration frequency in the sample population was greater than that of the control population at 45 generations, it would appear that the high LET radiation exposure may have served to enhance the spontaneous chromosomal instability at this point. However, the difference in total aberration frequency in control populations from the 30th to the 45th post-irradiation generation was greater by a factor of more than 4x the population derived from cells surviving irradiation exposure. This might actually indicate that the irradiation decreased the effect of senescence that was seen in the control population. Furthermore, it should be noted that although these cells were left in confluent culture for over a month after the last collection, no foci appeared, indicating a lack of immortalization or transformation along with a lack of radiation-induced transmissible chromosomal instability.

CHAPTER 3

Chromosomal Instability in Clones of HeLa Tumor Cells and Irradiated Normal Cells

ABSTRACT

As a background study to characterize some properties of chromosomal instability in a classical tumor-derived cell line, I isolated clones of HeLa cells to determine the extent to which the clonal populations displayed a narrow or broad distribution of chromosome numbers per cell. The starting population of cells exhibits a broad range of chromosome numbers. In both primary and secondary clonal isolates, the modal chromosome number was not narrow and the population rapidly reverted back to the original broad distribution, regardless of the chromosome number within the initial parent clonal cell. It was interesting that even though clones rapidly developed a spread of chromosome numbers among individual cells in the population, the DNA content per cell was remarkably constant. Next, we set out to determine if ionizing radiation (IR) induced chromosomal instability that was expressed in the clonal populations derived from individual surviving AG1521A normal human fibroblasts after exposure in G_0 to ^{137}Cs γ -rays or an equitoxic dose of 1 GeV/nucleon ^{56}Fe particles. Clones of single cells were isolated and expanded for a total of ~20-25 cell generations after exposure and were then analyzed using WCP-FISH.

We observed a high frequency of unstable clones, but this was unrelated to radiation exposure. Chromosomal instabilities were judged on the basis of whether cells in a clonal population contained karyotypically different subpopulations. These included cells with numerical and structural changes, including ploidy changes, chromatid-type aberrations, dicentrics that did not have associated acentric fragments and cells containing a combination of both numerical and structural changes. Cell population growth data for these clones indicated these clones were approaching the end of their *in vitro* lifespan, and this was apparently accompanied by the increased frequency of development of new aberrations probably due to telomere shortening or premature aging associated with excessive stress incurred during the cloning process.

INTRODUCTION

Since cancer is widely accepted as being a clonal phenomenon, the next portion of my study concerned the isolation, expansion and cytogenetic characterization of clonal isolates from human tumor and normal cell cultures for the study of the development of chromosomal instability in clonal subpopulations.

To characterize some features of this phenomenon in cells from a tumor, which would be expected to display instability, I carried out some initial studies involving HeLa cells. The HeLa cell line was isolated from a cervical adenocarcinoma over 50 years ago (120) (cited in (121) and has since maintained an elevated chromosomal number distribution among cells in bulk cultures through many years of continuous subculturing (121). How this cell line maintains a fairly constant modal chromosome number, despite the numerical instability that had to have occurred at some point in the tumor's development, led us to investigate the possibility of isolating clonal cell lines to determine whether sublines with different modal chromosome number distributions could be derived. Although a population of cells might contain a broad distribution of chromosomes, each individual cell of course, has a specific number. Therefore, isolation of a single cell and expansion of its clonal progeny might be expected to yield a population of cells containing a narrow chromosomal number distribution about the number in the initial founder cell, providing that little or no instability exists to alter this distribution.

I showed in the previous chapter on chromosomal instability in mixed populations of AG1521A cells, that no instability was induced in the progeny of

surviving cells by exposure to ionizing radiation, although elevated levels of aneuploidy and chromosomal aberrations appeared near the end of the *in vitro* lifespan of the cultures. However, we felt that two questions needed to be answered. First, in the case of reports indicating an induction of chromosomal instability in mixed populations of cells (62) (74) (73), it was unclear as to whether the clonal progeny of a few cells were actually showing a very high degree of instability while the remaining cells were not, or whether a lower level of instability existed, but in a much larger proportion of the population. Secondly, if instability was occurring in only a small number of clones within a population, they may go undetected in a mixed population of cells if aberration levels are low and near the background frequencies found in untreated cells. Therefore, it seemed necessary to isolate clones of cells surviving the same exposures as studied in the previous chapter to determine if elevated levels of aberrations occurred in some clones but not in others.

All progeny of a cell containing a stable radiation-induced aberration should contain that aberration. Any different aberrations later found in a cell from a clone would therefore not have been produced directly in the irradiated cell by the radiation, but by some subsequent event occurring in later generations of the clone arising from that cell. The timing, or number of cell divisions after exposure, of these subsequent events could be determined based upon the fraction of cells in the clonal population that contained these subsequent aberrations. The appearance of multiple different aberrations in cells of the clonal isolates could

then be used as an indicator of the induction of chromosomal instability in the clone.

It is possible that a second or third aberration might occur spontaneously at a very low frequency. It has been shown that the spontaneous dicentric frequency in human cells is ~1 dicentric in 1000-2000 cells (122) and the spontaneous reciprocal translocation frequency is ~10x greater than that (1 in 100-200 cells) (118). Furthermore, the occurrence of a derived chromosome-type aberration in the daughter cells of an irradiated cell containing a chromatid aberration might also occur at a low frequency. In normal human cells irradiated in G₀/G₁, chromatid aberrations, mostly gaps and breaks, are seen in the 1st post-irradiation mitosis at a frequency of ~1 in 10 cells at 5 Gy for low LET radiation, whereas the frequency of chromosome-types after this dose may be as high as 10 to 15 in 10 cells. Chromatid-types could give rise to up to ~10% of clones with derived chromosome-type aberrations in half the cells and therefore two karyotypic subpopulations induced by the radiation exposure.

Therefore, we have chosen very strict criteria for radiation-induced instability in clones of cells surviving exposure. Our working definition is that a clone is scored as unstable if three or more karyotypically distinct subpopulations are present in 50 analyzed cells. The probability of seeing 2 spontaneous aberrations in 50 cells if each occurs at a frequency of 10^{-2} is extremely low. For example, if reciprocal translocations occur spontaneously at a frequency of 10^{-2} per cell per generation, then for two such events, the frequency would be $(10^{-2})^2 = 10^{-4}$ and therefore would likely not be detected in 50 scored cells.

We chose to study these clones using whole chromosome painting by fluorescence *in situ* hybridization (WCP- FISH) using a combination of chromosomes 1, 2, 4 and X paints. Chromosome libraries were pooled, labeled with digoxigenin and then hybridized to metaphase spreads from clonal populations of cells surviving radiation exposure and then expanded for 20-25 generations post-irradiation. After hybridization, the probes were detected using Rhodamine anti-digoxigenin and scored through a DAPI/rhodamine dual emission filter. This probe combination (1+2+4+X) covers approximately 30% of the human genome. Therefore, by scoring 50 cells per clone we were able to score >10 genome equivalents per clone, putting us in line with published reports using G-banding analysis of clones (72).

As a test of the validity of our analysis method, we initially repeated the experiments of Grosovsky and coworkers using the human tumor-derived lymphoblastoid cell line TK6 (72). In our brief analysis, two of nine clones surviving exposure to 2Gy ¹³⁷Cs γ -rays were determined to demonstrate chromosomal instability using our multi-probe FISH method due to the presence of three or more karyotypic subpopulations.

MATERIALS AND METHODS

Numerical Instability in Clones of HeLa Cells

S3 HeLa cells were incubated in F-12 medium (Gibco, Gaithersburg, MD) supplemented with 10% FBS (Summit, Ft. Collins, CO) in a 37°C, 5% CO₂ incubator. Near confluent cells were trypsinized and counted. 5×10^5 cells were inoculated into a T25 flask for mitotic cell collection. 100 cells were plated into each of 4 x 100 mm dishes and incubated for 8 days. Colonies of cells were then randomly picked and transferred to 6-well plates for expansion for an additional 10-14 days. Each of 12 expanded clonal populations was then trypsinized and subcultured into 2 x T25 flasks for continued expansion. After three days in culture, mitotic cells were collected from 1 x T25 flask for all 12 clonal isolates, ~21 generations after initial single-cell culture. After another three days the second T25 flask from three of the clones, A5, B3 and D4 was subcultured for mitotic collection at ~24 generations after initial inoculation. Clone D4 was then subcloned in the same manner as with the bulk parental population and mitotic cells from several clones were collected at ~43 generations from the initial single-cell inoculation. Chromosome number distributions were determined by staining metaphase spreads for 5 min with a 10% solution of Gurr's Giemsa R66 stain (Bio/medical Specialties, Inc., Santa Monica, CA) and counting the number of chromosomes in each of 100 cells per sample using a Zeiss Axioskop microscope (Carl Zeiss, Germany).

Chromosomal Instability in Clones of TK6 Cells

TK6 cells were incubated in RPMI-1640 (Gibco, Gaithersburg, MD) supplemented with 10% FBS (Summit, Ft. Collins, CO) in a 37°C, 5% CO₂ incubator. Log-phase cells were irradiated to a dose of 2 Gy using a 6000Ci J.L Shepherd Mark-1 ¹³⁷Cs irradiator at a dose rate of 3.9 Gy/min. Cells were then inoculated into 96-well plates at ~0.1 viable cells/well and incubated for 11 days. All detectable clones were then transferred to individual wells of 6-well plates and incubated an additional 4 days. The clones were then subcultured for mitotic collection. For each clone, 20% of the cells were inoculated into new 6-well plates and the remaining cells were cryopreserved for future study. Cells were incubated for 30 h at which time Colcemid (Gibco, Gaithersburg, MD) was added to each well to a final concentration of 0.1 µg/ml. All cells were collected and fixed 3.5 hrs later using standard fixation methods as described below. Fixed cells were dropped onto cold, wet ethanol rinsed slides, dried and aged at room temperature for >3 days up to a maximum of ~3 months. WCP-FISH was done on the slides as described below.

Isolation and Expansion of AG1521A Clones

Cell culture and irradiations were done as described in Chapter 2. The same initial cultures of cells were used in these experiments. Cells from control and irradiated pools were plated into 100 mm cell culture dishes at a viable cell density to yield ~25 clones after 10-14 days in culture. The location of each clone was then marked on the underside of the dishes and clones were transferred to

6-well plates, 1 clone/well, using sterile glass cloning cylinders sealed to the plates with sterile high vacuum silicone grease (Dow Corning, Midland, MI). Clonal isolates were grown an additional 7-10 days in the 6-well plates with fresh medium changes every 2-4 days. Upon reaching confluence or near confluence, the clones were then transferred to individual T25 flasks and incubated until confluent ($1-2 \times 10^5$ cells, ~20-25 post-irradiation generations, including corrections for cell death during subcultures). Upon reaching confluence, clones were trypsinized and 1/3 of the cells were replated for mitotic collection. The remaining 2/3 of the cells were frozen down for later analysis if necessary.

Metaphase Spread Preparation

Cells were incubated for 30 hr after inoculation. Colcemid (Gibco, Gaithersburg, MD) was added to the flask to a final concentration of $0.1 \mu\text{g/ml}$. Four to eight hours after colcemid addition, depending on the cell line, the cells were trypsinized, collected, spun down and incubated at 37°C in 12 ml 0.075M KCl hypotonic solution. Two ml of 3:1 methanol: acetic acid (Fix) was then added, followed by an additional 15 min incubation at room temperature (RT). The cells were again centrifuged. Next, we added 4ml of fix dropwise and incubated overnight at 4°C . The suspensions were centrifuged and resuspended in 4 ml fix for 10-15 min at RT. The suspension was again centrifuged and the cells were resuspended in 1-2 ml fix and dropped in $40 \mu\text{l}$ aliquots onto ethanol washed, cold, wet slides, followed by 3 x $40 \mu\text{l}$ fix rinses. Slides were then allowed to air-dry and stored at RT.

Chromosome Probe Preparation

Degenerate oligonucleotide primed (DOP) whole chromosome libraries for human chromosomes #1, 2 and 4 were kindly provided by Dr. Allen Christian of Lawrence Livermore National Laboratory. DOP-chromosome X library was created by microdissection by Dr. Mari Muhlmann-Diaz at CSU. PCR amplification was done in a 30 μ l volume containing 12U ThermoSequenase polymerase (USB), 26 mM Tris-HCl, pH9.5, 6.5 mM MgCl₂, 200 μ M each dTTP, dCTP, dATP and dGTP (ROCHE Molecular), 4 μ M Telenius primer (5'-CCGATCGAGNNNNNATGTGG-3') (MacroMolecularResources, Fort Collins, CO) and 100 ng combined 1, 2, 4 and X libraries in a ratio of 2:2:6:1. The reaction was run in a MJR Thermocycler (MJ Research, Boston, MA) using a profile of 95°C for 5 min followed by 15 cycles of 94°C for 1min, 56°C for 1min, 72°C for 3 min. This was followed by 5 min at 72°C and a hold at 4°C until samples were removed. Products were purified for labeling using Qiagen's Qiaquick PCR Purification Kit (Qiagen, Inc., Valencia, CA) following the manufacturer's instructions. The labeling reaction was done in a 50 μ l volume containing 10U Amplitaq LD polymerase, (Applied Biosystems, Beverly, MA) 26 mM Tris-HCL, pH 9.5, 6.5 mM MgCl₂, 4 μ M each dTTP, dCTP, dATP and dGTP (Roche Molecular, Indianapolis, IN), 4 μ M Telenius primer (MMR, Fort Collins, CO), 1 nmol digoxigenin-dUTP (Roche Molecular, Indianapolis, IN) and 10 ng pooled library DNA. The same reaction profile as above was used. No further purification was done on the products.

Fluorescence *in situ* hybridization

The digoxigenin-labeled PCR product was combined and mixed with a 20-fold excess of human Cot-1 DNA (Roche Molecular, Indianapolis, IN) and precipitated overnight at -4°C by adding $1/20^{\text{th}}$ volume 3M sodium acetate and 2x volume 100% ethanol. The probe mix was spun down, rinsed 2x in 70% ethanol, dried and resuspended in a hybridization mixture. The hybridization mixture consisted of 50% formamide, 30% SSC and 20% dextran sulfate. Coded, aged (3 days to 3 months at room temperature) slides were dehydrated in an ethanol series consisting of 2 min rinses in 70, 85 and 100% ethanol. The slides were air-dried and then denatured in 70% formamide, 30% 2xSSC at 72°C for approximately 2-3 min, depending on the age of the slides. The slides were then dehydrated in the same ethanol series and air-dried. While the slides were being prepared, the hybridization mixture was denatured in a thermocycler by heating to 84°C for 10 min followed by a 45-60 min hold at 37°C to allow reannealing of repetitive sequences between the unlabeled Cot-1 DNA and the labeled repetitive DNA in the probe. Next, 10 μl of hybridization cocktail was then placed on the target area of each of the prepared slides and a 22x22 mm coverslip was placed over the hybridization mix and sealed with rubber cement. The slides were placed in a sealed box and incubated for 18-36 hrs in a 37°C warm room. Following incubation the coverslips were gently removed and the slides were immediately immersed in 0.4x SSC/0.3% Igepal CA-630 (Sigma, St. Louis, MO) at 72°C . Slides were agitated for 1-3 seconds and removed after 2 min. The slides were

then rinsed in room temperature 2xSSC/0.1% NP-40 for 5 sec to 1 min. Next, the slides were rinsed 2x for 3min. each in 1x PN buffer at room temperature and 10 μ l of 5% nonfat dry milk in PN buffer were placed on the target area of each slide and covered with a 25x25 mm coverslip and left at room temperature for 5min. The coverslip was gently lifted and 10 μ l of 50 ng/ml rhodamine anti-digoxigenin (Roche Molecular, Indianapolis, IN) was placed on the target area of each slide. The coverslip was replaced and the slides were incubated for 20 min at 37°C in a humid chamber. The coverslips were then gently removed and the slides were again rinsed 2x in 1xPN for 3min per rinse. Finally, 10 μ l of antifade solution containing 42 ng/ μ l DAPI was dropped onto slide and covered with a fresh 22x22 mm coverslip. Metaphase spreads were then viewed and scored on a Zeiss Axioskop fluorescence microscope (Carl Zeiss, NY, NY) using a dual DAPI/rhodamine emission filter (Chroma Technology, Burlington, VT).

Image Acquisition

Metaphase spreads were photographed on an Olympus Provis AX70 fluorescence microscope (Olympus America, Melville, NY) equipped with a Photometrics SenSys cooled CCD camera (Photometrics, Tuscon, AZ). Images were acquired and processed using Applied Imaging's PowerGene MacProbe software (Applied Imaging, Santa Clara, CA)

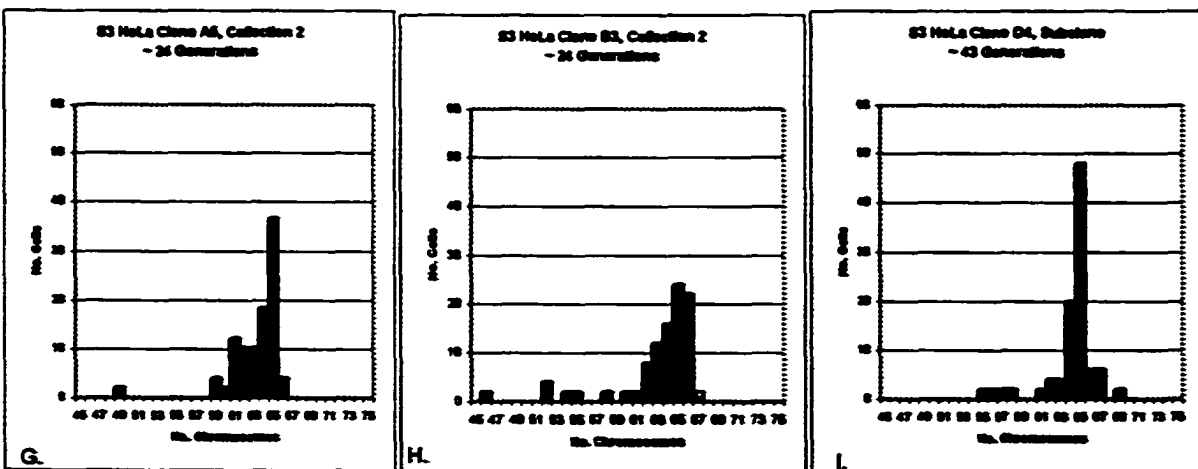
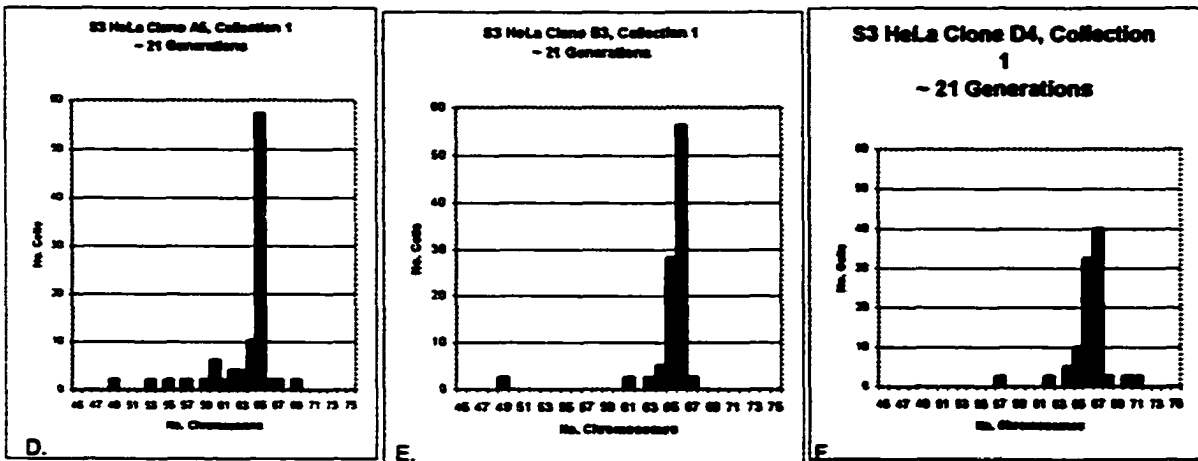
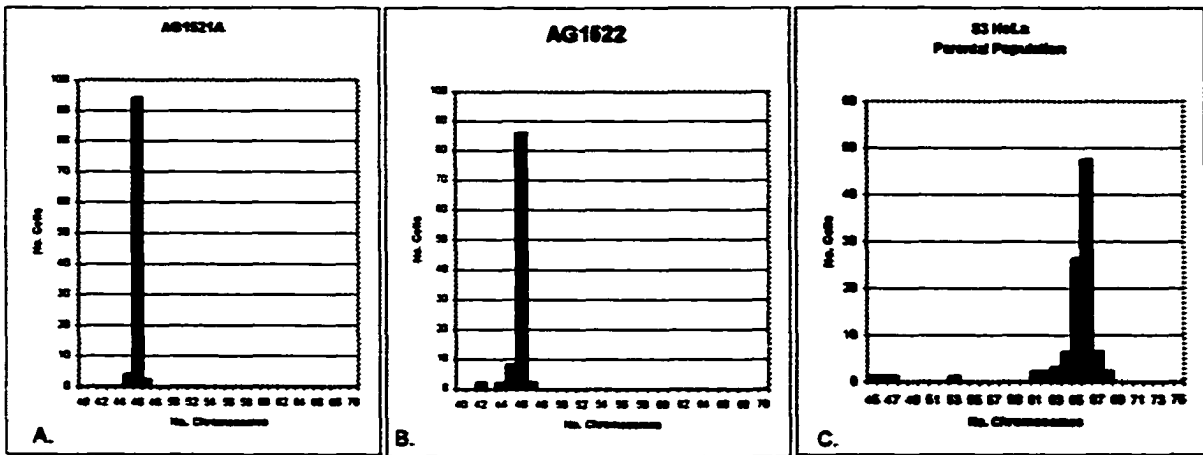
RESULTS

HeLa Cells: Assay for Numerical Chromosome Instability

Distribution of chromosome numbers among cell populations after isolation and expansion of primary and secondary HeLa cell clone populations are shown in Figure 3-1. Panels A and B show distributions of chromosome numbers for two phenotypically normal human diploid fibroblast cell lines, AG1521A and AG1522, respectively, both of which contain a modal number of 46 chromosomes, with a very tight distribution around this mode. Panel C shows the distribution for the S3 HeLa parental cell line determined after counting the chromosomes in 100 mitotic cells. Panels D, E and F depict the distributions for three primary clones, A5, B3 and distributions for two of these clones, A5 and B3, respectively, after further expansion to ~24 generations. Finally, panel I shows the distribution of a secondary subclone from the initial D4 clone that has been expanded for ~43 generations. Figure 3-2 shows a comparison of DNA histograms obtained by flow cytometric measurements of log-phase cultures of phenotypically normal AG1521A fibroblasts (panel A) and HeLa tumor cells (panel B). Despite a broader modal chromosome number per cell, the HeLa culture maintains a narrow G1 peak.

Figure 3-1

Numerical chromosome instability in HeLa clone pedigrees. Panels A and B indicate chromosome number distributions for apparently normal human fibroblast lines AG1521A and AG1522, respectively. Panel C shows the distribution of the S3 HeLa CCL2.2 parental line, while panels D, E and F show the distributions for three subclones (A5, B3, D4, respectively) expanded for ~21 generations. Panels G and H show the further expansion of clones A5 and B3, respectively, for an additional three generations. Panel I shows the distribution for a secondary subclone from the D4 clone that was expanded for a total of ~43 generations from the initial cloning inoculation.



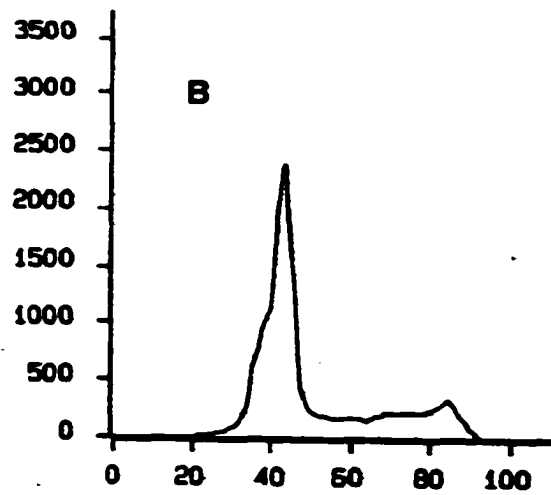
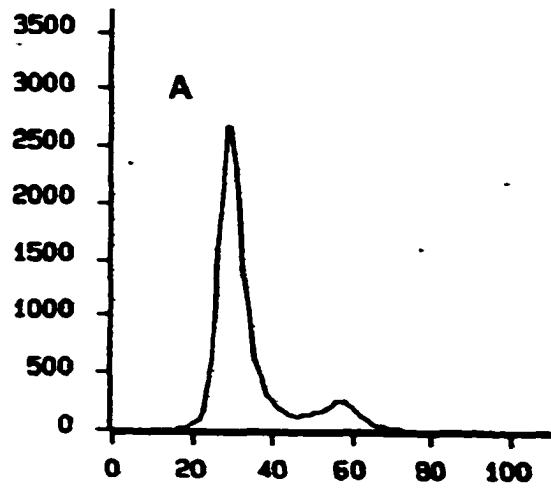


Figure 3-2

DNA histogram comparison between log-phase populations of AG1521A normal human fibroblasts (A) and S3 HeLa CCL2.2 cells (B).

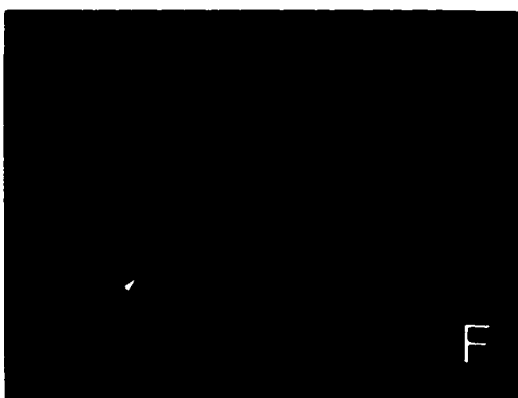
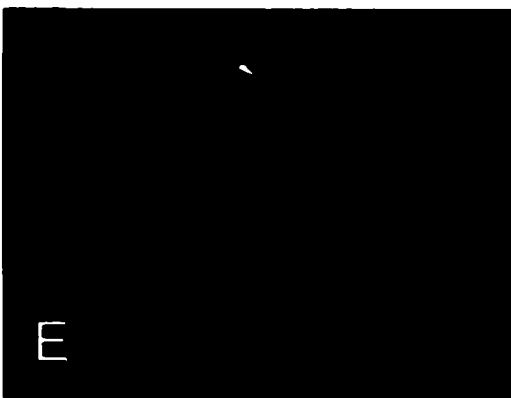
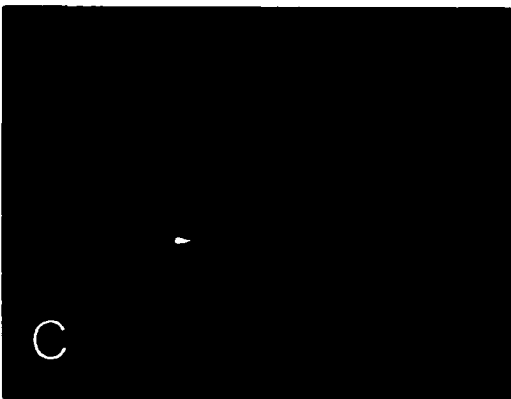
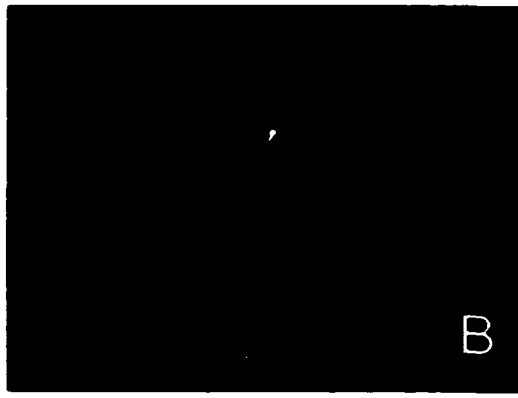
Normal AG1521A Human Fibroblasts: Assays for Radiation-induced Numerical and Structural Chromosome Instability

Figure 3-3 illustrates the combination of structural and numerical rearrangements found in an unstable AG1521A clone, designated 5 γ -41, selected after a dose of 5Gy of ¹³⁷Cs γ -rays. In 48 of 50 scored cells, aneuploidy was seen. In all 50 cells a reciprocal translocation involving 4q and an unlabeled chromosome was seen as shown in panel A, indicating that this was present in the original cell surviving the 5Gy dose. However, in one cell, one of the translocation products of the aberration was further involved in a dicentric with another unlabeled chromosome as shown in panel B. Additional aberrations were also seen in other cells in this clone. An "apparently non-reciprocal" translocation (panel C), a dicentric involving two unlabeled chromosomes (panel D), a chromatid break (panel E) and a dicentric involving chromosome 2 and an unlabeled chromosome (panel F) were among other aberrations also detected in cells from this clone.

Figure 3-4 shows the frequency of clones scored that were classified as unstable. These results were derived from scoring a total of 90 control and sample clones. The numbers above the columns indicate the number of unstable clones (numerator) and the total number of clones (denominator) scored for that sample. Error bars are 95% confidence intervals using Poisson statistics as described by Johnson and Kotz (123).

Figure 3-3

Chromosomal instability in AG1521A clone 5 γ -41. Aneuploidy was detected in 48 of 50 cells scored. A reciprocal translocation involving chromosome 4 and an unlabeled chromosome indicated by arrow in panel A, this aberration was found in all 50 cells, except where a second aberration was found involving it as seen in panel B where one half of this aberration is also involved in a dicentric, as indicated by the arrow. A non-reciprocal aberration was also detected in a cell as shown in panel C. Panel D shows a dicentric chromosome involving two unlabeled chromosomes, while a chromatid break is shown in panel E and a dicentric involving chromosome 2 and an unlabeled chromosome is shown in panel F.



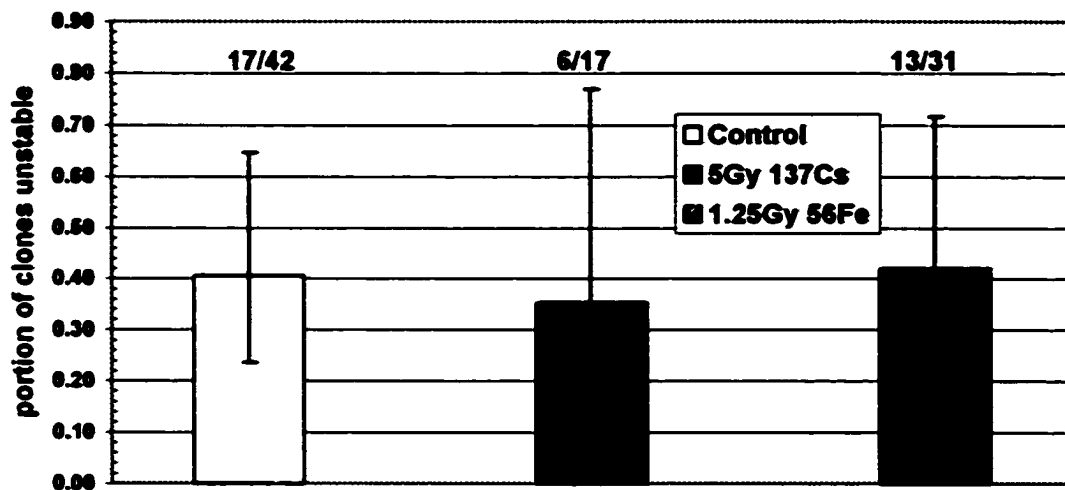


Figure 3-4

Proportion of AG1521A clonal populations scored as unstable after analysis of 50 mitotic cells using WCP-FISH with probes for chromosomes 1, 2, 4 and X. Clonal populations were derived from individual cells isolated and expanded for approximately 25 generations after exposure to ionizing radiation. Numbers above bars are unstable clones/total clones scored. Error bars are 95% confidence intervals using Poisson statistics.

Figure 3-5 shows a breakdown of the analyzed clones by sample and number of karyotypic subpopulations, 1, 2 or greater than or equal to 3, in 50 cells for each clone scored.

Figure 3-6 shows a breakdown of the kinds of abnormalities in unstable clones by sample and whether the clone contained numerical aberrations only (N), structural aberrations only (S) or a combination of both types, i.e. mixed (M), in situations where a clone contained cells with both structural and numerical aberrations. In some cases, an individual cell within a clone may have contained both structural and numerical aberrations, as seen in Figure 3-3. However, in other cases, individual cells within a clone may have contained either a structural or a numerical aberration, but overall the clone was scored as mixed due to the presence of both classes of aberrations.

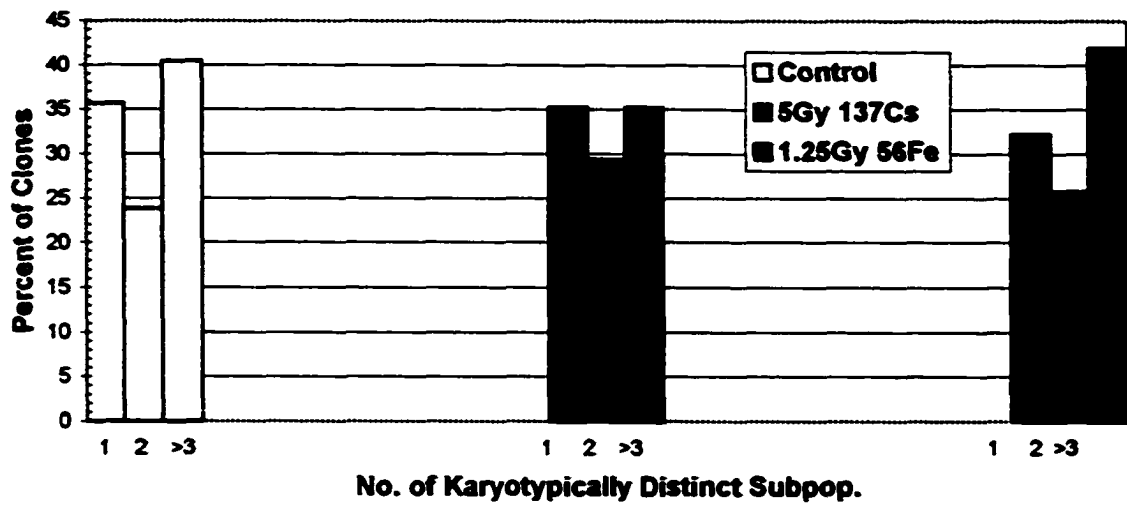


Figure 3-5

Percentage of total clones scored as a function of the number of karyotypic subpopulations.

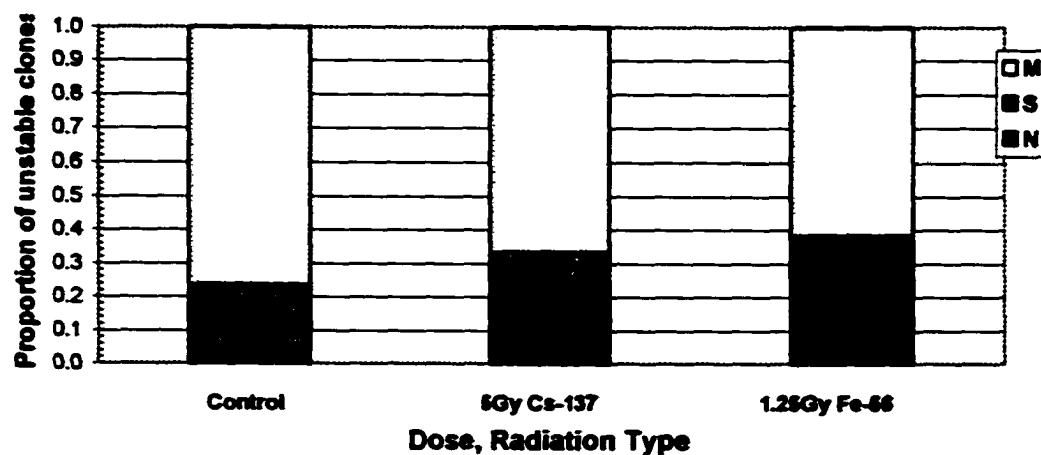


Figure 3-6

Frequency of unstable clones containing numerical aberrations only (N), structural aberrations only (S) or mixed (M) populations of numerical and structural aberrations.

DISCUSSION

The phenotypically normal human diploid fibroblast cell lines, AG1521A and AG1522, maintained a discrete chromosome number distribution near 46 chromosomes/cell in low passage bulk culture, while S3 HeLa cells show a broader distribution with a modal number of 65-66 chromosomes/cell. Cloning of individual HeLa cells, each of course possessing a discrete chromosome number, leads to numerical instability within the first 20 generations after isolation of the cell which is virtually the earliest time the distribution can be measured. By this time there is already a broad chromosomal number/cell distribution similar to that seen in the original parent population. Furthermore, this same distribution is then maintained many generations without further spread of the distribution. It is interesting that this spread in chromosome number is not also reflected by a broad G1 peak in a DNA histogram obtained from flow cytometric analysis of a log-phase population of cells, as shown in Figure 3-2. It can be seen in this figure that the HeLa culture (B) has a narrow G1 peak similar to the AG1521A culture (A). These results indicate that the selection of a stable tumor cell line with regard to DNA content per cell has occurred after some initial numerical instability, even though there is a fairly broad range of chromosome number per cell among cells in the populations.

For the initially normal AG1521A human fibroblast cells, we have analyzed numerous control and sample clones for the occurrence of radiation-induced chromosomal instability. Our results indicate that there is no biologically significant difference in the frequency of unstable clones, comparing clones

derived from either control or irradiated cells. In both control and irradiated cells, clones containing cells with numerical (aneuploidy, tetraploidy, polyploidy) and/or structural aberrations were seen. The structural aberrations were mainly dicentrics, but also exchanges and chromatid aberrations or a combination of both. Since I only looked at approximately 30% of the genome with our chromosome paints, it is possible that a higher frequency of symmetrical exchanges existed in the clones, but went undetected due to lack of probe coverage. Levels of instability in individual clones ranged from our minimum criteria, which is three karyotypically distinct subpopulations up to clones where nearly every cell was karyotypically different. Aneuploidy and increased levels of dicentrics have also been found to occur in human fibroblasts as they approach senescence (119) (105). Bacchetti and coworkers demonstrated that an increase in dicentric chromosome frequency at senescence in human embryonic kidney (HEK) cells was associated with critically short telomeres (124)

The cells that were initially cloned varied in age at the time of their initial inoculation prior to isolation. Cells inoculated for colony formation were anywhere from 25-35 generations old. Upon reaching confluence in a T25 flask, these cells were from 50-60 generations old. It might be possible that this age difference had an additional adverse effect on some of the samples. In fact, we were unable to clone control cells from one experiment in which the cells were >35 generations old at the time of irradiation, similar to previously published reports (125). Therefore, we cloned and expanded passage 5 (P5) cells that were ~20 generations old at inoculation. This is currently the earliest available generation

for this cell line as the supply of earlier generations is now exhausted. Upon reaching confluence in a T25 flask, these cells were then ~45 generations old. Even in this case, a very high frequency of unstable clones was detected (7 unstable clones out of 22 clones scored or 32%). Therefore, it does not appear that cell age at inoculation has a great affect on the final instability frequency, although it may affect the ability to obtain viable clones.

Attempts to clone control and irradiated cells from the BNL-5 run yielded unexpected results. These cells were approximately 30-35 generations old at irradiation and cloning. I was unable to collect any control clones from two cloning attempts involving plating a total of 2800 cells at densities of 200-600 cells/dish. Thirteen clones from irradiated cells were collected in one attempt after plating 10^4 cells at 2.5×10^3 cells/dish. In a second attempt, zero clones were collected after plating 2.2×10^4 cells. The fact that no control clones were collected is not unexpected since previous reports have shown this effect in attempts to clone older cells (125). What was surprising, however, was that clones were isolated from the irradiated cell population. It would appear that in this case the exposure to IR may have conferred an extended lifespan over the control cells as reported by others (62). However, of the 11 clones from the irradiated population that were scored, six were chromosomally unstable and their instabilities contained all the hallmarks of senescent cells, including telomeric association dicentrics, aneuploidy and polyploidy. Of the five other analyzed clones, no aberrations were detected in three clones, one clone had one tetraploid cell and the other clone contained two tetraploid cells.

It is interesting to note a comparison here between the mixed population experiments and the clonal isolate experiments. At ~25 generations post-irradiation, the clones were showing very high levels of instability, near 40% for control and sample clones. The mixed populations, however, did not show a corresponding level of instability at this same cell age. This is evident from both the chromatid-type aberration data and the WCP-FISH data for both ^{137}Cs and ^{56}Fe -irradiated samples. In the mFISH analysis of ^{56}Fe -irradiated mixed population cells, we begin to see similar types of karyotype changes at 45 post-irradiation generations in both the controls and the samples. Perhaps the process of cloning this particular cell line induced elevated levels of stress to the cells that manifested itself as chromosomal instability in the clonal isolates in a shorter time frame than in the mixed populations.

In conclusion, clones of AG1521A normal human fibroblast cells surviving exposure in G_0 to 1.25Gy of 1GeV/nucleon ^{56}Fe particles or 5Gy of ^{137}Cs γ -rays did not contain elevated levels of chromosomal instability compared to parallel samples drawn from unirradiated control clones. Some extension of lifespan may have been induced by the exposure of G_0 cells to ^{56}Fe nuclei as seen with the BNL-5 cloning experiment, although many of these clones showed a pattern of instability similar to that of control clones. We feel that the chromosomal instabilities seen in the control and irradiated clones were due to aging effects, probably involving telomere shortening at senescence similar to that seen in the mixed population study and that the cloning of these cells accelerated the effect compared to the mixed populations. It appears from our results in phenotypically

normal AG1521A human fibroblast cell cultures that exposure of non-cycling cells to either ^{137}Cs γ -rays or 1 GeV/nucleon ^{56}Fe particles did not induce a transmissible chromosomal instability in the progeny of cells surviving the exposures; at least at the level of resolution of these experiments. Exposure to 1 GeV/nucleon ^{56}Fe particles may have extended the lifespan of some surviving cells, as seen in the BNL-5 clones; however, cells from these clones eventually became senescent in a manner similar to controls. The cloning of cells in these experiments had the apparent effect of accelerating senescence, regardless of whether or not a lifespan extension had been induced by IR.

CHAPTER 4

Chromosomal Aberrations in G₀-irradiated GM7166A Nijmegen Breakage Syndrome Fibroblasts

ABSTRACT

Nijmegen Breakage Syndrome is a recessively inherited genetic disorder and among other things is characterized by hypersensitivity to ionizing radiation and chromosomal instability. NBS1 (nibrin or p95), the product of the NBS1 gene, complexes with Rad50 and Mre11 in response to DNA damage, especially double-strand breaks and is required for cell cycle control and possibly telomere maintenance during S-phase. The defect in DNA repair and the resulting hypersensitivity to ionizing radiation in cells from NBS patients led us to hypothesize that exposure to ionizing radiation may lead to elevated levels of complex aberrations at doses considerably lower than would produce a similar effect in repair competent cells. Therefore, as an initial step in comparing radiation-induced chromosomal instability in a repair deficient human cell against our previous research in repair competent human cells, we analyzed 1st post-irradiation mitotic cells for various aberration frequencies including complex exchange aberrations. Our results indicate that the GM7166 NBS fibroblasts contain an elevated frequency of spontaneous chromatid-type as well as chromosome-type aberrations, and are hypersensitive with respect to radiation-induced chromatid-type and chromosome-type aberrations compared to a

phenotypically normal human fibroblast, AG1521A. An elevated level of endoreduplication was also observed in the irradiated NBS cells. Finally, the proportion of radiation-induced aberrations that were complex was higher in the NBS fibroblasts than previously reported for normal lymphocytes as determined by mFISH analysis. These results suggest that the major defect in this NBS cell line concerns the ability to correctly repair DNA damage and leads to elevated levels of both simple and complex aberrations after exposure to ionizing radiation.

INTRODUCTION

Maintenance of genomic integrity in cells that experience continuous endogenous and/or exogenous DNA damaging insults requires the coordinated functions of many repair and cell-cycle checkpoint systems in a way that is only just beginning to be appreciated. The breakdown of this process can lead to genomic and chromosomal instability and eventually even to tumorigenesis. Several syndromes have been diagnosed in which the fidelity of one or more of these processes has been compromised. For the most part these result from autosomal recessive inherited genetic diseases and occur at very low frequencies in the general population. These syndromes are collectively referred to as chromosomal instability syndromes and include, for example, Ataxia-telangiectasia (AT), BRCA1/BRCA2, Werner's syndrome, Nijmegen Breakage Syndrome (NBS), Bloom's syndrome, Li-Fraumeni syndrome, Fanconi anemia and Xeroderma pigmentosum (XP). Mutant alleles of these genes generally play some role in DNA damage repair. Phenotypic effects include chromosomally unstable genomes and a predisposition of the affected individual to cancer. These include lymphomas and leukemias in the case of AT, NBS and Bloom's syndrome (reviewed in (126) and (127)), sarcomas, breast cancer and brain tumors in the case of Li-Fraumeni syndrome (reviewed in (128)), acute myeloid leukemia in Fanconi anemia (reviewed in (127)) and sunlight-induced skin cancers in XP patients (reviewed in (129)). The affected individuals, or probands, in some cases also tend to be hypersensitive to ionizing radiation and are at elevated risk for second cancers from radiation therapy. Furthermore, although

the frequency of affected individuals may be low, the numbers of carrier individuals can be relatively high in the population and they may also be at risk for radiation sensitivity and cancer. Further, there are many genes that can lead to cancer proneness as a result of DNA damage processing defects, so collectively the problem is much larger than for any one disorder. It is also noteworthy that heterozygosity, which occurs at a much higher frequency, may also result in increased cancer risk. For example, AT heterozygotes are believed to comprise up to 1% of the general population (130) (131) and their radiosensitivity and susceptibility to cancer has been shown to be elevated (132) (130).

Ataxia-telangiectasia was first described as a disease in the late 1950's by Boder and Sedgwick (133) and reviewed in (134). The AT gene, *ATM* (mutated in A-T), is located on chromosome 11q22-23 and produces a 350kDa protein kinase that is a member of phosphatidylinositol-3-kinase (PI 3-kinase) family (135). DNA-PKcs, ATR, Mei-40 (*D. melanogaster*), Mec1 (*S. cerevisiae*) and Rad3 (*S. pombe*) are other members of this family and all have some function in maintaining genomic integrity (reviewed in (126)).

ATM is believed to be an overseer of DNA damage and activates a number of response pathways after damage has been detected (136) (137). *ATM* phosphorylates p53 leading to a G1 cell cycle checkpoint (138). G1, S and G2 checkpoints are activated by *Atm* phosphorylation of Chk1 and Chk2 proteins (139) and reviewed in (140). Additionally, *ATM* has been shown to phosphorylate p95/nbs1/nibrin in response to ionizing radiation (141) (142) (142) (143).

Nijmegen Breakage Syndrome (NBS) was first described by Taalman and coworkers in 1983 (144). They observed elevated levels of spontaneous and radiation-induced chromatid-type and chromosome-type aberrations in NBS fibroblasts compared to fibroblasts from a phenotypically normal individual and elevated levels of chromatid breaks in G2/S-irradiated NBS lymphocytes compared to normal lymphocytes (144). Cultured T cells from NBS patients often contain rearrangements involving chromosomes 7 and 14 at the same breakpoints as in AT cells (145) which (perhaps not coincidentally) are where the immunoglobulin and T-cell receptor genes are located (146).

The gene for NBS has been mapped to chromosome 8q21 (147) (148) and encodes a 95 kDa protein that contains a forkhead-associated (FHA) domain and a breast cancer carboxy-terminal (BRCT) domain (149) (150). Proteins with FHA and BRCT domains have been shown to function in DNA replication, repair and in cell cycle checkpoints (reviewed in (151)). This protein, p95/nibrin/NBS1, has been shown to complex with the hMre11/hRad50 protein complex (149) in an ATM dependent manner in response to DNA double strand breaks (141) (142) (142) (143). The phosphorylation of NBS1 by ATM serves to inhibit DNA synthesis (142) and may serve as an initiating step in homologous recombination repair and/or non-homologous end-joining repair of DNA double strand breaks (reviewed in (140)) or "as a key organizer that determines the type of processing to be used on double-strand breaks" (152).

The high spontaneous frequency of chromatid-type and chromosome-type aberrations identified in NBS cells (144) (153) combined with reports suggesting

that a lack of cell-cycle delay may not account for the high radiosensitivity of NBS cells (154) led us to hypothesize that the defect in DNA double strand break repair response caused by the mutation in the NBS gene may lead to elevated frequencies of complex chromosome exchange aberrations and that this increase in aberrations might at least partly account for the radiation hypersensitivity of NBS cells. The best approach to test this idea would be to utilize multiplex fluorescence *in situ* hybridization (mFISH) of 1st post-irradiation mitotic cells.

The advent of fluorescence in situ hybridization (FISH) (155) led to the determination that a significant fraction of chromosome exchange aberrations were actually complex in nature and often involved many more than two chromosomes. A complex exchange aberration is defined as an aberration involving three or more breaks in two or more chromosomes (156). Simpson and Savage irradiated confluent HF12 human fibroblasts with 4Gy of X-rays, subcultured them at a lower cell density and then collected the 1st mitotic cell population. These mitotic cells were then analyzed by FISH for exchange aberration frequencies and complex exchange aberrations. They estimated that 35% of the exchanges scored were complex in nature (156). This group then went on to examine complex exchange aberration frequencies induced by exposure to increasing doses of ²³⁸Pu α -particles in the same cell line. In this case they determined that complex exchange aberrations accounted for 38–47% of all the exchange aberrations (157). It is noteworthy that with a single or even two-color FISH many of the complex aberrations are still invisible and are seen

as "apparently simple." This group later showed that a dose effect does exist for low LET radiation and that the proportion of aberrations that were complex increased as the dose increased (158).

The development by two groups in 1996 (159) (160) of combinatorial labeling schemes and computer software to analyze the labeling patterns has allowed for the identification of all homologous human chromosomes in mitotic cells as distinct, pseudocolored pairs. This has allowed for genome-wide assessment of simple and complex exchange aberrations in tumor specimens and more recently in human lymphocytes exposed to ionizing radiation (161). Loucas and Cornforth used mFISH analysis to identify simple and complex chromosome aberrations in human lymphocytes exposed to doses of ^{137}Cs γ -rays ranging from 0 to 4Gy. They determined that for low LET radiation exposure, a dose-effect was present for the formation of complex exchange aberrations. The fraction of complex exchange aberrations on a per exchange aberration basis rose from 0.0 at 0Gy to 0.14 at 1Gy and to 0.26 at 4Gy. Furthermore, they showed that the fraction of cells containing at least one complex exchange also increased with dose and that at 4Gy, almost half the cells contained at least one complex exchange (161).

Finally, to determine if entry of confluent, G₀-irradiated cells into the cell cycle has any effect on the formation of complex exchange aberrations, or if they form during the initial repair process, regardless of any cell cycle effects, I initiated a pilot study analysis of G₀ prematurely condensed chromosomes (PCCs) hybridized with mFISH probes. The PCC technique was first described

by Johnson and Rao in 1970 (162) and involves the fusion of mitotic HeLa or CHO cells (inducer cells) to interphase cells via Sendai virus or polyethylene glycol. The inducer cells cause the chromosomes in the interphase cells to condense and allows for the cytogenetic analysis of G1 and G2 chromosomes. This technique has been used to show that in G1 irradiated HeLa cells a much higher frequency of chromosome breaks is detected in G1 PCCs than in cells entering the 1st post-irradiation mitosis (163). Cornforth and Bedford improved this technique by incorporating BrdU into the HeLa inducer cells and using differential staining to quench the signal of the HeLa inducer cells (164). This technique has also been used to study initial chromosome exchange aberration frequencies in noncycling AG1522 human fibroblasts exposed to 6Gy of ¹³⁷Cs γ -rays using FISH (165) (166) and more recently in the blood lymphocytes of astronauts after varying periods of space travel (167). However, the application of mFISH analysis to a comparison of noncycling cells after exposure to ionizing radiation against cells allowed to cycle through to the next mitosis appeared to present an efficient method to test whether complex exchange aberration formation required the cellular machinery involved in entrance into the cell cycle or formed at a high frequency prior to exit from G0 and was therefore due exclusively to the DNA damage response.

MATERIALS AND METHODS

Cell Culture

Frozen passage-8 AG1521A normal human fibroblasts, which had been derived from expanded cultures of low passage number (P4-P5) cells obtained from American Type Culture Collection (ATCC) were thawed and inoculated into a T25 flask. Cells were cultured in α -MEM medium (Gibco BRL, Gaithersburg, MD) supplemented with 15% fetal bovine serum (FBS) (Summit Labs, Ft. Collins, CO) and incubated at 37°C in a humidified atmosphere of 5% CO₂ in air. Confluent T25 flasks were split 1:10 into new T25 flasks. Passage-8 GM7166A cells originally from a 20 year old NBS-affected female, whose phenotype included short stature, microcephaly and developmental delay were obtained from ATCC. The subject was found to be homozygous for a deletion of 5 nucleotides in exon 6 of the NBS1 gene, which resulted in a frameshift and premature termination at codon 218. NBS cells were cultured in α -MEM medium (Gibco BRL, Gaithersburg, MD) supplemented with 15% fetal bovine serum (FBS) (Summit Labs, Ft. Collins, CO) and 2x essential and non-essential amino acids and 2x vitamins (Gibco BRL, Gaithersburg, MD). Cells were incubated at 37°C in a humidified atmosphere of 5% CO₂ in air. Confluent T25 flasks were split 1:3 into new T25 flasks. Upon reaching confluence again, fresh medium was added to the flask and cells were incubated for an additional 4 days prior to irradiation.

Irradiations

Confluent, non-cycling T25 flasks were irradiated using a 6000Ci JL Shepherd Mark-1 ¹³⁷Cs irradiator (JL Shepherd, CA) at a dose rate of 3.9 Gy/min. The dose rate was obtained from the slope of a calibration curve created from data obtained by thermoluminescence dosimetry (TLD) readings over a range of exposure times from 0.01 to 0.1 min. Flasks were then returned to incubators for 24hrs to allow for complete DNA repair.

Premature Chromosome Condensation

For induction of premature chromosome condensation, we used a procedure similar to that described by Cornforth and Bedford (164). 2×10^6 HeLa cells were plated into T175 flasks, 1 flask/PCC sample, two days prior to the PCC experiment. Thymidine was added to HeLa medium to a final concentration of 2.5 mM 24 hrs prior to the fusion to block cycling cells in G1. After 12 hrs, flasks were rinsed with glucose-free Hank's balanced salt solution (HBSS-G) to remove thymidine and allow the cells to reenter the cell cycle and after adding fresh medium, they were incubated for an additional 7-8 hrs to proceed through S-phase. Loose cells were then lightly shaken off and removed and fresh medium containing Colcemid (Gibco BRL, Gaithersburg, MD) at a concentration of 0.1 μ g/ml was added back. The HeLa cells were then incubated to collect mitotic cells for an additional 5-6 hrs. Approximately 24 hrs after irradiation, coinciding with the end of the colcemid block of the HeLa cells, the normal human AG1521A

and GM7166 NBS sample cells were trypsinized and counted. 10^6 cells were set aside for PCC experiment. The remaining cells were reinoculated into T75 flasks for collection of 1st post-irradiation mitotic cells. HeLa mitotic cells were shaken off by modest agitation, collected and counted. Sample and HeLa cells were rinsed 2x in ice-cold HBSS-G containing 0.1 μ g/ml Colcemid and resuspended in 5 ml of the same and kept on ice. For each sample, 10^6 sample and 10^6 HeLa mitotic cells were combined in a tube and centrifuged. They were resuspended in 0.5 ml HBSS-G containing 0.1 μ g/ml Colcemid and UV-inactivated Sendai virus was added to a final load of 200 HAU/ml. The cell suspension was gently mixed and placed back on ice for 15 min. The samples were then gently centrifuged by hand spinning and placed in a 37°C waterbath for 10 min. Next, 5ml of HBSS-G containing 0.1 μ g/ml Colcemid was then added to each tube and the tubes were further incubated for an additional 50 min at 37°C to provide adequate PCC condensation. The suspensions were then split in three, spun down and resuspended in 12 ml of 0.075M KCl hypotonic solution and incubated at 37°C for 20 min. Two ml of freshly prepared 3:1 methanol:acetic acid (fix) was then added, followed by an additional 15 min incubation at room temperature. The cells were centrifuged again. Next, 4 ml of fix was added dropwise and incubated for 15 min at room temperature. This step was then repeated. Finally, the cells were resuspended in 1-2 ml of fix and dropped onto cold, wet, ethanol-washed microscope slides. Slides were then aged at room temperature for up to one week. Slides older than one week tend to produce poor mFISH hybridizations and were therefore not used.

Mitotic Cell Collection and Giemsa Staining

Two T75 flasks, each containing 5×10^5 cells per sample were incubated for 30 hrs after inoculation of suspensions of the G_0 treated or untreated cells. Colcemid (Gibco, Gaithersburg, MD) was then added to one flask/sample to a final concentration of $0.1 \mu\text{g/ml}$. Cells were incubated an additional 6–8 hrs, trypsinized and fixed using method described above. After 36 hrs, Colcemid was added to the 2nd flask, again at $0.1 \mu\text{g/ml}$. This flask was also incubated for an additional 6–8 hrs and then cells were harvested and fixed. Fixed cell suspensions were dropped onto cold, wet ethanol-rinsed slides and allowed to air-dry overnight. Slides were then coded and stained in 10% Gurr's Giemsa solution for 4 min, washed with deionized H_2O and air-dried.

BrdU Incorporation and Detection

In one experiment a parallel 2Gy-irradiated NBS sample contained 10^{-5} M 5-bromo 2'-deoxyuridine (BrdU) (Sigma, St. Louis, MO) in the medium from 4 hrs prior to irradiation until subculturing the following day. This was done to determine the proportion of cycling cells in the culture and the proportion of mitotic cells scored that might have been in S-phase at the time of irradiation rather than in G_1 or G_0 . Mitotic cells from this sample were collected and fixed in parallel with the samples used for scoring. Slides were aged for two to seven days at room temperature and were then denatured in 70% formamide, 2x SSC at 70°C for 2 min, rinsed 2x for 3 min/rinse in 2x SSC and hybridized with mouse monoclonal anti-BrdU, clone BU-33 (Sigma, St. Louis, MO) for 20 min in a

humidified chamber at 37°C. Slides were then rinsed 2x for 3 min/rinse in 1xPN buffer and hybridized with goat anti-mouse IgG FITC conjugate (Sigma, St. Louis, MO) for 20 min in a humid chamber at 37°C. Slides were again rinsed 2x in 1xPN buffer and 30µl of antifade solution containing 42 ng/µl DAPI was placed on the slide and covered with a 22x50 mm coverslip. A total of 1000 interphase and mitotic cells were scored for BrdU incorporation to determine labeling indices and an additional 400+ mitotic cells were scored for BrdU incorporation to determine a labeled mitotic index.

Multiplex FISH (mFISH)

Vysis' SpectraVysion Assay mFISH probe set (Vysis, Downers Grove, IL) was used following the manufacturer's instructions, with slight modifications as described in chapter two.

RESULTS

Giemsa Staining: Classical Scoring of Aberrations

The first experiment using the parallel sample of NBS cells containing BrdU before and after irradiation was scored for labeling index and labeled mitotic index using a FITC/Texas red/DAPI triple band-pass filter on a Zeiss Axiophot fluorescence microscope. A total of 1000 cells (mitotic and interphase) were scored of which a total of 33 were stained for BrdU incorporation for a labeling index of 3.3%. Additionally, 404 mitotic cells were scored of which 4 were stained for BrdU incorporation for a labeled mitotic index of 1%. The samples scored for aberrations in the first post-irradiation mitosis could not, therefore, have derived from more than a 1% contamination of S-phase cells.

The summary of aberrations scored is tabulated in Table 4-1 and the results are plotted in Figure 4-1. Data for AG1521A cells is for one experiment, while data for NBS cells is pooled from two experiments.

Table 4-2 compares the endoreduplication (ER) frequencies determined for our samples. Only the irradiated NBS sample contained endoreduplicated cells.

mFISH Analysis of Aberrations

First post-irradiation mitotic cells from unirradiated and 2Gy irradiated NBS fibroblasts were analyzed by mFISH and the results are given in Table 4-3. Chromatid-type aberrations in 2Gy irradiated NBS cells were detected at a frequency of 0.53 per cell, slightly higher than in the control population, 0.31/cell. In the irradiated population of NBS cells, chromosome-type aberrations

Table 4-1

Frequency of first division aberrations detected in AG1521A normal fibroblasts and GM7166A NBS fibroblasts analyzed by classical scoring after Giemsa staining. Cells were irradiated in confluent, non-cycling culture and subcultured 24 hrs later.

Cell line		AG1521 (normal)			GM7166 (NBS)	
Dose (Gy)		0	2	6	0	2
No. scored		100	100	100	200	250
Chromatid-type (per cell)	Gaps	0.02	0.01	0.05	0.05	0.14
	Breaks	0.05	0.08	0.07	0.4	0.61
	Exchanges	0.0	0.0	0.0	0.04	0.09
	Total chromatids	0.07	0.09	0.12	0.49	0.86
Chromosome-type (per cell)	Int del/ac. Ring	0.0	0.09	0.43	0.01	0.24
	Term. del	0.0	0.02	0.08	0.01	0.1
	Centric rings	0.0	0.01	0.1	0.0	0.05
	Dicentrics	0.0	0.17	0.93	0.02	0.58
	Total chromosomes	0.0	0.2	1.57	0.04	0.98
	Induced		0.2	1.57		0.95

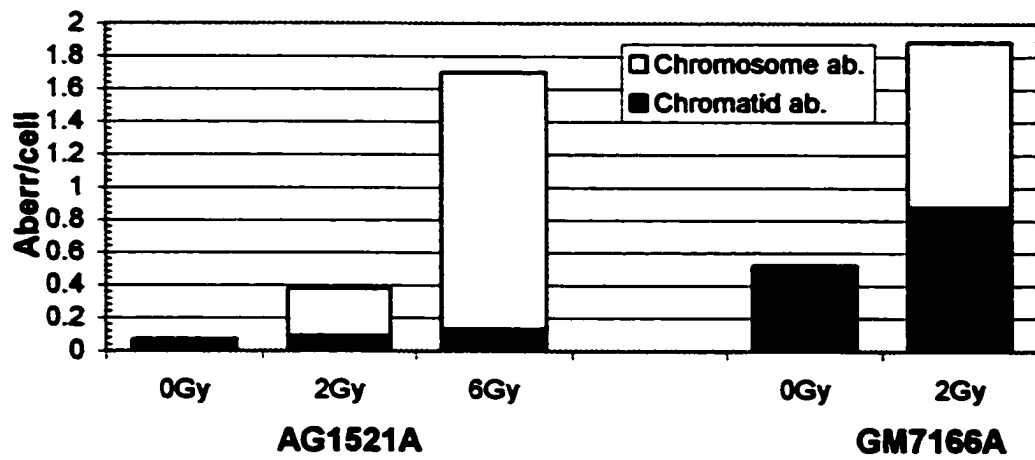


Figure 4-1

Comparison of total aberration frequencies between phenotypically normal AG1521A fibroblasts and GM7166A NBS fibroblasts determined by scoring Giemsa stained 1st post-irradiation mitotic cells after G₀ irradiation.

Table 4-2

Frequency of endoreduplicated mitotic cells detected in unirradiated and irradiated AG1521A and GM7166A fibroblast cultures in the first post-irradiation mitosis.

Sample	No. mitotics scored	No. ER mitotics	Freq ER mitotics
AG1521A 0Gy	400	0	0
AG1521A 2Gy	400	0	0
AG1521A 6Gy	314	0	0
GM7166A 0Gy	353	0	0
GM7166A 2Gy	653	11	0.017

Table 4-3

Frequency of first division aberrations detected in GM7166A NBS fibroblasts analyzed by mFISH. Cells were irradiated in confluent, non-cycling culture and subcultured 24 hrs later. AG1521A data is taken from 10th and 30th post-irradiation generation mixed population samples from experiment Fe-1 described in Chapter 2.

Cell line		AG1521 (normal)	GM7166 (NBS)	
Dose (Gy)		0	0	2
No. scored		84	42	40
Chromatid- type	Gaps	0	1	0
	Breaks	0	12	21
	Total chromatid (/cell)	0	13 (0.31)	21 (0.53)
	Induced (/cell)			8 (0.2)
Chromosome- type	Int del/ac. Ring (/cell)	0	2 (0.05)	14 (0.35)
	Term. del (/cell)	1 (0.01)	3 (0.07)	9 (0.23)
	Dic. (/cell)	0	3 (0.07)	18 (0.45)
	Centric rings (/cell)	0	1 (0.02)	0 (0.0)
	Symm. Exch. (/cell)	1 (0.01)	12 (0.29)	25 (0.63)
	Complex Exch. (/cell)	0	1 (0.02)	17 (0.425)
	Other (/cell)	0	4 (0.1)	1 (0.025)
	Total chromosomes (/cell)	2 (0.02)	26 (0.62)	84 (2.1)
	Induced (/cell)	0		58 (1.48)
	Total Aberrat (/cell)	2 (0.02)	36 (0.86)	105 (2.63)
	Induced (/cell)			66 (1.77)
	Induced complex (/cell)			16 (0.04)
	Induced complex per induced exchange			0.36
	Ploidy		0	0

were detected at a frequency of 2.08 per cell, compared to 0.62/cell in the unirradiated controls. Complex aberrations were detected at a frequency of 0.43 per cell, but on a per exchange aberration frequency (including asymmetrical, symmetrical and complex exchanges) they were detected at a frequency of 0.28. One complex aberration was detected in 42 unirradiated control cells, a frequency of 0.02/cell or 0.06/exchange aberration. Since the background frequency of exchange aberrations is high in these NBS cells, it is quite possible that this complex aberration, seen in the unirradiated control population, could have arisen from sequential exchange aberrations occurring over a number of cell cycles. Table 4-4 details the number of chromosome breaks per aberration for the above samples. The majority of complex aberrations (13 of 17) involve three breaks. Figures 4-2 through 4-6 illustrate some examples of cells containing multiple aberrations, including complex exchange aberrations that were detected in unirradiated control NBS cells and in irradiated NBS cells. Nomenclature for the indicated aberrations is as follows: n' indicates the centromeric portion of chromosome n ; Tn' indicates a truncation of chromosome n ; $(n'-m)(m'-n)$ indicates a translocation, one part of the aberration includes the centromeric portion of n with an acentric portion of m attached, the other half of the translocation involves the centric portion of m with an acentric portion of n attached; $n' br$ indicates a chromatid break on chromosome n , similarly, $n' gap$ indicates a chromatid gap on chromosome n ; $n id$ indicates an acentric ring or interstitial deletion arising from chromosome n ; $n td$ indicates a terminal deletion

Table 4-4

Number of chromosome breaks determined for each complex exchange aberration detected by mFISH in unirradiated and irradiated GM7166A NBS fibroblasts in the first post-irradiation mitosis.

Dose, Gy	No. Complex Exchanges	No. breaks/complex exchange			
		3	4	5	6
0	1	1	0	0	0
2	17	13	3	0	1

Figure 4-2

"Tinted" pseudocolored image of a chromosome spread (panel A) and its karyotype (panel B) from an unirradiated control GM7166 NBS fibroblast in which a complex exchange aberration involving chromosomes 2, 14 an X was detected.

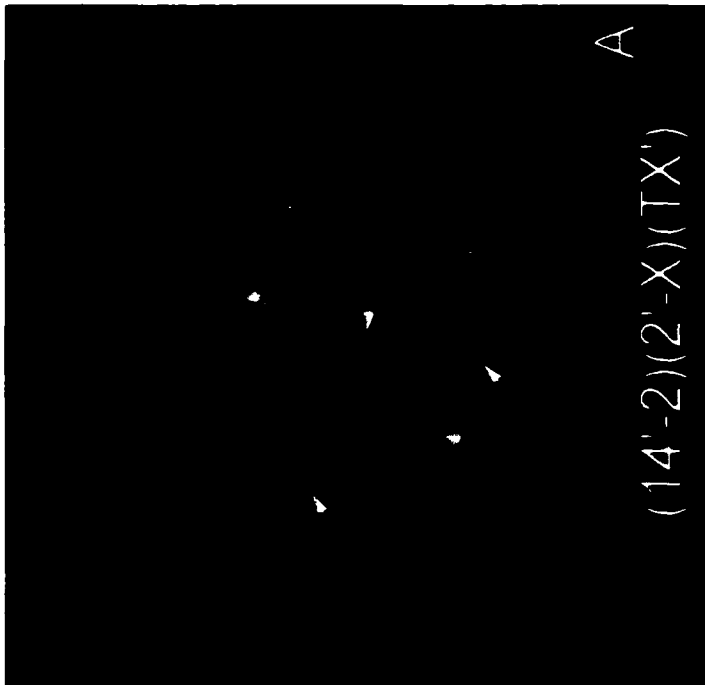
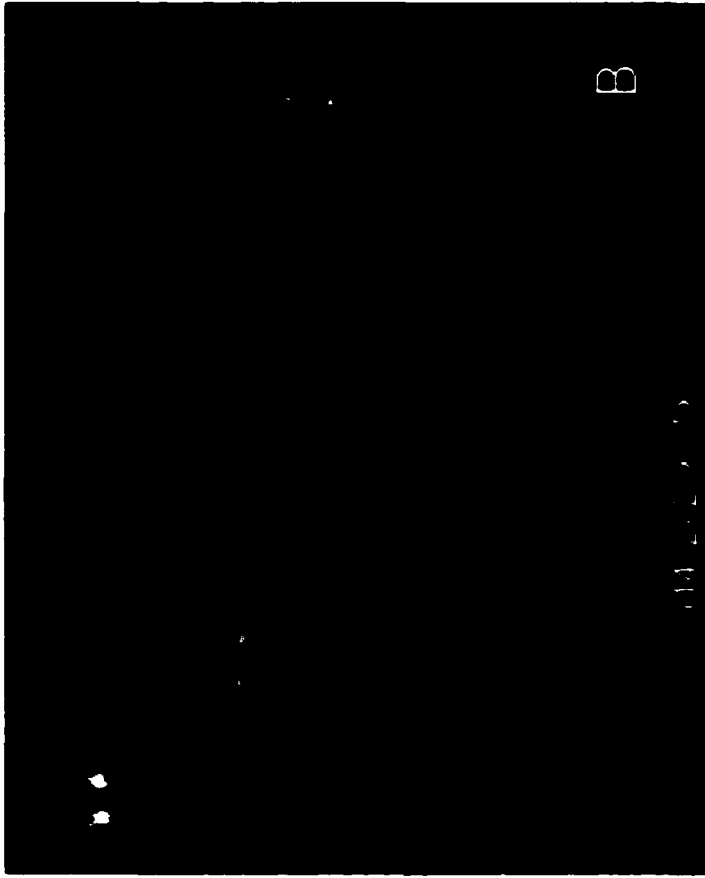


Figure 4-3

“Tinted” pseudocolored image of a chromosome spread (panel A) and its karyotype (panel B) from a GM7166A NBS fibroblast that had been irradiated with 2Gy of ^{137}Cs γ -rays. A complex exchange aberration involving chromosomes 8, 10 and 20 was detected in this cell, indicated in panel A by yellow arrows and text. A chromatid break on chromosome 6 (red arrow and text) was also detected. A terminal deletion of the other homologue of chromosome 6 was detected (blue arrows and text). Finally, an interstitial deletion from chromosome 4 was also detected (green arrows and text).

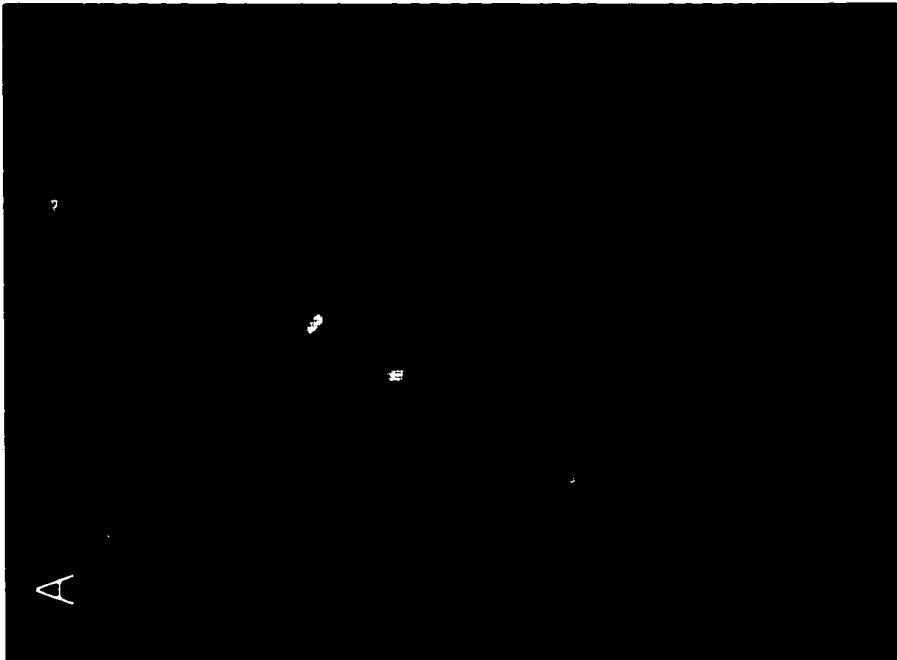
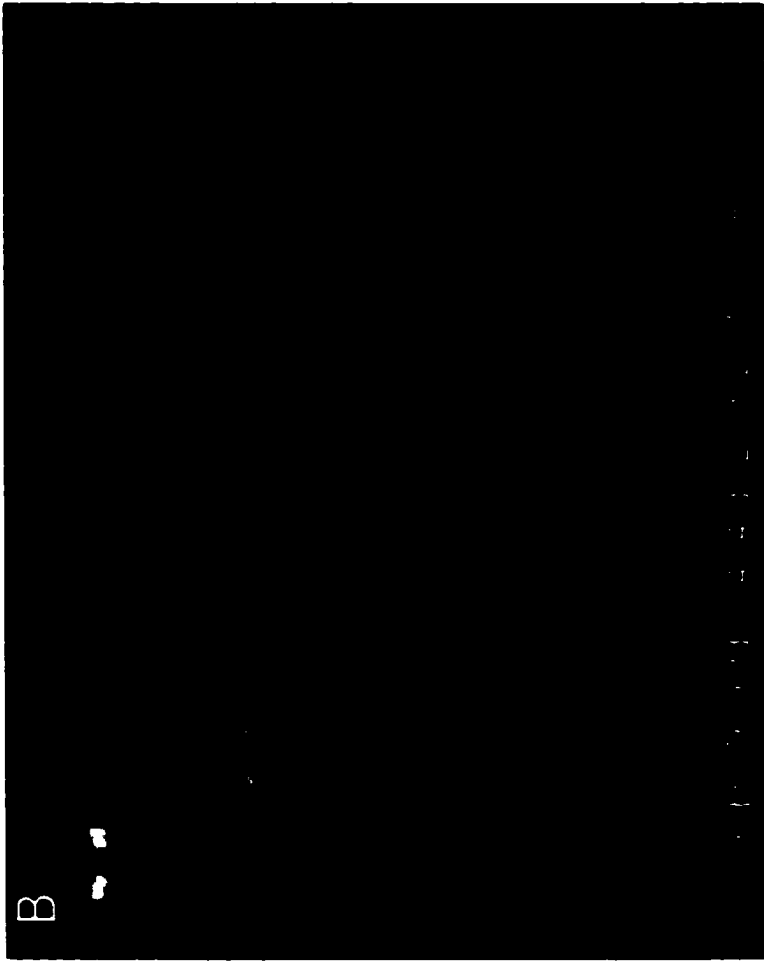


Figure 4-4

"Tinted" pseudocolored image of a chromosome spread (panel A) and its karyotype (panel B) from a GM7166A NBS fibroblast that had been irradiated with 2Gy of ^{137}Cs γ -rays. A complex exchange aberration involving chromosomes 3 and 8 was detected in this cell, indicated in panel A by blue arrows and text. A second complex exchange aberration was also detected and involved chromosomes 1, 2, 7, 10 and X (white arrows and text). A chromatid break on chromosome 2 (red arrow and text) was also detected. Finally, an additional copy of chromosome 9, minus the p-arm was detected (yellow arrow and text).

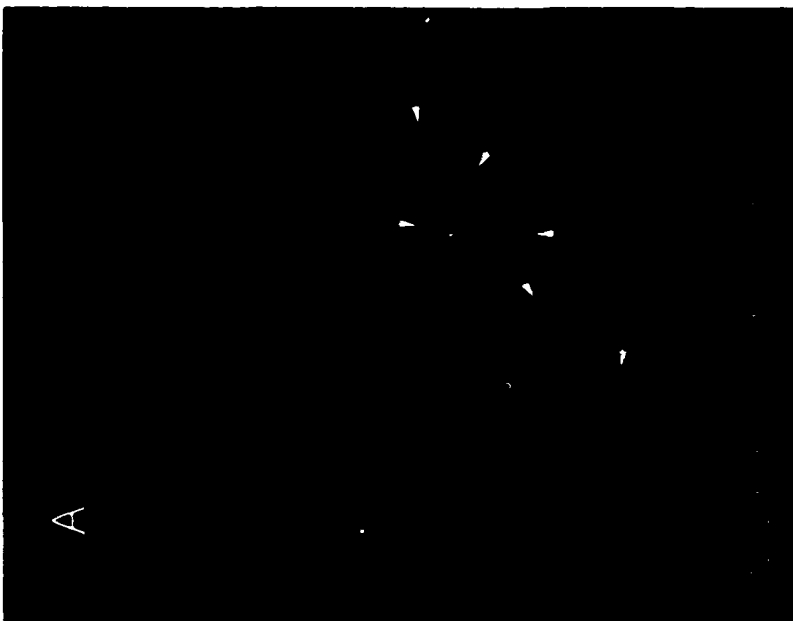
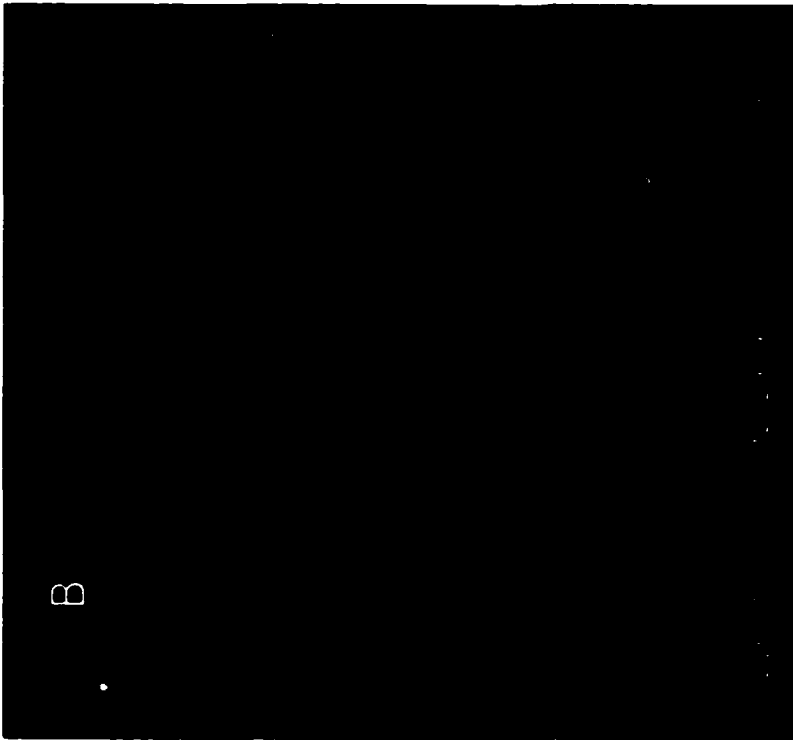
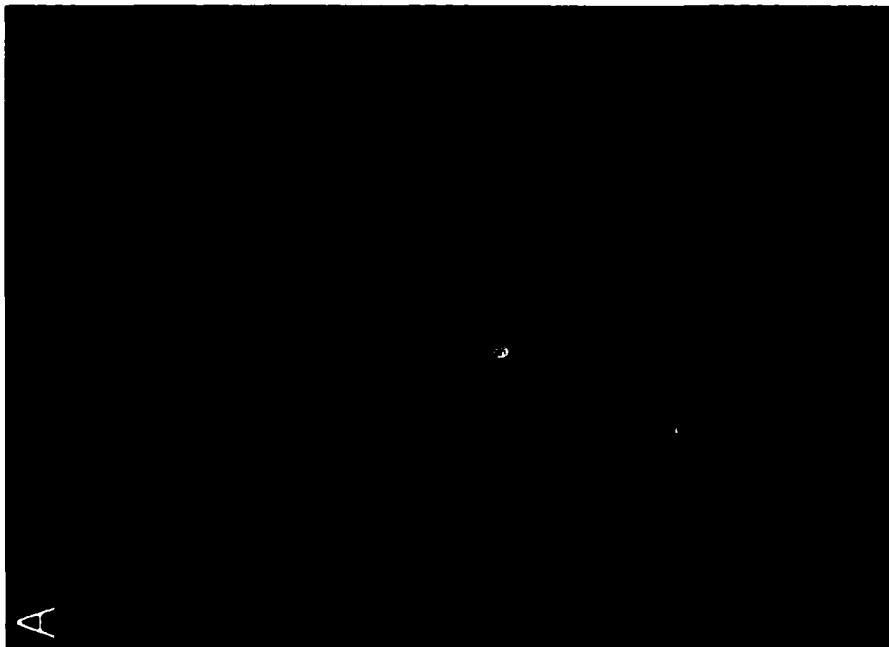


Figure 4-5

“Tinted” pseudocolored image of a chromosome spread (panel A) and its karyotype (panel B) from a GM7166A NBS fibroblast that had been irradiated with 2Gy of ^{137}Cs γ -rays. A complex exchange aberration involving chromosomes 3, 6 and X was detected in this cell, indicated in panel A by blue arrows and text. An asymmetrical exchange aberration was also detected and involved chromosomes 1 and 18 (red arrows and text). A one-way exchange involving chromosomes 9 and 15 was detected (yellow text and arrows). Finally, a chromatid break on chromosome 4 (orange arrow, text) was also detected.



NOTE TO USERS

**Page(s) missing in number only; text follows.
Microfilmed as received.**

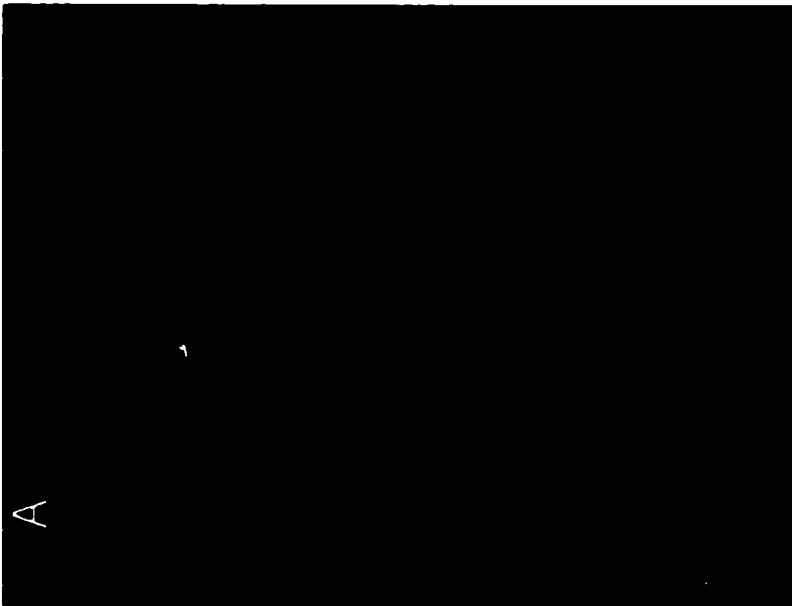
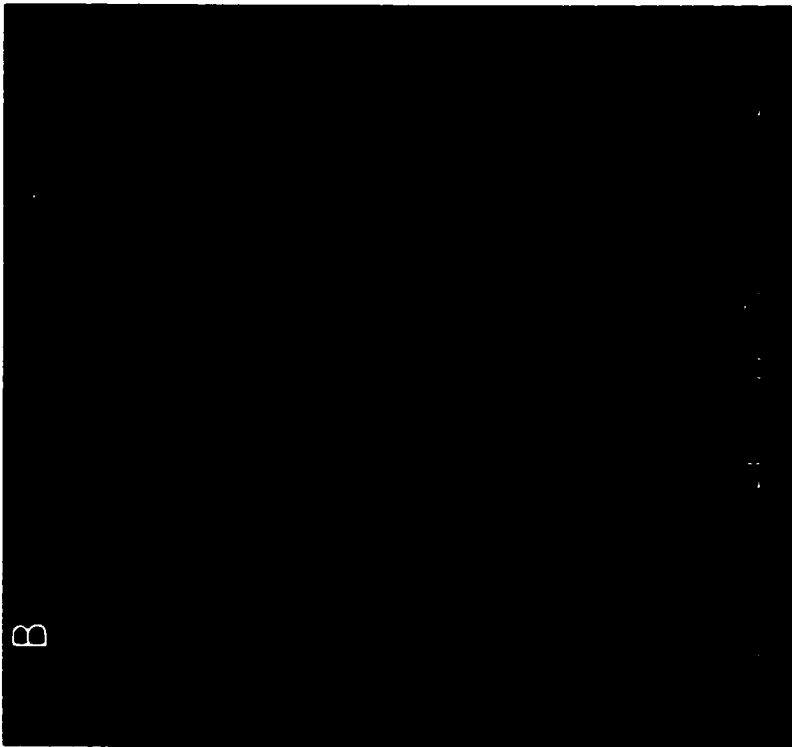
154

This reproduction is the best copy available.

UMI

Figure 4-6

“Tinted” pseudocolored image of a chromosome spread (panel A) and its karyotype (panel B) from a GM7166A NBS fibroblast that had been irradiated with 2Gy of ^{137}Cs γ -rays. Two complex exchange aberrations were detected in this cell. The first, involving chromosomes 8, and 11, was a dicentric with an extra acentric fragment, indicated in panel A by red arrows and text. The second involved chromosomes 3, 5 and 12 (blue arrows and text). Three chromatid breaks were also detected, one on chromosome 1 (yellow arrow and text), one on chromosome 2 (orange arrow and text) and the third on chromosome 17 (green arrow and text).



arising from chromosome n; +n' indicates an amplification of chromosome n and finally a dicentric chromosome would be indicated by (n'-m')(m-n).

Aberrations in PCC's

Several G₀ PCC cells from the 2Gy NBS irradiated population were analyzed for complex aberrations. Although we were unable to perform a quantitative analysis of this sample due to technical difficulties, especially the inability to fully remove cytoplasmic background noise in large multi-nuclear heterokaryons, we did identify one complex aberration in a total of five cells scored. These cells contained a total of ten aberrations, including symmetrical and asymmetrical exchanges, interstitial and terminal deletions. A second complex exchange aberration may have been present in another cell, but analysis was not conclusive. Figure 4-7 and 4-8 show examples of these cells.

NOTE TO USERS

**Page(s) missing in number only; text follows.
Microfilmed as received.**

158

This reproduction is the best copy available.

UMI

Figure 4-7

“Tinted” pseudocolored image of a G₀ PCC spread (panel A) and its karyotype (panel B) from a GM7166A NBS fibroblast that had been irradiated with 2 Gy of ¹³⁷Cs γ-rays. An asymmetrical exchange (dicentric) aberration involving both homologues of chromosome 21 (red arrows and text) was detected in this cell. Also, a terminal deletion involving chromosome 16 (blue arrows and text) was detected.

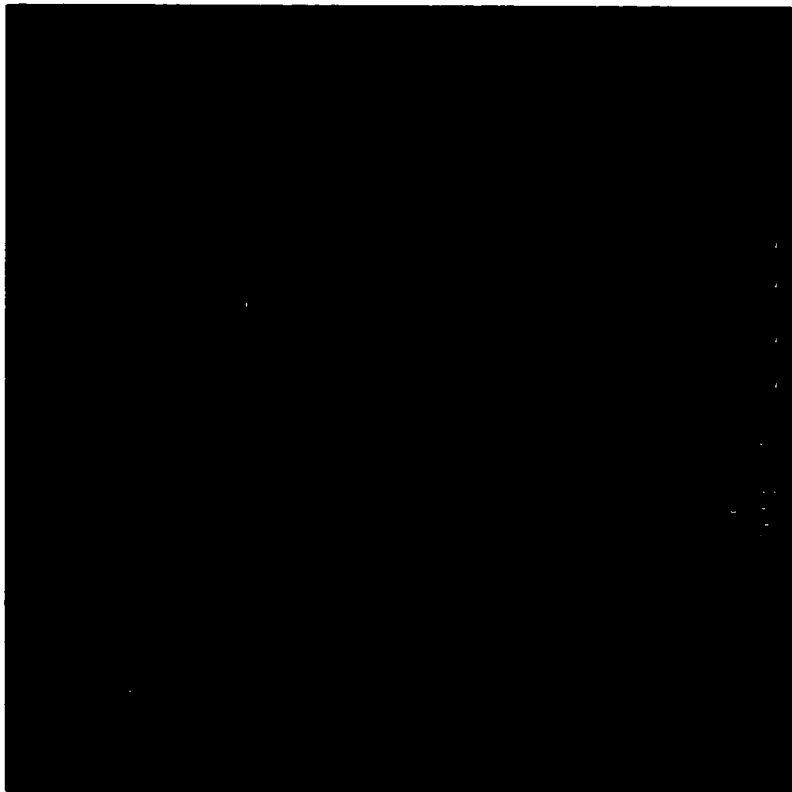


Figure 4-8

“Tinted” pseudocolored image of a G0 PCC spread (panel A) and its karyotype (panel B) from a GM7166A NBS fibroblast that had been irradiated with 2Gy of ¹³⁷Cs γ -rays. A complex exchange aberration involving an insertion of a portion of chromosome 1 into chromosome 2 (blue arrows and text) was detected in this cell. A symmetrical exchange involving chromosomes 6 and 16 (white arrows and text) was observed. Also, a terminal deletion involving chromosome 18 (red arrows and text) was detected.



DISCUSSION

Our data indicate that the defect in the NBS cell line, GM7166A, likely leads to high levels of spontaneous chromatid-type and chromosome-type aberrations. Furthermore, in response to DNA damage induced by ionizing radiation, this cell line is severely compromised in its ability to correctly reconstitute the damage. Using solid Giemsa staining and classical cytogenetic analysis of the 1st post-irradiation mitosis, I detected high levels of spontaneous chromatid-type aberrations, 0.49/cell (98 aberrations in 200 cells), including 6 chromatid exchange aberrations and a low level of spontaneous chromosome-type aberrations, 0.035/cell (7 aberrations in 200 cells) in unirradiated GM7166A fibroblasts. These levels were significantly elevated after 2Gy ¹³⁷Cs γ -radiation. Chromatid-type aberrations increased to 0.86/cell (215 aberrations in 250 cells), including 22 chromatid exchange aberrations and chromosome-types increased to 0.98/cell (245 aberrations in 250 cells). Compared to a phenotypically normal fibroblast culture, AG1521A, also irradiated in G₀, the level of induced chromatid-type aberrations was significantly greater in the NBS cell culture at 2Gy, 0.39/cell vs. 0.02/cell and 0.06/cell after 2Gy and 6Gy, respectively, in the normal fibroblast cell culture. Furthermore, the induced chromosome-type aberration frequency in 2Gy irradiated NBS fibroblasts was much greater than seen at 2Gy in a phenotypically normal control cell line, 0.98/cell vs. 0.29/cell, although it was lower than that detected in 6Gy irradiated AG1521A cells, 1.57/cell. Overall, the radiation-induced aberration frequency was significantly greater in the NBS culture than in the normal fibroblast culture at the same dose, 2Gy, 1.37

aberrations/cell vs. 0.31/cell, respectively, but was slightly lower than the total aberration frequency in the normal fibroblast culture exposed to 6Gy, which was 1.63/cell.

A comparison of radiation-induced aberration frequencies in 1st post-irradiation mitotic cells is given in Table 4-4 for several non-radiation sensitive (AG1521A, CHO 10B2, 4364A and AG1522) and radiation-sensitive (NBS, Irs-20 (deficient in DNA-PK_{cs}), XR-1 (deficient in Ku-70) and Ataxia) cell lines analyzed in this lab. In all the radiation-sensitive cell lines, a high proportion of the induced aberrations detected were chromatid-type.

Analysis of the NBS cell culture using mFISH allowed for a more complete picture concerning the induction of aberrations by exposure to 2Gy of ¹³⁷Cs γ -rays. A high spontaneous background level of chromatid-type aberrations was again detected, 0.31/cell (13 aberrations in 42 cells), although it was somewhat lower than that seen with Giemsa staining, 0.49/cell. Similarly, in the 2Gy exposed cells, a lower chromatid-type aberration frequency was detected by mFISH, 0.53/cell (21 aberrations in 40 cells) as compared to the Giemsa staining results (0.86/cell). This discrepancy in the chromatid-type aberration frequency may have been partially due to the difficulty in identifying chromatid gaps and small breaks in mitotic spreads that have been enzymatically digested, denatured and hybridized with chromosome probes and then counterstained with DAPI. This process tends to induce a loss of morphology (puffiness) and causes other distortions due to fluorescence. Larger breaks are still usually detectable, however.

Table 4-5

Frequency of radiation-induced first-division metaphase aberrations per cell in several normal and radiation-sensitive cell lines analyzed in our laboratory after confluent fibroblast cultures were exposed to X- or γ -rays and subcultured 24 hours later.

^a Data from this study.

^b Data from Cornforth and Bedford, 1987.

^c Data from Stackhouse and Bedford, 1994.

^d Data from Bahari and Bedford, 1989.

Cell line		AG1521 ^a		NBS ^d	AG1522 ^b						Ataxia ^c
Dose (Gy)		2	6	2	1	2	4	6	9	12	1
No. scored		100	100	250	100	100	150	250	100	150	100
% w/ Aberr.		68	83	88							
% w/o Aberr.		32	17	12	83	70	37	16	4	1	15
Chromatid-type (per cell)	Gaps	0	0.03	0.09	0	0	0	0	0	0	0
	Breaks	0.03	0.02	0.21	0	0	0	0	0	0.03	0.37
	Exchanges	0	0	0.05	0	0	0	0	0	0	0.01
Chromosome-type (per cell)	Int del/ac. ring	0.09	0.43	0.23	0.06	0.12	0.48	0.78	1.72	2.8	1.05
	Term. del	0.02	0.08	0.09	0.06	0.02	0.22	0	0.46	0.7	0
	Centric rings	0.01	0.1	0.05	0	0.01	0.06	0.08	0.21	0.26	0
	Dicentrics	0.17	0.93	0.56	0.04	0.05	0.25	0.79	1.31	1.89	0.25
Total Aberr./cell		0.32	1.63	1.33	0.16	0.2	1.0	1.66	3.7	5.49	1.7
% chromatid-type		9.4	3.7	28.2	0	0	0	0	0	0.8	23.3
% chromosome-type		90.6	96.3	71.8	100	100	100	100	100	99.2	76.7

Cell line		CHO 10B2 ^a	hrs-20 ^a	4364A ^a			XR-1 ^a		
Dose (Gy)		7.4	3.8	6	8	14	0.35	0.75	1.5
No. scored		97	125	130	100	150	100	100	130
% w/ Aberr.									
% w/o Aberr.									
Chromatid-type (per cell)	Gaps	0	0.36	0.01	0	0	0.07	0.08	0.19
	Breaks	0	0.53	0.01	0.01	0.03	0.12	0.18	0.39
	Exchanges	0	2.21	0.01	0	0.01	0.16	0.91	1.26
Chromosome-type (per cell)	Int del/ac. ring	3.32	3.42	0.62	1.3	2.8	0.17	0.53	1.11
	Term. del	0.76	1.64	0.15	0.17	0.36	0	0.02	0.13
	Centric rings	0.05	0.19						
	Dicentrics	0.76	0.43	0.55	0.69	1.36	0	0.28	0.64
Total Aberr./cell		4.89	10.38	1.34	2.17	4.56	0.52	2.0	3.71
% chromatid-type		0	45.3	1.6	0.6	0.9	67.4	58.4	49.5
% chromosome-type		100	54.7	96.4	99.4	99.1	32.6	41.6	50.5

A high spontaneous frequency of chromosome-type aberrations was also detected in the unirradiated control NBS cells. A total of 28 chromosome-type aberrations were detected in 42 cells, a frequency of 0.62/cell. Of these, the majority were symmetrical exchanges (12 aberrations) that would not have been detected in the Giemsa scoring, thus accounting for the much of the difference in this frequency determined by mFISH (0.67/cell) compared to Giemsa staining (0.035/cell). Furthermore, one complex exchange aberration was detected in the NBS control cells analyzed. It consisted of an exchange between chromosomes 14, 2 and X and is shown in Figure 4-2. Panel A shows the mitotic spread with the chromosomes involved indicated by arrows, while panel B shows the karyotype of this cell. In the 2Gy irradiated NBS cells, a total of 83 chromosome-type aberrations were detected in 40 cells, 2.08/cell. Of these, 60 were exchange aberrations and of these, 17 were complex. The majority of these complex exchange aberrations involved three breaks as indicated in Table 4-3, three involved four breaks and one highly complex exchange involved six breaks. Several of these cells are shown in Figures 4-3 through 4-6. Figure 4-3 shows a cell containing a chromatid break in one copy of chromosome 6 (red) along with a truncated chromosome 6 (blue). A copy of chromosome 4 has lost an interstitial deletion (green) and a complex exchange aberration involving chromosomes 8, 10 and 20 (yellow) was also detected. Figure 4-4 shows a cell that contained a chromatid break in the q-arm of one copy of chromosome 2 (red), an additional copy of chromosome 9q (yellow), a complex dicentric involving chromosomes 3 and 8 (blue) and a highly complex exchange involving five chromosomes (1, 2, 7,

10 and X) and six breaks (white). Figure 4-5 shows a cell containing an asymmetrical exchange (dicentric) involving chromosomes 1 and 18 (red), a one-way exchange involving chromosomes 9 and 15 (yellow), a chromatid break on chromosome 4 (orange) and a complex exchange involving chromosomes 3, 6 and X (blue). Finally, Figure 4-6 shows a cell containing three chromatid breaks on different chromosomes, 1 (yellow), 2 (orange) and 17 (green). This cell also contained two complex aberrations. The first is a dicentric involving chromosomes 8 and 11 that also contains a small acentric fragment of chromosome 11 (red). The second involves chromosomes 3, 5 and 12 (blue). However, two of these fragments also contain chromatid-type aberrations. One is on chromosome 5, the other is on chromosome 12. Currently, there is no consensus opinion on how to score chromatid-complex chromosome exchange aberrations. Apparently, this is also common in A-T cells exposed to ionizing radiation, although as yet this has not been published (M. Cornforth, personal communication).

A comparison of spontaneous aberration frequencies in the NBS cell culture against data obtained from mFISH analysis of phenotypically normal AG1521A cells held in continuous log phase culture for 10 to 30 post-irradiation generations and described in chapter 2, indicates that the phenotypically normal cell culture had much lower frequencies of spontaneous chromatid-type aberrations (0 aberrations in 84 cells) compared to the radiation-sensitive NBS culture (13 aberrations in 42 cells). Furthermore the AG1521A culture had fewer chromosome-type aberrations (2 in 84 cells) than did the unirradiated control

NBS culture (28 aberrations in 42 cells). Further comparison of aberration frequencies detected by mFISH in our NBS cultures vs. published reports for phenotypically normal human lymphocytes (161) indicates that the NBS cultures exposed to 2Gy of ¹³⁷Cs γ -rays studied in this work had a much greater frequency of complex aberrations per cell than lymphocytes exposed to the same dose, 0.43 vs. 0.12, respectively and a greater frequency on a per exchange aberration basis, 0.28 vs. 0.14, respectively. Furthermore, our results indicate that the complex aberration frequencies produced in NBS cultures were more similar to a dose of 4Gy given to the phenotypically normal human lymphocytes on a per cell basis, 0.43 vs. 0.59, respectively and on a per exchange aberration basis, 0.28 vs. 0.26, respectively.

In a brief analysis of non-cycling NBS cells exposed to 2Gy of ¹³⁷Cs γ -rays while in a confluent culture, mFISH analysis of prematurely condensed chromosomes, I detected a total of 10 aberrations in five cells. One of these aberrations was clearly a complex exchange. In an additional cell, I observed what appeared to be a complex exchange, but was unable to fully classify it. Figure 4-7 illustrates a cell containing a terminal deletion involving chromosome 16 (blue arrows and text) and an asymmetrical exchange involving both homologues of chromosome 21 (red arrows and text). Figure 4-8 illustrates a PCC cell containing a complex exchange aberration involving an insertion of a portion of chromosome 1 into chromosome 2 (blue arrows and text), along with a terminal deletion of chromosome 18 (red arrows and text) and a symmetrical exchange involving chromosomes 6 and 16 (white arrows and text). The

presence of a complex exchange in a non-cycling cell after exposure to ionizing radiation indicates that their formation may occur without the need for the cell to be cycling. However, since I was only able to look at a select few cells due to technical difficulties, I am unable to present any quantitative analysis at this time. Since we detected one complex exchange in the unirradiated control NBS population, we cannot rule out the possibility that the complex exchange detected in the PCCs was not already present and therefore not induced by the radiation exposure. However, although the appearance of complex exchange aberrations involving several chromosomes can be explained by the possible occurrence of sequential exchanges over several cell divisions in a background where a high frequency of exchange events are occurring, it is difficult to envision the occurrence of an insertion involving more than one event in the cell cycle prior to its appearance. Therefore, it is my opinion that the complex exchange seen in this PCC cell (Figure 4-8) was due to the exposure to ionizing radiation.

Taken together, these data indicate that the GM7166A NBS fibroblast cell line is highly susceptible to radiation-induced chromosome-type and complex exchange aberration formation. Furthermore, the cell line is highly susceptible to spontaneous and radiation-induced chromatid-type aberration formation.

Finally, the irradiated NBS cells also showed a significant level of endoreduplication (1.7%). Endoreduplication, the duplication of chromosomes without proceeding through mitosis, leads to chromosomes with double sets of chromatids and a tetraploid chromosome number. Several types of endoreduplication have been identified, including multiple initiations within S-

phase, a recurring S-phase and repeated S and Gap phases (reviewed in (168)). Since NBS cells have been shown to fail to induce the p53 G1/S checkpoint in response to DNA damage after exposure to ionizing radiation (169), it is possible that some cells escaped their confluent, G0 state and entered S-phase prior to release of the entire culture from G0. However, the presence of endoreduplicated cells only in the population exposed to ionizing radiation, suggests a further role for NBS1, possibly in regulating the exit from S-phase into G2 or in the duplication of the centrosome which begins at the G1/S border and is completed prior to entering mitosis (170) and may be mediated somehow by p53 (171). Disjunction of centrosome duplication from DNA replication would produce cells with 4N DNA content, but would lack the ability for proper chromosome segregation at the ensuing mitosis. This might then lead to re-replication of the DNA in a subsequent S-phase leading to the appearance of endoreduplicated cells.

Overall, it appears that the defect in the NBS gene in GM7166A fibroblasts causes misrecognition of DNA damage, leading to misrepair, and elevated levels of chromatid-type and chromosome-type aberrations along with complex exchange aberrations. This likely contributes significantly to the radiation-sensitivity of the cell line, regardless of any role NBS might have in cell cycle control.

Summary of Dissertation

Most cancers show some degree of genomic instability, of which chromosomal instability is a major player. Furthermore, several chromosomal instability syndromes exist in the general population. These syndromes are for the most part due to mutations in genes involved in DNA damage recognition and repair and/or cell cycle control. Affected individuals are, among other things, radiation sensitive and prone to a number of cancers. Finally, ionizing radiation has been shown to induce carcinogenesis and chromosomal instability both *in vitro* and *in vivo*. Since a link has been shown between chromosomal aberrations and carcinogenesis, it has been suggested that radiation-induced chromosomal instability is an initial, or at least very early step, in radiation carcinogenesis. In order to study some aspects of the phenomenon of chromosomal instability, I set out to analyze unirradiated and irradiated normal human cells, unirradiated human tumor cells and unirradiated and irradiated human cells from a chromosomal instability syndrome for structural and/or numerical chromosomal aberrations as markers for chromosomal instability.

Structural and numerical chromosomal instabilities were detected in both mixed populations and clonal populations of unirradiated and irradiated phenotypically normal AG1521A fibroblast cells in a manner and time-frame expected for primary cells as they enter senescence. Clonal descendents of HeLa tumor cells showed numerical chromosomal instability at a point early on in the expansion process which was followed by a return to a somewhat stable, albeit, elevated chromosomal distribution similar to the original bulk cell

population from which the clones were derived. Finally, although a complete instability analysis was not performed due to time constraints, I was able to determine that the Nijmegen Breakage Syndrome fibroblast cell line, GM7166A, showed elevated levels of spontaneous and radiation-induced chromatid-type and chromosome-type aberrations. Furthermore, the proportion of radiation-induced aberrations in this cell line that were complex was higher than previously reported for normal human lymphocytes.

Taken together, this data along with recently published reports, indicate that although chromosomal instability may play an important role in systems with some predisposing factor, such as a defect in DNA damage processing or cell cycle control, it does not appear to occur universally and therefore, may not be the initiating step in radiation carcinogenesis in all cases.

BIBLIOGRAPHY

1. American Cancer Society. Statistics for 2002. American Cancer Society . 3-28-2002. Ref Type: Electronic Citation
2. T. Boveri, Über mehrpolige Mitosen als Mittel zur Analyse des Zellkerns, *Phys. -Med. Ges. Wurzburg* **35**, 67-90 (1902).
3. T. Caspersson, G. Lomakka and L. Zech, 24 fluorescence patterns of human metaphase chromosomes -distinguishing characters and variability., *Hereditas* **67**, 89 (1971).
4. A. T. Summer, H. J. Evans and R. A. Buckland, A new technique for distinguishing between human chromosomes., *Nature New Biol.* **232**, 31 (1971).
5. P. C. Nowell and D. Hungerford, A minute chromosome in human granulocytic leukemia, *Science* **132**, 1497 (1960).
6. J. D. Rowley, Identificaton of a translocation with quinacrine fluorescence in a patient with acute leukemia, *Ann. Genet.* **16**, 109-112 (1973).
7. R. Dalla-Favera, M. Bregni, J. Erikson, D. Patterson, R. C. Gallo and C. M. Croce, Human c-myc onc gene is located on the region of chromosome 8 that is translocated in Burkitt lymphoma cells, *Proc. Natl. Acad. Sci. U. S. A* **79**, 7824-7827 (1982).
8. R. Taub, I. Kirsch, C. Morton, G. Lenoir, D. Swan, S. Tronick, S. Aaronson and P. Leder, Translocation of the c-myc gene into the immunoglobulin heavy chain locus in human Burkitt lymphoma and murine plasmacytoma cells, *Proc. Natl. Acad. Sci. U. S. A* **79**, 7837-7841 (1982).
9. P. C. Nowell and C. M. Croce, Chromosomes, genes, and cancer, *Am. J. Pathol.* **125**, 7-15 (1986).
10. L. Foulds, The experimental study of tumor progression: a review., *Cancer Res.* **14**, 317-339 (1954).
11. P. C. Nowell, The clonal evolution of tumor cell populations, *Science* **194**, 23-28 (1976).
12. I. P. Tomlinson, M. R. Novelli and W. F. Bodmer, The mutation rate and cancer, *Proc. Natl. Acad. Sci. U. S. A* **93**, 14800-14803 (1996).
13. L. A. Loeb, Mutator phenotype may be required for multistage carcinogenesis, *Cancer Res.* **51**, 3075-3079 (1991).

14. R. Baserga, The Relationship of the Cell Cycle to Tumor Growth and Control of Cell Division: A Review, *Cancer Res.* **25**, 581-595 (1965).
15. G. D. Weinstein, J. L. McCullough and P. Ross, Cell proliferation in normal epidermis, *J. Invest Dermatol.* **82**, 623-628 (1984).
16. J. B. Little, H. Nagasawa, T. Pfenning and H. Vetrovs, Radiation-induced genomic instability: delayed mutagenic and cytogenetic effects of X rays and alpha particles, *Radiat. Res.* **148**, 299-307 (1997).
17. L. A. Loeb, A mutator phenotype in cancer, *Cancer Res.* **61**, 3230-3239 (2001).
18. C. Lengauer, K. W. Kinzler and B. Vogelstein, Genetic instabilities in human cancers, *Nature* **396**, 643-649 (1998).
19. K. W. Kinzler and B. Vogelstein, Lessons from hereditary colorectal cancer, *Cell* **87**, 159-170 (1996).
20. M. Varella-Garcia, T. Boomer and G. J. Miller, Karyotypic similarity identified by multiplex-FISH relates four prostate adenocarcinoma cell lines: PC-3, PPC-1, ALVA-31, and ALVA-41, *Genes Chromosomes. Cancer* **31**, 303-315 (2001).
21. C. Lengauer, K. W. Kinzler and B. Vogelstein, Genetic instability in colorectal cancers, *Nature* **386**, 623-627 (1997).
22. T. D. Tlsty, B. H. Margolin and K. Lum, Differences in the rates of gene amplification in nontumorigenic and tumorigenic cell lines as measured by Luria-Delbruck fluctuation analysis, *Proc. Natl. Acad. Sci. U. S. A* **86**, 9441-9445 (1989).
23. D. J. Brenner, *Radon: Risk and Remedy*. W.H. Freeman and Company, NY, NY (1989).
24. D. Trichopoulos, F. P. Li and D. J. Hunter, What causes cancer?, *Sci. Am.* **275**, 80-87 (1996).
25. J. J. McCormick and V. M. Maher, Towards an understanding of the malignant transformation of diploid human fibroblasts, *Mutat. Res.* **199**, 273-291 (1988).
26. D. A. Trott, A. P. Cuthbert, R. W. Overell, I. Russo and R. F. Newbold, Mechanisms involved in the immortalization of mammalian cells by ionizing radiation and chemical carcinogens, *Carcinogenesis* **16**, 193-204 (1995).

27. M. S. Crane, Mutagenesis and cell transformation in cell culture, *Methods Cell Sci.* **21**, 245-253 (1999).
28. M. Terzaghi and J. B. Little, X-radiation-induced transformation in a C3H mouse embryo-derived cell line, *Cancer Res.* **36**, 1367-1374 (1976).
29. A. Han and M. M. Elkind, Transformation of mouse C3H/10T1/2 cells by single and fractionated doses of X-rays and fission-spectrum neutrons, *Cancer Res.* **39**, 123-130 (1979).
30. R. Miller and E. J. Hall, X-ray dose fractionation and oncogenic transformations in cultured mouse embryo cells, *Nature* **272**, 58-60 (1978).
31. M. Lun, R. L. Wells, S. Lang, N. Chawapun and M. M. Elkind, The neoplastic transformation of SCID cells by radiation, *Radiat. Res.* **152**, 180-189 (1999).
32. C. Borek, A. Ong and H. Mason, Distinctive transforming genes in x-ray-transformed mammalian cells, *Proc. Natl. Acad. Sci. U. S. A* **84**, 794-798 (1987).
33. C. A. Reznikoff, D. W. Brankow and C. Heidelberger, Establishment and characterization of a cloned line of C3H mouse embryo cells sensitive to postconfluence inhibition of division, *Cancer Res.* **33**, 3231-3238 (1973).
34. G. J. Todaro and H. Green, Quantitative studies of the growth of mouse embryo cells in culture and their development into established lines., *J. Cell Biol.* **17**, 299-313 (1963).
35. T. Kuroki and N. H. Huh, Why are human cells resistant to malignant cell transformation in vitro?, *Jpn. J. Cancer Res.* **84**, 1091-1100 (1993).
36. A. C. Riches, Z. Herceg, P. E. Bryant and D. Wynford-Thomas, Radiation-induced transformation of SV40-immortalized human thyroid epithelial cells by single and fractionated exposure to gamma- irradiation in vitro, *Int. J. Radiat. Biol.* **66**, 757-765 (1994).
37. M. R. Kuettel, P. J. Thraves, M. Jung, S. P. Varghese, S. C. Prasad, J. S. Rhim and A. Dritschilo, Radiation-induced neoplastic transformation of human prostate epithelial cells, *Cancer Res.* **56**, 5-10 (1996).
38. A. Riches, C. Peddie, S. Rendell, P. Bryant, H. Zitzelsberger, J. Bruch, J. Smida, L. Hieber and M. Bauchinger, Neoplastic transformation and cytogenetic changes after Gamma irradiation of human epithelial cells expressing telomerase, *Radiat. Res.* **155**, 222-229 (2001).

39. P. Brown, *American Martyrs to Science Through Roentgen Ray*. Charles C. Thomas, Springfield, MA (1936).
40. A. C. Upton, *Cancer Research 1964: Thoughts of the Contributions of Radiation Biology, Cancer Res.* **24**, 1861-1868 (1964).
41. J. Bedford and W. C. Dewey, *Historical and Current Highlights in Radiation Biology: Has Anything Important Been Learned By Irradiating Cells?*, *Radiat. Res.* **158** (2002) (in Press).
42. E. J. Hall, *Radiobiology for the Radiologist* (4 Edn). J.B. Lippincott Company, Philadelphia, PA (1994).
43. J. D. Boice, Jr., *Carcinogenesis—a synopsis of human experience with external exposure in medicine, Health Phys.* **55**, 621-630 (1988).
44. J. D. Boice, Jr., *Studies of atomic bomb survivors. Understanding radiation effects, JAMA* **264**, 622-623 (1990).
45. H. L. Liber, D. W. Yandell and J. B. Little, *A comparison of mutation induction at the tk and hprt loci in human lymphoblastoid cells; quantitative differences are due to an additional class of mutations at the autosomal tk locus, Mutat. Res.* **216**, 9-17 (1989).
46. R. J. Albertini, J. P. O'Neill, J. A. Nicklas, N. H. Heintz and P. C. Kelleher, *Alterations of the hprt gene in human in vivo-derived 6-thioguanine-resistant T lymphocytes, Nature* **316**, 369-371 (1985).
47. J. Thacker and R. Cox, *The relationship between specific chromosome aberrations and radiation-induced mutations in cultured mammalian cells. In Radiation-induced Chromosome Damage in Man* Chap. 12. Alan R. Liss, Inc., NY, NY (1983).
48. A. J. Grosovsky, J. G. de Boer, P. J. de Jong, E. A. Drobetsky and B. W. Glickman, *Base substitutions, frameshifts, and small deletions constitute ionizing radiation-induced point mutations in mammalian cells, Proc. Natl. Acad. Sci. U. S. A* **85**, 185-188 (1988).
49. J. Thacker, *The nature of mutants induced by ionising radiation in cultured hamster cells. III. Molecular characterization of HPRT-deficient mutants induced by gamma-rays or alpha-particles showing that the majority have deletions of all or part of the hprt gene, Mutat. Res.* **160**, 267-275 (1986).
50. S. L. Nelson, K. K. Parks and A. J. Grosovsky, *Ionizing radiation signature mutations in human cell mutants induced by low-dose exposures, Mutagenesis* **11**, 275-279 (1996).

51. C. Waldren, C. Jones and T. T. Puck, Measurement of mutagenesis in mammalian cells, *Proc. Natl. Acad. Sci. U. S. A* **76**, 1358-1362 (1979).
52. C. Waldren, L. Correll, M. A. Sognier and T. T. Puck, Measurement of low levels of x-ray mutagenesis in relation to human disease, *Proc. Natl. Acad. Sci. U. S. A* **83**, 4839-4843 (1986).
53. R. Brown and J. Thacker, The nature of mutants induced by ionising radiation in cultured hamster cells. I. Isolation and initial characterisation of spontaneous, ionising radiation-induced, and ethyl methanesulphonate-induced mutants resistant to 6-thioguanine, *Mutat. Res.* **129**, 269-281 (1984).
54. S. A. Amundson, D. J. Chen and R. T. Okinaka, Alpha particle mutagenesis of human lymphoblastoid cell lines, *Int. J. Radiat. Biol.* **70**, 219-226 (1996).
55. T. K. Hei, L. J. Wu, S. X. Liu, D. Vannais, C. A. Waldren and G. Randers-Pehrson, Mutagenic effects of a single and an exact number of alpha particles in mammalian cells, *Proc. Natl. Acad. Sci. U. S. A* **94**, 3765-3770 (1997).
56. A. R. Kennedy and J. B. Little, Evidence that a second event in X-ray-induced oncogenic transformation in vitro occurs during cellular proliferation, *Radiat. Res.* **99**, 228-248 (1984).
57. J. B. Little, Radiation carcinogenesis, *Carcinogenesis* **21**, 397-404 (2000).
58. R. L. Ullrich and B. Ponnaiya, Radiation-induced instability and its relation to radiation carcinogenesis, *Int. J. Radiat. Biol.* **74**, 747-754 (1998).
59. M. A. Kadhim, S. A. Lorimore, M. D. Hepburn, D. T. Goodhead, V. J. Buckle and E. G. Wright, Alpha-particle-induced chromosomal instability in human bone marrow cells, *Lancet* **344**, 987-988 (1994).
60. M. A. Kadhim, S. J. Marsden and E. G. Wright, Radiation-induced chromosomal instability in human fibroblasts: temporal effects and the influence of radiation quality, *Int. J. Radiat. Biol.* **73**, 143-148 (1998).
61. M. A. Kadhim, S. J. Marsden, D. T. Goodhead, A. M. Malcolmson, M. Folkard, K. M. Prise and B. D. Michael, Long-Term Genomic Instability in Human Lymphocytes Induced by Single- Particle Irradiation, *Radiat. Res.* **155**, 122-126 (2001).
62. M. B. Martins, L. Sabatier, M. Ricoul, A. Pinton and B. Dutrillaux, Specific chromosome instability induced by heavy ions: a step towards transformation of human fibroblasts?, *Mutat. Res.* **285**, 229-237 (1993).

63. L. Sabatier, J. Lebeau and B. Dutrillaux, Chromosomal instability and alterations of telomeric repeats in irradiated human fibroblasts, *Int. J. Radiat. Biol.* **66**, 611-613 (1994).
64. K. Holmberg, A. E. Meijer, G. Auer and B. O. Lambert, Delayed chromosomal instability in human T-lymphocyte clones exposed to ionizing radiation, *Int. J. Radiat. Biol.* **68**, 245-255 (1995).
65. U. Weissenborn and C. Streffer, Analysis of structural and numerical chromosomal anomalies at the first, second, and third mitosis after irradiation of one-cell mouse embryos with X-rays or neutrons, *Int. J. Radiat. Biol.* **54**, 381-394 (1988).
66. M. A. Kadhim, S. A. Lorimore, K. M. Townsend, D. T. Goodhead, V. J. Buckle and E. G. Wright, Radiation-induced genomic instability: delayed cytogenetic aberrations and apoptosis in primary human bone marrow cells, *Int. J. Radiat. Biol.* **67**, 287-293 (1995).
67. G. E. Watson, S. A. Lorimore, S. M. Clutton, M. A. Kadhim and E. G. Wright, Genetic factors influencing alpha-particle-induced chromosomal instability, *Int. J. Radiat. Biol.* **71**, 497-503 (1997).
68. B. A. Marder and W. F. Morgan, Delayed chromosomal instability induced by DNA damage, *Mol. Cell Biol.* **13**, 6667-6677 (1993).
69. C. L. Limoli, M. I. Kaplan, J. W. Phillips, G. M. Adair and W. F. Morgan, Differential induction of chromosomal instability by DNA strand-breaking agents, *Cancer Res.* **57**, 4048-4056 (1997).
70. C. L. Limoli, J. J. Corcoran, J. R. Milligan, J. F. Ward and W. F. Morgan, Critical target and dose and dose-rate responses for the induction of chromosomal instability by ionizing radiation, *Radiat. Res.* **151**, 677-685 (1999).
71. M. Jamali and K. R. Trott, Persistent increase in the rates of apoptosis and dicentric chromosomes in surviving V79 cells after X-irradiation, *Int. J. Radiat. Biol.* **70**, 705-709 (1996).
72. A. J. Grosovsky, K. K. Parks, C. R. Giver and S. L. Nelson, Clonal analysis of delayed karyotypic abnormalities and gene mutations in radiation-induced genetic instability, *Mol. Cell Biol.* **16**, 6252-6262 (1996).
73. B. Ponnaiya, M. N. Cornforth and R. L. Ullrich, Induction of chromosomal instability in human mammary cells by neutrons and gamma rays, *Radiat. Res.* **147**, 288-294 (1997).

74. B. Ponnaiya, M. N. Cornforth and R. L. Ullrich, Radiation-induced chromosomal instability in BALB/c and C57BL/6 mice: the difference is as clear as black and white, *Radiat. Res.* **147**, 121-125 (1997).
75. Y. Yu, R. Okayasu, M. M. Weil, A. Silver, M. McCarthy, R. Zabriskie, S. Long, R. Cox and R. L. Ullrich, Elevated breast cancer risk in irradiated BALB/c mice associates with unique functional polymorphism of the Prkdc (DNA-dependent protein kinase catalytic subunit) gene, *Cancer Res.* **61**, 1820-1824 (2001).
76. R. L. Ullrich and C. M. Davis, Radiation-induced cytogenetic instability in vivo, *Radiat. Res.* **152**, 170-173 (1999).
77. T. Stamato, R. Weinstein, B. Peters, J. Hu, B. Doherty and A. Giaccia, Delayed mutation in Chinese hamster cells, *Somat. Cell Mol. Genet.* **13**, 57-65 (1987).
78. T. D. Stamato, E. Richardson and M. L. Perez, UV-light induces delayed mutations in Chinese hamster cells, *Mutat. Res.* **328**, 175-181 (1995).
79. J. B. Little, L. Gorgojo and H. Vetrovs, Delayed appearance of lethal and specific gene mutations in irradiated mammalian cells, *Int. J. Radiat. Oncol. Biol. Phys.* **19**, 1425-1429 (1990).
80. B. D. Loucas and M. N. Cornforth, Postirradiation growth in HAT medium fails to eliminate the delayed appearance of 6-thioguanine-resistant clones in EJ30 human epithelial cells, *Radiat. Res.* **149**, 171-178 (1998).
81. K. Suzuki, R. Takahara, S. Kodama and M. Watanabe, In situ detection of chromosome bridge formation and delayed reproductive death in normal human embryonic cells surviving X irradiation, *Radiat. Res.* **150**, 375-381 (1998).
82. O. V. Belyakov, K. M. Prise, K. R. Trott and B. D. Michael, Delayed lethality, apoptosis and micronucleus formation in human fibroblasts irradiated with X-rays or alpha-particles, *Int. J. Radiat. Biol.* **75**, 985-993 (1999).
83. W. K. Sinclair, X-ray-induced Heritable Damage (Small-Colony Formation) in Cultured Mammalian Cells, *Radiat. Res.* **21**, 581-611 (1964).
84. C. B. Seymour, C. Mothersill and T. Alper, High yields of lethal mutations in somatic mammalian cells that survive ionizing radiation, *Int. J. Radiat. Biol. Relat Stud. Phys. Chem. Med.* **50**, 167-179 (1986).
85. L. Gorgojo and J. B. Little, Expression of lethal mutations in progeny of irradiated mammalian cells, *Int. J. Radiat. Biol.* **55**, 619-630 (1989).

86. W. P. Chang and J. B. Little, Delayed reproductive death as a dominant phenotype in cell clones surviving X-irradiation, *Carcinogenesis* **13**, 923-928 (1992).
87. M. Jamali and K. R. Trott, Increased micronucleus frequency in the progeny of irradiated Chinese hamster cells, *Int. J. Radiat. Biol.* **69**, 301-307 (1996).
88. L. Manti, M. Jamali, K. M. Prise, B. D. Michael and K. R. Trott, Genomic instability in Chinese hamster cells after exposure to X rays or alpha particles of different mean linear energy transfer, *Radiat. Res.* **147**, 22-28 (1997).
89. B. Paquette and J. B. Little, In vivo enhancement of genomic instability in minisatellite sequences of mouse C3H/10T1/2 cells transformed in vitro by X-rays, *Cancer Res.* **54**, 3173-3178 (1994).
90. Y. E. Dubrova, M. Plumb, J. Brown and A. J. Jeffreys, Radiation-induced germline instability at minisatellite loci, *Int. J. Radiat. Biol.* **74**, 689-696 (1998).
91. K. Salassidis, V. Georgiadou-Schumacher, H. Braselmann, P. Muller, R. U. Peter and M. Bauchinger, Chromosome painting in highly irradiated Chernobyl victims: a follow-up study to evaluate the stability of symmetrical translocations and the influence of clonal aberrations for retrospective dose estimation, *Int. J. Radiat. Biol.* **68**, 257-262 (1995).
92. S. Salomaa, K. Holmberg, C. Lindholm, R. Mustonen, M. Tekkel, T. Veidebaum and B. Lambert, Chromosomal instability in in vivo radiation exposed subjects, *Int. J. Radiat. Biol.* **74**, 771-779 (1998).
93. C. S. Griffin, A. Neshasateh-Riz, R. J. Mairs, E. G. Wright and T. E. Wheldon, Absence of delayed chromosomal instability in a normal human fibroblast cell line after 125I iododeoxyuridine, *Int. J. Radiat. Biol.* **76**, 963-969 (2000).
94. C. A. Whitehouse and E. J. Tawn, No evidence for chromosomal instability in radiation workers with in vivo exposure to plutonium, *Radiat. Res.* **156**, 467-475 (2001).
95. L. Abramsson-Zetterberg, G. Zetterberg, S. Sundell-Bergman and J. Grawe, Absence of genomic instability in mice following prenatal low dose-rate gamma-irradiation, *Int. J. Radiat. Biol.* **76**, 971-977 (2000).
96. E. J. Tawn, C. A. Whitehouse and F. A. Martin, Sequential chromosome aberration analysis following radiotherapy - no evidence for enhanced genomic instability, *Mutat. Res.* **465**, 45-51 (2000).

97. S. D. Bcuffler, J. W. Haines, A. A. Edwards, J. D. Harrison and R. Cox, Lack of detectable transmissible chromosomal instability after in vivo or in vitro exposure of mouse bone marrow cells to 224Ra alpha particles, *Radiat. Res.* **155**, 345-352 (2001).
98. C. R. Hunt, J. E. Sim, S. J. Sullivan, T. Featherstone, W. Golden, C. Kapp-Herr, R. A. Hock, R. A. Gomez, A. J. Parsian and D. R. Spitz, Genomic instability and catalase gene amplification induced by chronic exposure to oxidative stress, *Cancer Res.* **58**, 3986-3992 (1998).
99. K. K. Sanford, R. Parshad, G. Jones, S. Handleman, C. Garrison and F. Price, Role of photosensitization and oxygen in chromosome stability and "spontaneous" malignant transformation in culture, *J. Natl. Cancer Inst.* **63**, 1245-1255 (1979).
100. I. Emerit, Reactive oxygen species, chromosome mutation, and cancer: possible role of clastogenic factors in carcinogenesis, *Free Radic. Biol. Med.* **16**, 99-109 (1994).
101. T. Duell, E. Lengfelder, R. Fink, R. Giesen and M. Bauchinger, Effect of activated oxygen species in human lymphocytes, *Mutat. Res.* **336**, 29-38 (1995).
102. S. M. Clutton, K. M. Townsend, C. Walker, J. D. Ansell and E. G. Wright, Radiation-induced genomic instability and persisting oxidative stress in primary bone marrow cultures, *Carcinogenesis* **17**, 1633-1639 (1996).
103. E. H. Blackburn, Structure and function of telomeres, *Nature* **350**, 569-573 (1991).
104. J. Meyne, R. J. Baker, H. H. Hobart, T. C. Hsu, O. A. Ryder, O. G. Ward, J. E. Wiley, D. H. Wurster-Hill, T. L. Yates and R. K. Moyzis, Distribution of non-telomeric sites of the (TTAGGG)_n telomeric sequence in vertebrate chromosomes, *Chromosoma* **99**, 3-10 (1990).
105. P. A. Benn, Specific chromosome aberrations in senescent fibroblast cell lines derived from human embryos, *Am. J. Hum. Genet.* **28**, 465-473 (1976).
106. S. M. Bailey, J. Meyne, D. J. Chen, A. Kurimasa, G. C. Li, B. E. Lehnert and E. H. Goodwin, DNA double-strand break repair proteins are required to cap the ends of mammalian chromosomes, *Proc. Natl. Acad. Sci. U. S. A* **96**, 14899-14904 (1999).
107. L. Alvarez, J. W. Evans, R. Wilks, J. N. Lucas, J. M. Brown and A. J. Giaccia, Chromosomal radiosensitivity at intrachromosomal telomeric sites, *Genes Chromosomes. Cancer* **8**, 8-14 (1993).

108. J. P. Day, C. L. Limoli and W. F. Morgan, Recombination involving interstitial telomere repeat-like sequences promotes chromosomal instability in Chinese hamster cells, *Carcinogenesis* **19**, 259-265 (1998).
109. J. L. Schwartz, R. Jordan and H. H. Evans, Characteristics of chromosome instability in the human lymphoblast cell line WTK1, *Cancer Genet. Cytogenet.* **129**, 124-130 (2001).
110. N. M. Tsang, H. Nagasawa, C. Li and J. B. Little, Abrogation of p53 function by transfection of HPV16 E6 gene enhances the resistance of human diploid fibroblasts to ionizing radiation, *Oncogene* **10**, 2403-2408 (1995).
111. M. A. Kadhim, D. A. Macdonald, D. T. Goodhead, S. A. Lorimore, S. J. Marsden and E. G. Wright, Transmission of chromosomal instability after plutonium alpha-particle irradiation, *Nature* **355**, 738-740 (1992).
112. C. Zeitlin, L. Heilbronn and J. Miller, Detailed characterization of the 1087 MeV/nucleon iron-56 beam used for radiobiology at the alternating gradient synchrotron, *Radiat. Res.* **149**, 560-569 (1998).
113. P. A. Benn and M. A. Perle, Chromosome Staining and Banding Techniques. In *Human Cytogenetics: Volume 1, Constitutional Analysis: A Practical Approach* (Edited by D. E. Rooney and B. H. Czepulkowski), Chap. 4. Oxford University Press, New York, NY (1992).
114. T. Straume and J. N. Lucas, A comparison of the yields of translocations and dicentrics measured using fluorescence in situ hybridization, *Int. J. Radiat. Biol.* **64**, 185-187 (1993).
115. M. S. Meyn, Ataxia-telangiectasia and cellular responses to DNA damage, *Cancer Res.* **55**, 5991-6001 (1995).
116. S. Casares, Y. Ionov, H. Y. Ge, E. Stanbridge and M. Perucho, The microsatellite mutator phenotype of colon cancer cells is often recessive, *Oncogene* **11**, 2303-2310 (1995).
117. M. A. Kadhim, C. A. Walker, M. A. Plumb and E. G. Wright, No association between p53 status and alpha-particle-induced chromosomal instability in human lymphoblastoid cells, *Int. J. Radiat. Biol.* **69**, 167-174 (1996).
118. J. N. Lucas, A. Awa, T. Straume, M. Poggensee, Y. Kodama, M. Nakano, K. Ohtaki, H. U. Weier, D. Pinkel, J. Gray and ., Rapid translocation frequency analysis in humans decades after exposure to ionizing radiation, *Int. J. Radiat. Biol.* **62**, 53-63 (1992).

119. E. Saksela and P. S. Moorhead, Aneuploidy in the degenerative phase of serial cultivation of human cell strains, *Proc. Natl. Acad. Sci. U. S. A* **50**, 390-395 (1963).
120. G. O. Gey, W. D. Coffman and M. T. Kubicek, Tissue culture studies of the proliferative capacity of cervical carcinoma and normal epithelium, *Cancer Res.* **12**, 264-265 (1952).
121. M. Macville, E. Schrock, H. Padilla-Nash, C. Keck, B. M. Ghadimi, D. Zimonjic, N. Popescu and T. Ried, Comprehensive and definitive molecular cytogenetic characterization of HeLa cells by spectral karyotyping, *Cancer Res.* **59**, 141-150 (1999).
122. A. Tonomura, K. Kishi and F. Saito, Types and Frequencies of Chromosome Aberrations in Peripheral Lymphocytes of General Populations. In *Radiation-induced Chromosome Damage in Man* (Edited by T. Ishihara and M. S. Sasaki), Chap. 28. Alan R. Liss, Inc., NY, NY (1983).
123. N. Johnson and S. Kotz, *Discreet Distributions*, 96-98. Wiley, New York, NY (1969).
124. C. M. Counter, A. A. Avilion, C. E. LeFeuvre, N. G. Stewart, C. W. Greider, C. B. Harley and S. Bacchetti, Telomere shortening associated with chromosome instability is arrested in immortal cells which express telomerase activity, *EMBO J.* **11**, 1921-1929 (1992).
125. L. Hayflick, The Limited in vitro Lifetime of Human Diploid Cell Strains, *Exp. Cell Res.* **37**, 614-636 (1965).
126. J. P. Carney, Chromosomal breakage syndromes, *Curr. Opin. Immunol.* **11**, 443-447 (1999).
127. E. G. Wright, Inherited and inducible chromosomal instability: a fragile bridge between genome integrity mechanisms and tumourigenesis, *J. Pathol.* **187**, 19-27 (1999).
128. D. W. Bell, J. M. Varley, T. E. Szydlo, D. H. Kang, D. C. Wahrer, K. E. Shannon, M. Lubratovich, S. J. Verselis, K. J. Isselbacher, J. F. Fraumeni, J. M. Birch, F. P. Li, J. E. Garber and D. A. Haber, Heterozygous germ line hCHK2 mutations in Li-Fraumeni syndrome, *Science* **286**, 2528-2531 (1999).
129. C. Masutani, R. Kusumoto, A. Yamada, N. Dohmae, M. Yokoi, M. Yuasa, M. Araki, S. Iwai, K. Takio and F. Hanaoka, The XPV (xeroderma pigmentosum variant) gene encodes human DNA polymerase eta, *Nature* **399**, 700-704 (1999).

130. M. Swift, L. Sholman, M. Perry and C. Chase, Malignant neoplasms in the families of patients with ataxia-telangiectasia, *Cancer Res.* **36**, 209-215 (1976).
131. C. S. Djuzenova, D. Schindler, H. Stopper, H. Hoehn, M. Flentje and U. Oppitz, Identification of ataxia telangiectasia heterozygotes, a cancer-prone population, using the single-cell gel electrophoresis (Comet) assay, *Lab Invest* **79**, 699-705 (1999).
132. P. C. Chen, M. F. Lavin, C. Kidson and D. Moss, Identification of ataxia telangiectasia heterozygotes, a cancer prone population, *Nature* **274**, 484-486 (1978).
133. E. Boder and R. P. Sedgwick, Ataxia-telangiectasia. A familial syndrome of progressive cerebellar ataxia, oculocutaneous telangiectasia and frequent pulmonary infection. A preliminar report on 7 children, an autopsy and a case history., *Univ Sth Calif Med Bull* **9**, 15-28 (1957).
134. M. F. Lavin and Y. Shiloh, Ataxia-telangiectasia: a multifaceted genetic disorder associated with defective signal transduction, *Curr. Opin. Immunol.* **8**, 459-464 (1996).
135. K. Savitsky, A. Bar-Shira, S. Gilad, G. Rotman, Y. Ziv, L. Vanagaite, D. A. Tagle, S. Smith, T. Uziel, S. Sfez and ., A single ataxia telangiectasia gene with a product similar to PI-3 kinase, *Science* **268**, 1749-1753 (1995).
136. C. E. Canman, D. S. Lim, K. A. Cimprich, Y. Taya, K. Tamai, K. Sakaguchi, E. Appella, M. B. Kastan and J. D. Siliciano, Activation of the ATM kinase by ionizing radiation and phosphorylation of p53, *Science* **281**, 1677-1679 (1998).
137. S. Banin, L. Moyal, S. Shieh, Y. Taya, C. W. Anderson, L. Chessa, N. I. Smorodinsky, C. Prives, Y. Reiss, Y. Shiloh and Y. Ziv, Enhanced phosphorylation of p53 by ATM in response to DNA damage, *Science* **281**, 1674-1677 (1998).
138. K. K. Khanna, H. Beamish, J. Yan, K. Hobson, R. Williams, I. Dunn and M. F. Lavin, Nature of G1/S cell cycle checkpoint defect in ataxia-telangiectasia, *Oncogene* **11**, 609-618 (1995).
139. P. Chaturvedi, W. K. Eng, Y. Zhu, M. R. Mattern, R. Mishra, M. R. Hurle, X. Zhang, R. S. Annan, Q. Lu, L. F. Faucette, G. F. Scott, X. Li, S. A. Carr, R. K. Johnson, J. D. Winkler and B. B. Zhou, Mammalian Chk2 is a downstream effector of the ATM-dependent DNA damage checkpoint pathway, *Oncogene* **18**, 4047-4054 (1999).

140. L. H. Thompson and D. Schild, Homologous recombinational repair of DNA ensures mammalian chromosome stability, *Mutat. Res.* **477**, 131-153 (2001).
141. M. Gatei, D. Young, K. M. Cerosaletti, A. Desai-Mehta, K. Spring, S. Kozlov, M. F. Lavin, R. A. Gatti, P. Concannon and K. Khanna, ATM-dependent phosphorylation of nibrin in response to radiation exposure, *Nat. Genet.* **25**, 115-119 (2000).
142. S. Zhao, Y. C. Weng, S. S. Yuan, Y. T. Lin, H. C. Hsu, S. C. Lin, E. Gerbino, M. H. Song, M. Z. Zdzienicka, R. A. Gatti, J. W. Shay, Y. Ziv, Y. Shiloh and E. Y. Lee, Functional link between ataxia-telangiectasia and Nijmegen breakage syndrome gene products, *Nature* **405**, 473-477 (2000).
143. D. S. Lim, S. T. Kim, B. Xu, R. S. Maser, J. Lin, J. H. Petrini and M. B. Kastan, ATM phosphorylates p95/nbs1 in an S-phase checkpoint pathway, *Nature* **404**, 613-617 (2000).
144. R. D. Taalman, N. G. Jaspers, J. M. Scheres, J. de Wit and T. W. Hustinx, Hypersensitivity to ionizing radiation, in vitro, in a new chromosomal breakage disorder, the Nijmegen Breakage Syndrome, *Mutat. Res.* **112**, 23-32 (1983).
145. D. B. van, I, K. H. Chrzanowska, D. Smeets and C. Weemaes, Nijmegen breakage syndrome, *J. Med. Genet.* **33**, 153-156 (1996).
146. C. Featherstone and S. P. Jackson, DNA repair: the Nijmegen breakage syndrome protein, *Curr. Biol.* **8**, R622-R625 (1998).
147. K. Saar, K. H. Chrzanowska, M. Stumm, M. Jung, G. Nurnberg, T. F. Wienker, E. Seemanova, R. D. Wegner, A. Reis and K. Sperling, The gene for the ataxia-telangiectasia variant, Nijmegen breakage syndrome, maps to a 1-cM interval on chromosome 8q21, *Am. J. Hum. Genet.* **60**, 605-610 (1997).
148. K. M. Cerosaletti, E. Lange, H. M. Stringham, C. M. Weemaes, D. Smeets, B. Solder, B. H. Belohradsky, A. M. Taylor, P. Karnes, A. Elliott, K. Komatsu, R. A. Gatti, M. Boehnke and P. Concannon, Fine localization of the Nijmegen breakage syndrome gene to 8q21: evidence for a common founder haplotype, *Am. J. Hum. Genet.* **63**, 125-134 (1998).
149. J. P. Carney, R. S. Maser, H. Olivares, E. M. Davis, M. Le Beau, J. R. Yates, III, L. Hays, W. F. Morgan and J. H. Petrini, The hMre11/hRad50 protein complex and Nijmegen breakage syndrome: linkage of double-strand break repair to the cellular DNA damage response, *Cell* **93**, 477-486 (1998).

150. R. Varon, C. Vissinga, M. Platzer, K. M. Cerosaletti, K. H. Chrzanowska, K. Saar, G. Beckmann, E. Seemanova, P. R. Cooper, N. J. Nowak, M. Stumm, C. M. Weemaes, R. A. Gatti, R. K. Wilson, M. Digweed, A. Rosenthal, K. Sperling, P. Concannon and A. Reis, Nibrin, a novel DNA double-strand break repair protein, is mutated in Nijmegen breakage syndrome, *Cell* **93**, 467-476 (1998).
151. M. Digweed, A. Reis and K. Sperling, Nijmegen breakage syndrome: consequences of defective DNA double strand break repair, *Bioessays* **21**, 649-656 (1999).
152. T. T. Paull and M. Gellert, Nbs1 potentiates ATP-driven DNA unwinding and endonuclease cleavage by the Mre11/Rad50 complex, *Genes Dev.* **13**, 1276-1288 (1999).
153. G. Barbi, J. M. Scheres, D. Schindler, R. D. Taalman, K. Rodens, K. Mehnert, M. Muller and H. Seyschab, Chromosome instability and X-ray hypersensitivity in a microcephalic and growth-retarded child, *Am. J. Med. Genet.* **40**, 44-50 (1991).
154. A. Antoccia, M. Stumm, K. Saar, R. Ricordy, P. Maraschio and C. Tanzarella, Impaired p53-mediated DNA damage response, cell-cycle disturbance and chromosome aberrations in Nijmegen breakage syndrome lymphoblastoid cell lines, *Int. J. Radiat. Biol.* **75**, 583-591 (1999).
155. D. Pinkel, J. Landegent, C. Collins, J. Fuscoe, R. Seagraves, J. Lucas and J. Gray, Fluorescence in situ hybridization with human chromosome-specific libraries: detection of trisomy 21 and translocations of chromosome 4, *Proc. Natl. Acad. Sci. U. S. A* **85**, 9138-9142 (1988).
156. P. J. Simpson and J. R. Savage, Estimating the true frequency of X-ray-induced complex chromosome exchanges using fluorescence in situ hybridization, *Int. J. Radiat. Biol.* **67**, 37-45 (1995).
157. C. S. Griffin, S. J. Marsden, D. L. Stevens, P. Simpson and J. R. Savage, Frequencies of complex chromosome exchange aberrations induced by ²³⁸Pu alpha-particles and detected by fluorescence in situ hybridization using single chromosome-specific probes, *Int. J. Radiat. Biol.* **67**, 431-439 (1995).
158. P. J. Simpson and J. R. Savage, Dose-response curves for simple and complex chromosome aberrations induced by X-rays and detected using fluorescence in situ hybridization, *Int. J. Radiat. Biol.* **69**, 429-436 (1996).
159. M. R. Speicher, B. S. Gwyn and D. C. Ward, Karyotyping human chromosomes by combinatorial multi-fluor FISH, *Nat. Genet.* **12**, 368-375 (1996).

160. E. Schrock, M. S. du, T. Veldman, B. Schoell, J. Wienberg, M. A. Ferguson-Smith, Y. Ning, D. H. Ledbetter, I. Bar-Am, D. Scenksen, Y. Garini and T. Ried, Multicolor spectral karyotyping of human chromosomes, *Science* **273**, 494-497 (1996).
161. B. D. Loucas and M. N. Cornforth, Complex chromosome exchanges induced by gamma rays in human lymphocytes: an mFISH study, *Radiat. Res.* **155**, 660-671 (2001).
162. R. T. Johnson and P. N. Rao, Mammalian cell fusion: induction of premature chromosome condensation in interphase nuclei, *Nature* **226**, 717-722 (1970).
163. C. A. Waldren and R. T. Johnson, Analysis of interphase chromosome damage by means of premature chromosome condensation after X- and ultraviolet-irradiation, *Proc. Natl. Acad. Sci. U. S. A* **71**, 1137-1141 (1974).
164. M. N. Cornforth and J. S. Bedford, High-resolution measurement of breaks in prematurely condensed chromosomes by differential staining, *Chromosoma* **88**, 315-318 (1983).
165. J. M. Brown and M. S. Kovacs, Visualization of nonreciprocal chromosome exchanges in irradiated human fibroblasts by fluorescence in situ hybridization, *Radiat. Res.* **136**, 71-76 (1993).
166. M. S. Kovacs, J. W. Evans, I. M. Johnstone and J. M. Brown, Radiation-induced damage, repair and exchange formation in different chromosomes of human fibroblasts determined by fluorescence in situ hybridization, *Radiat. Res.* **137**, 34-43 (1994).
167. K. George, M. Durante, H. Wu, V. Willingham, G. Badhwar and F. A. Cucinotta, Chromosome aberrations in the blood lymphocytes of astronauts after space flight, *Radiat. Res.* **156**, 731-738 (2001).
168. G. Grafi, Cell cycle regulation of DNA replication: the endoreduplication perspective, *Exp. Cell Res.* **244**, 372-378 (1998).
169. W. Jongmans, M. Vuillaume, K. Chrzanowska, D. Smeets, K. Sperling and J. Hall, Nijmegen breakage syndrome cells fail to induce the p53-mediated DNA damage response following exposure to ionizing radiation, *Mol. Cell Biol.* **17**, 5016-5022 (1997).
170. A. Kramer and A. D. Ho, Centrosome aberrations and cancer, *Onkologie.* **24**, 538-544 (2001).
171. K. Fukasawa, T. Choi, R. Kuriyama, S. Rulong and G. F. Vande Woude, Abnormal centrosome amplification in the absence of p53, *Science* **271**, 1744-1747 (1996).